The Dissertation Committee for Gwendolyn Motz Stovall Certifies that this is the approved version of the following dissertation:

Evaluation of Protein Aggregation and Organismal Fitness

Committee:

Andrew D. Ellington, Supervisor

Edward Marcotte

Marvin Whiteley

Claus Wilke

Katherine Willets

Evaluation of Protein Aggregation and Organismal Fitness

by

Gwendolyn Motz Stovall, B.S. Chem.; B.S.

Dissertation

Presented to the Faculty of the Graduate School of

The University of Texas at Austin

in Partial Fulfillment

of the Requirements

for the Degree of

Doctor of Philosophy

The University of Texas at Austin

May 2011

Dedication

To my husband, Drew.

Acknowledgements

I must begin by thanking Andy Ellington for the opportunities, support, and guidance that you have provided me over the years. The Ellington lab, including past and present members, shaped me into the scientist and person that I am today and I am very appreciative to be part of such a fantastic group of "Buddies". I would like to thank my past and present committee members Edward Marcotte, Marvin Whiteley, Kallie Willets, Claus Wilke, and Barrie Kitto for the depth of your insight and molding my project into what it is today. I am deeply grateful to have had the opportunity to work with Akash Patel. His calm, yet dogged work effort is unlike anyone that I have ever met and have learned so much from him. I would like to thank the "punctate" researchers, Ram Swamy, Edward Marcotte, Jeremy O'Connell, Mark Tsechansky, Alice Zhao, Akash Patel, Brandon Plost, and Jennifer Mirrielees for your insight and expertise, which significantly enriched my research. I would like to thank Adam (T) Meyer, Eric Davidson, Tony Hwang, and Steven Chirieleison for your thoughtful discussions, patience, and, possibly above all else, humor. Thank you Alex Miklos and Randy Hughes for your expertise and guidance in protein design and expression. Thank you Adam Meyer, Michelle Byrom, Amrita Singh, Angel Syrett, and Christien Kluwe for reviewing my dissertation. Thank you Xi Chen for your brilliance and guidance. Michelle Byrom, thank you for teaching me that the smallest things can make the biggest difference in a day (green). Thank you Paulina Dlugosz for your considerate words of wisdom to keep me going and to Brad Hall for showing me the ropes and making it all look so easy. And, Angel Syrett, thank you for being you and a little ray of happiness. I would also like to thank past and present members of the administrative staff, including

Sarah Caton, Jorge Villafana, Stephanie Huntzis Achebe, Alisha Hall, Ashley Rasmussen, and Dorothy Podgornoff.

Without my family, none of this would have been possible. I would like to thank my Mom, Dad, brother, and sister for your continued support and patience. My sister has provided the encouragement worthy of a team of cheerleaders and came through for us in the end to keep the household up and running. I would like to thank my son, Sam. Thank you for reminding me to push towards my dreams, but that I still have to change a diaper or two the end of the day. Most importantly, I'd like to thank Drew, my husband. You are an inspiration to me, picked me up when I was down, "fixity" me right when I was wrong, and the glue that keeps our little family together. You are a remarkable person and I'm most grateful to have you in my life.

Evaluation of Protein Aggregation and Organismal Fitness

Publication No._____

Gwendolyn Motz Stovall, Ph.D.

The University of Texas at Austin, 2011

Supervisor: Andrew D. Ellington

In quiescent yeast, the widespread reorganization of cytosolic proteins into punctate has been observed (Narayanaswamy et al. 2009). We seek to better understand and describe this reorganization, which we hypothesize to be a protein aggregation phenomenon. To test this hypothesis, we examined mutant proteins (Ade4p protein variants) in yeast with predicted non-native aggregation propensities and measured their punctate formation kinetics. Monitoring punctate formation kinetics involved the validation of an automated quantification technique using an Amnis ImageStream imaging flow cytometer. The automated punctate counts were strongly correlated with the manual punctate counts, with usual R^2 values of 0.99 or better, but evaluated 50-fold more cells per run. Fitness evaluations of the mutant yeast in the form of growth curves and batch competition experiments revealed the slowed growth of the Ade4-1286 strain and the functional inequality to the wild type strain of the Ade4-mtoin2034, Ade4-mtoin2105, and Ade4-2800 strains in competition experiments, especially when the mutants were forced to generate their own adenine. Subsequent structural analysis of the mutant proteins revealed destabilizing mutations for 4 of the 6 mutant proteins with 2 of

the mutations classified as significantly destabilizing ($\Delta\Delta G$ >2 kcal/mol). We concluded that the reduction in protein fitness was likely due to the destabilizing effects of the mutations. Evaluation of the punctate formation kinetics revealed little difference between strains in the rate of punctate formation. Further examination revealed the wild type Ade4p and all of the mutants (with the exception of the Ade4-1286 mutant) were predicted to have similar aggregation propensities according to a secondary aggregation predicting algorithm (Zyggregator, Pawar et al. 2005). Additionally, solvent accessibility calculations estimate ~3-19% of the side chain surface area to be solvent accessible, which indicates proximity of mutations to the protein surface. However, mutating buried amino acids likely would have generated a greater disturbance (Matthews 1993, Tokuriki et al. 2007). We concluded that the mutations, although destabilizing, altered the aggregation propensity very little. Deletion of chaperone proteins (Hsp82p, Hsc82p, and Ssa1p) revealed no difference in the Ade4-GFP punctate formation kinetics, although a slight kinetic difference was detected in the chaperone (Hsp82p) knockout, Gln1-GFP strain and the wild type strain. While further workup is necessary in the chaperone knockout, Gln1-GFP work, the initial results are promising and suggest the involvement of protein folding machinery in punctate formation.

Table of Contents

List of Tables

List of Figures

Chapter 1: Introduction

Living cells are in flux as requirements fluctuate with the cell cycle. As they transition from proliferation to stationary phase (quiescence, Gray et al. 2004), macromolecular reorganization has been observed. This restructuring is visible in the assembly or disassembly of macromolecular complexes, as in the case of actin bodies (Sagot et al. 2006). It can involve molecular commerce between two of more bodies, such as in the case of mRNA exchange between polysomes and P-bodies (Brengues et al. 2005). Reorganization within the cell may be associated with mobility, such as the active actin cytoskeleton in proliferating cells (Pruyne et al. 2004), or a static phase, such as in the case of stationary phase stalled RNA polymerase II upstream of genes and prepped for reentry into growth phase (Radonjic et al. 2005). Recently, a large scale reorganization of proteins upon nutrient depletion has been reported. This phenomenon involves the assembly of cytoplasmic proteins into punctate foci in *Saccharomyces cerevisiae* (Narayanaswamy et al. 2009).

Normal cellular processes rely on the ordered molecular proximity of proteins, nucleic acids, and metabolites, and the avoidance of aggregation. Aggregates, in the form of misfolded proteins or amyloid filaments, are potentially toxic and metabolically costly. Protein aggregation has been implicated in a number of neurodegenerative diseases, including Alzheimer's disease, amyotrophic lateral sclerosis (ALS), Parkinson's disease, Huntington's disease, and prion diseases (reviewed in Ross and Poirier 2004).

A Model Organism: *Saccharomyces cerevisiae*

Saccharomyces cerevisiae has a long history of cultivation for use in wine and beer making, as a leavening agent in bread baking, and as a model eukaryotic organism in

the laboratory. This unicellular organism offers itself as a model eukaryotic organism for a number of reasons: It is nonpathogenic. Many of its cellular processes are conserved across species, including humans. Yeast grow with great speed and ease, and can be maintained economically. *S. cerevisiae* was the first eukaryotic genome sequenced in its entirety (reviewed in Dujon 1996). The annotated yeast sequence information is readily available. Additionally, there is a large community of yeast researchers, who offer access to a wide range of data. Most notable is the *Saccharomyces* Genome Database (http://www.yeastgenome.org), which provides a comprehensive view of the annotated genome, function based datasets, transcriptome, chromatin landscape, as well as regulatory sequence elements.

Furthermore, the *S. cerevisiae* haploid and diploid cell cycle permits genetic manipulation. For instance, mutant strains can be generated and isolated by mating haploid yeast and sporulating the diploid strain. Using diploid cells permits the propagation of recessive mutations for analysis. Additionally, homologous recombination occurs with a high efficiency and may be exploited. Simple introduction of exogenous DNA with flanking homologous sequences is all that is required for recombination into the yeast genome. This in addition to the high transformation efficiency, which readily permits yeast genetic manipulation, such as insertion or deletion of genes (reviewed in Sugiyama et al. 2009).

The impact of such genetic manipulation is perhaps best exemplified in the variety of yeast libraries. In genomic libraries, the open reading frames (ORF) on the chromosome may be tagged with an affinity or fluorescent tag (i.e. 1 tag per ORF per yeast strain) (Huh et al. 2003, Kumar et al. 2002). Alternatively, genomic knockout collections replace ORFs with a selectable marker (such as Geneticin resistance using the *KanMX* module) (Winzeler et al. 1999). Plasmid encoded ORF libraries are also

available, many offering promoter driven over-expression (Gelperin et al. 2005, Ma et al. 2008, Zhu et al. 2001, Martzen et al. 1999). Table 1-1 summarizes some of the available yeast libraries, including libraries used in this work.

Table 1-1 Yeast libraries/collections.

Library	Genomic or Plasmid Expression?	*Available as S. cerevisiae, E. coli*, or plasmid?	Number of Strains or Genes	Location of Tag	Tag (affinity or fluorescent)	Vendor	Website	Reference
Yeast ORF Collection	Plasmid, over-expressed under GAL1 promoter	both	5,500 genes	C-terminal	Protein A Domain, 6xHis Domains, and Hemagglutinin (HA) Tag (affinity tag)	Open Biosystems	https://www.openbiosystems.com/GeneExpression/Yeast/ORF/	Gelperin et al. 2005
Yeast GFP Clone Collection	Genomic	*S. cerevisiae*	4,159 strains (~75% of yeast proteome)	C-terminal	GFP Tag (fluorescent tag)	Invitrogen	http://clones.invitrogen.com/cloneinfo.php?clone=yeastgfp	Huh et al. 2003
Yeast YFP Fusion Collection	Gateway Donor Vector	plasmid	120 kinase genes	N-terminal	YFP Tag (fluorescent tag)	Open Biosystems	https://www.openbiosystems.com/GeneExpression/YeastYeastYFPFusionCollection/	Ma et al. 2008
Yeast HA-Tagged Strains	Genomic	*S. cerevisiae*	>2,400 strains	Within Coding Region	3 Hemagglutinin (HA) Tag (affinity tag)	Open Biosystems	http://www.openbiosystems.com/GeneExpression/Yeast/HA-Tagged/	Kumar et al. 2002
Yeast GST-Tagged Collection	Plasmid, over-expressed under GAL1/10 promoter	*S. cerevisiae*	>5,000 strains	N-terminal	Glutathione S-Transferase (GST) Tag (affinity tag)	Open Biosystems	http://www.openbiosystems.com/GeneExpression/Yeast/GST/	Zhu et al. 2001
Yeast GST-Fusion Collection	Plasmid, inducible CUP1 promoter	*S. cerevisiae*	6,144 strains (~85-90% of all ORFs)	N-terminal	GST Tag (affinity tag)	Not Commercially Available	N/A	Martzen et al. 1999
Yeast Knock-Out Collection	Genomic	*S. cerevisiae*	4,828 MATα haploid clones, 4,848 MATa haploid clones, 5,996 heterozygous diploid clones, and 4,741 homozygous diploid clones	N/A	N/A	Invitrogen and Open Biosystems	http://clones.invitrogen.com/cloneinfo.php?clone=yeast https://www.openbiosystems.com/GeneExpression/YeastYKO/	Winzeler et al. 1999
Yeast Tet-Promoter Hughes Collection	Genomic, under Tet down-titratable promoter	*S. cerevisiae*	800 genes	N/A	N/A	Open Biosystems	http://openbiosystems.com/GeneExpression/Yeast/Tet-Promoters/	Mnaimneh et al. 2004
Yeast DAmP Library (decreased expression)	Genomic, antibiotic resistance in the 3' UTR destabilizes mRNA and reduces expression	*S. cerevisiae*	>950 diploid strains and >800 haploid strains	N/A	N/A	Open Biosystems	https://www.openbiosystems.com/GeneExpression/Yeast/DAmP%20Yeast%20Library/	Breslow et al. 2008

Although the study of yeast might have begun as a humble subject of study for beer brewers, *S. cerevisiae* has become one of the most studied eukaryotic organisms, and has yielded a myriad of information regarding more complex organisms, including *Homo sapiens*. The yeast model will continue to yield useful results, in both its ability to ferment sugar into ethanol and for its use as a simplified eukaryote in the laboratory.

QUIESCENCE

Yeast cells, like all living cells, have a growth phase and a "resting" phase or quiescent phase. A majority of eukaryotic cells spend most of their life in a quiescent state (Lewis and Gattie 1991), making quiescence a valuable subject of study

In conceivably the simplest definition, quiescence is a reversible resting state of cells. This reversible non-proliferative phase is normal to all cells and in yeast is triggered by nutrient depletion.

Perhaps quiescence is best defined by what it "does not" have or "lacks" (reviewed in Gray et al. 2004). Proliferation ceases and cells do not accumulate mass or volume (Pringle and Hartwell 1981). Transcription is reduced to 1/3rd – 1/5th of log phase transcription (Choder 1991). The expression of a large subset of genes is repressed (Werner-Washburne et al. 1996). The degradation of mRNA is inhibited (Jona et al. 2000). Protein synthesis is reduced to ~0.3% that of log phase cells (Fuge et al. 1994) and proteasome proteolytic activity is lowered (Bajorek et al. 2003). Autophagy is induced (Noda and Ohsumi 1998). The cell wall thickens, making cells more resistant to zymolase digestion (de Nobel et al. 2000). Cells are more thermotolerant and osmotolerant (Plesset et al. 1987).

This operational definition of quiescence includes stationary phase cultures. Stationary phase cultures, or cultures grown to saturation, contain a significant number of quiescent cells, though the exact population ratio of quiescent cells is unknown (reviewed in Gray et al. 2004). Additionally, quiescent cells have been identified in cultures that have been rapidly starved, depleted of nitrogen, sulfur, or phosphate or upon transfer to water (Thevelein et al. 2000).

REORGANIZATION OF MACROMOLECULAR COMPLEXES IN STATIONARY PHASE

Yeast readily and reversibly transition from a nutrient-rich environment ripe for cellular proliferation to quiescence in a nutritionally starved environment. Nutritionally starved cells of the stationary phase demonstrate numerous changes, from decreased transcription to decreased translation. It is therefore not surprising to observe widespread cellular reorganization.

Such macromolecular reorganization has only been observed recently, specifically, in the formations of actin bodies. In stationary phase, the actin cytoskeleton of cables and patches is rearranged into actin bodies. In contrast to the polarized, mobile, and dynamic actin network of cables and patches, actin bodies are depolarized, immobile, and actin turnover has not been observed. Actin bodies are comprised of F-actin, the actin binding proteins fimbrin, and capping protein. These reversible actin bodies dissolve into actin cables and patches upon adding fresh media, even in the absence of protein synthesis (Sagot et al. 2006).

Another example of macromolecular rearrangement is the relocation of proteasome subunits described by Laporte et al. In quiescence, proteasome subunits relocate from the nucleus into cytoplasmic structures. Reorganization occurs without

protein synthesis, which implies their use as a storage depot according to the authors. Laporte et al. named the structures proteasome storage granules (PSGs). PSGs were observed in *S. cerevisiae* and the evolutionary distant yeast *Schizosaccharomyces pombe* (Laporte et al. 2008).

Quiescence reorganization was observed using chromatin immunoprecipitation experiments and RNA polymerase II. In quiescence, RNA polymerase II remains stalled immediately upstream of genes that are induced upon return to cell proliferation (Radonjic M, et al. 2005).

Another example of cellular reorganization is in the exchange of mRNA between polysomes and processing bodies (P-bodies). Large P-bodies in stationary phase contain mRNAs that reenter translation when cell proliferation returns (Brengues et al. 2005).

An et al. reported the reversible colocalization of six enzymes involved in purine biosynthesis upon purine depletion. The so called "purinosomes" in HeLa cells were dissolved upon the addition of purine-rich media and again induced with purine depleted media. The clustering of enzymes involved in the same metabolic pathway implied a functional relevance, perhaps substrate channeling across catalytic sites (An et al. 2008). Much of this work, though, has not been reproduced and recent work indicates the biosynthetic enzyme clustering may be independent of purine (personal communication, A. Zhao, University of Texas at Austin)

PUNCTATE FOCI IN NUTRIENT STARVED YEAST (NARAYANASWAMY ET AL. 2009)

With the observation of multiple system-specific examples of cellular reorganization, an exploratory systematic survey of cytosolic proteins was undertaken in search of widespread rearrangements. Systematic examination of *S. cerevisiae* cytosolic

proteins revealed the concentrated localization into punctate foci in stationary phase cells. The proteins, diffuse in log phase, form reversible punctate foci that return to their diffuse state upon the addition of fresh media. Further investigation revealed that protein puncta (*singular* punctate, *plural* puncta), of unknown conformation, may be induced through stationary phase or nutrient dropout media (Narayanaswamy et al. 2009).

Foundation Experiments

The phenomenon was first observed using the yeast GFP-tagged library (Huh et al. 2003). ~800 strains expressing GFP-tagged cytosolic proteins were grown to stationary phase (5 day growth). Cells were fixed and printed on polylysine coated slides or "chips". Fluorescent images were obtained using automated microscopy and GFP localization was evaluated by visual inspection. More than 200 cytosolic proteins formed puncta (Narayanaswamy et al. 2009).

The results of the cell chip experiment were manually confirmed. Of the 256 GFP-tagged yeast strains tested, 180 of these strains were manually confirmed to contain punctate foci (Narayanaswamy et al. 2009).

Mass spectrometry results independently validated the previous results. Puncta containing cells could be "recovered" or diffused of puncta by the addition of fresh media. Recovered cell lysate was centrifuged, fractionating the insoluble pellet from the supernatant. The fractionated recovered cell lysate was compared to centrifugation fractionated stationary phase lysate. Puncta were detected by visual inspection in the pellet fraction of stationary phase yeast lysate. Both the pellet and the supernatant fractions from the stationary phase yeast lysate were analyzed by LC-MS/MS and compared to recovered fractions. The mass spectrometry results indicated an enrichment

of the stationary phase pellet proteins in the recovered supernatant proteins. Additionally, the mass spectrometry results confirmed 33 punctate forming proteins, which were identified in the GFP-tag localization screen, and identified many more punctate forming candidate proteins (Narayanaswamy et al. 2009).

Punctate Proteins: Canonical Examples

A significant number of punctate forming proteins are involved in stress response or intermediary metabolism (i.e. involved in generation or storage of energy). Among the most robust punctate forming proteins are Ade4, Gln1, and Ura7 (Narayanaswamy et al. 2009).

Ade4p is phosphoribosylpyrophosphate amidotransferase. This enzyme catalyzes the first step of *de novo* purine biosynthesis, generating phosphoribosylamine from phosphoribosylpyrophosphate (Woods et al. 1983, Smolina and Bekker 1982). *ADE4* is not essential in yeast, but the deletion of *ADE4* results in slow growth and adenine auxotrophy (Li et al. 2009, Roberts et al. 2003). Expression of *ADE4* is repressed by purines and derepressed by the absence of purines (Som et al. 2005, Ludin et al. 1994).

The nutritional requirements of yeast Ade4p puncta formation and dissolution have been evaluated. GFP and YFP tagged Ade4p puncta have been detected in stationary phase cells (Figure 1-1), as well as Ade4-TAP puncta detected using immunofluorescence. In adenine dropout media, Ade4-GFP puncta are induced in early log phase cells within two hours, reaching a maximum puncta penetrance (i.e. percentage of cells with puncta) of ~50-60%. Such adenine dropout induced Ade4-GFP puncta may be dissolved by the addition of fresh media, adenine, or the related nucleotide hypoxanthine, although guanosine and histidine have no effect. An inhibitor of protein

translation, cycloheximide, inhibited Ade4-GFP puncta formation, although it did not affect punctate dissolution. Additionally, Ade4-GFP puncta were not affected by a serine protease inhibitor, PSMF, which inhibits vacuole proteases (Narayanaswamy et al. 2009).

Gln1p is glutamine synthetase and plays an important role in nitrogen metabolism. Gln1p requires ATP to catalyze the condensation reaction of glutamate and ammonia to form glutamine. In *S. cerevisiae*, *GLN1* is essential and the encoded protein is a homo-oligmer of 10 monomers, each 43,000 Da (Mitchell and Magasanik 1983, Unno et al. 2006).

The nutritional requirements of yeast Gln1p puncta formation and dissolution have been evaluated. A number of Gln1p punctate induction methods have been established: stationary phase, water, and glucose dropout media. GFP and YFP tagged Gln1p puncta have been detected in stationary phase cells, and Gln1-TAP puncta have been detected using immunofluorescence. In glucose dropout media, Gln1-GFP puncta are induced in log phase cells within two hours, reaching a maximum puncta penetrance of ~90%. Such glucose dropout induced Gln1-GFP puncta may be dissolved by the addition of fresh media or glucose. An inhibitor of protein translation, cycloheximide, has no effect on Gln1-GFP puncta formation, although it inhibited punctate dissolution with glucose addition. Additionally, Gln1-GFP puncta (like Ade4-GFP puncta) were not affected by a serine protease inhibitor, PSMF (Narayanaswamy et al. 2009).

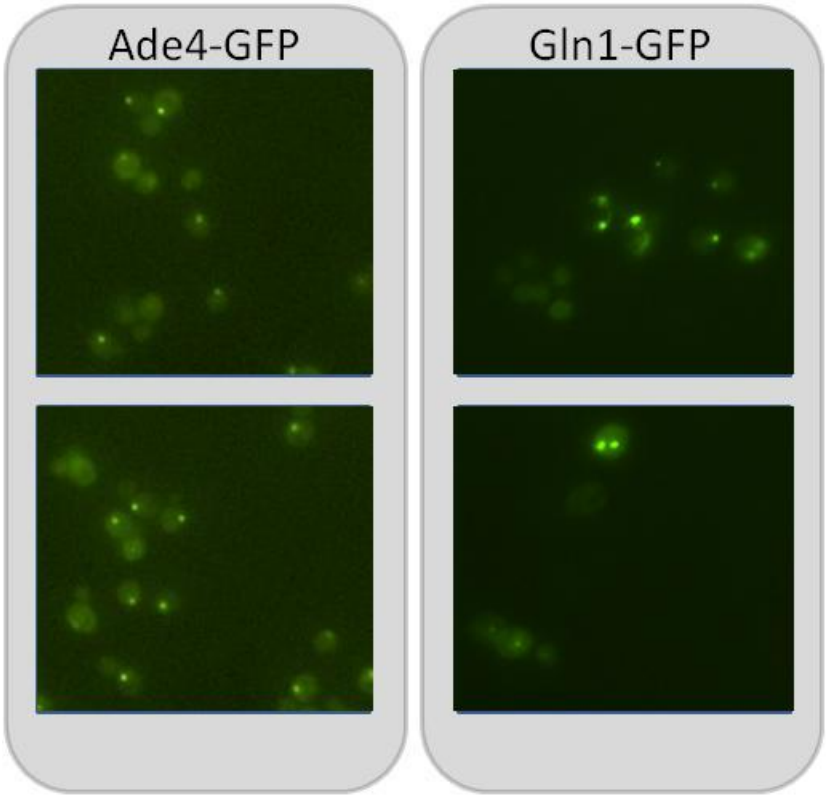

FIGURE 1-1 YEAST ADE4-GFP AND GLN1-GFP. These are fluorescent images of yeast cells with Ade4-GFP puncta and Gln1-GFP puncta. Yeast Ade4-GFP puncta are induced through stationary phase or in adenine dropout media. Yeast Gln1-GFP puncta are induced through stationary phase, water, or glucose dropout media.

Ura7p and Ura8p are CTP synthetase isozymes and share ~78% amino acid sequence identity (Ozier-Kalogeropoulos et al. 1994). The enzymes catalyze the ATP-dependent conversion of UTP to CTP, the final step in the CTP biosynthetic pathway (Ozier-Kalogeropoulos et al. 1994, Ozier-Kalogeropoulos et al. 1991). In *S. cerevisiae*, Ura7p and Ura8p are expressed 5-fold more in log phase growth than stationary phase growth. The *URA7* mRNA is 2-fold more abundant than *URA8* mRNA (Nadkarni et al. 1995).

Ura7-GFP puncta form in stationary phase and dissolve with the addition of fresh media (Narayanaswamy et al. 2009). Ura7-GFP stationary phase cells reach a maximum puncta penetrance of roughly 40% (personal communication, J.D. O'Connell, University of Texas at Austin). Ura7p cytoplasmic structures are not unique to *S. cerevisiae*. Three independent studies identified CTP synthetase foci and filamentous structures in bacteria, yeast, fruit flies, and mammalian cells (reviewed in Liu 2010).

PROTEIN AGGREGATION

Normal cellular processes rely on the ordered molecular proximity of proteins, nucleic acids, and metabolites, and the avoidance of protein aggregation. In its simplest form, protein aggregation is the self-association of misfolded proteins, producing extracellular and/or intracellular aggregates. These insoluble, precipitating aggregates are classified as amorphous aggregates or amyloid aggregates.

Amorphous aggregate formation is driven by amino acid hydrophobicity, charge (preferably neutral), as well as secondary structure propensity and may be enriched in cross β-structure (Chiti et al. 2002, Chiti et al. 2002, Chiti et al. 2003). The β-extended structure is preferred in amorphous aggregates, leaving maximum space between amino acid side chains. Additionally, it is likely that covalent modifications such as phosphorylation and oxidative modifications are involved in aggregate formation (Ross and Poirier 2004). Almost all proteins form amorphous aggregates when concentrations are high enough (Dobson 2004).

However, fewer proteins form highly ordered amyloid aggregates or fibrils (Dobson 2003). Amyloid fibrils are organized aggregates in ~6-10 nm diameter fibrils (Shirahama and Cohen 1967, Malinchik et al. 1998). Amyloid fibrils typically have cross

β-structure, where the β-strands of the proteins stack perpendicular to the fibril axis (Sunde et al. 1997). However, β-sheet structure is not essential for amyloid fibril formation, as is the case with the α-helical structure of the yeast Ure2 prion protein (Bousset et al. 2002).

Multiple aggregate forms might imply multiple mechanisms of formation. However, a misfolding event appears to be the primary instigator. A nucleation or "seeded polymerization" event around the initiating protein/peptide generates the aggregate (Lansbury et al. 1997). The delayed onset of aggregation pathology suggests unfavorable kinetics of such misfolding events and aggregation fibril formation (Jarrett and Lansbury 1993, Perutz and Windle 2001).

MISFOLDED PROTEINS, AGGREGATION, AND MUTATIONS IMPACT FITNESS

When errors occur, such as translational or misfolding errors, organismal fitness can be affected. It is not surprising that proteins, functioning as enzymes, structural units, or signaling molecules, significantly contribute to fitness. With regard to essential proteins and organismal fitness, it has been found that essential proteins in yeast, fly, and worm are predicted to have a lower aggregation propensity than nonessential proteins (Chen and Dokholyan 2008).

The fitness cost of misfolded proteins comes in many forms (reviewed by Drummond and Wilke 2009). One such cost is the "gain of toxic function," which occurs when an alternative harmful function manifests or the protein misfolds to generate a toxic product. Such toxic misfolded proteins are implicated in many neurodegenerative diseases, which are discussed further in the following section. Misfolded proteins may initiate other misfolding events, depleting natively folded protein from the protein

population. Additionally, there are numerous costs in the expression as well as the energetic costs (i.e. ATP) of chaperone proteins and/or degradation proteins, which are necessary to repair and/or "clean-up" the flawed protein. When ribosomes are engaged in the production of flawed protein, they are occupied and therefore unavailable for protein synthesis (Drummond and Wilke 2009).

There are numerous examples of fitness reduction due to protein mutations introduced during translation (reviewed by Drummond and Wilke 2009). Perhaps one of the most obvious examples is that antibiotics (such as streptomycin and kanamycin) target ribosomes leading to mistranslation events, which result in the death of bacteria. Additionally, the introduction of protein mutations by a mutant aminoacyl-tRNA synthetase with a defective editing domain ambiguously inserting amino acids into proteins led to retarded growth rates (Bacher et al. 2005) and altered cell morphology (Nangle et al. 2006). Similarly, the loss of translational fidelity in a defective editing domain of an aminoacyl-tRNA-synthetase resulted in the accumulation of misfolded proteins at neuronal cells and cell death in mice (Lee et al. 2006).

The Tawfik laboratory found error-prone transcription on an essential protein (β-lactamase) resulted in significant fitness loss. The experiments hinged on *E. coli* with an error-prone mutant T7 RNA polymerase and the TEM-1 β-lactamase gene under the control of the T7 RNA polymerase promoter. β-lactamase confers ampicillin resistance to *E. coli*. The error-prone RNA polymerase averaged 1.3 mutations per TEM-1 transcript, as opposed to the 0.05 mutations with the wild type RNA polymerase. Of the cells containing the error-prone RNA polymerase, less than 40% of the colonies containing survived at 1500 ug/mL ampicillin compared to ~100% of the colonies with the wild type polymerase. Much of this reduction in colony survival was due to the inefficient transcription by the mutant polymerase and subsequently lower concentrations

of the β-lactamase, while, to a lesser extent, the deleterious mRNA mutations compromised the β-lactamase activity. Clones that exhibited compromised β-lactamase activity (i.e. low or no ampicillin resistance) were sequenced. 25% contained nonsense mutations (deletions, insertions, or stop codons); 8.3% contained active site mutations, and 66.7% contained protein destabilizing mutations (Goldsmith and Tawfik 2009).

PROTEIN AGGREGATION: DISEASE IMPLICATIONS

Protein aggregates present as potentially toxic and metabolically costly complexes. Protein aggregation has been implicated in a number of neurodegenerative diseases, including Alzheimer's disease, amyotrophic lateral sclerosis (ALS), Parkinson's disease, Huntington's disease, and prion diseases (reviewed in Ross and Poirier 2004) (Figure 1-2). Additionally, the metabolic expense in the generation of the aggregating proteins and the removal/sequestration of functional protein species from the general population remains as an uncalculated cost.

TABLE 1-2 AGGREGATION IMPLICATED DISEASES. Table adapted from Haataja et al. (2008) and Selkoe (2003).

Disease	Protein	Diseased Cells	Aggregate Location
Alzheimer's disease	Amyloid β-protein	Cortical neurons	Extracellular plaques
	Tau		Tangles in neuronal cytoplasm
Amyotrophic lateral sclerosis	Superoxide dismutase	Motor neurons	Neuronal cytoplasm
Creutzfeldt–Jakob disease (mad cow disease)	Prion protein (PrPsc)	Cortical neurons	Extracellular plaques; Oligomers inside and outside neurons
Diabetes mellitus type 2	Islet amyloid polypeptide/ Amylin (IAPP)	β-cells	Extracellular amyloid; Oligomers inside and outside cells
Frontotemporal dementia with parkinsonism	Tau		Tangles in neuronal cytoplasm
Parkinson's disease (dementia with Lewy bodies)	α-Synuclein	Dopaminergic neurons	Neuronal cytoplasm
Polyglutamine associated diseases (Huntington's disease, spinocerebellar ataxias, etc.)	Polyglutamine	Pyramidal neurons	Neuronal nuclei and cytoplasm

Amyloid aggregates appear to be the precursor to amyloidosis, a symptom of a disease state. It is almost widely accepted that the toxicity lies in the pre-fibrillar aggregates and not in the mature fibrils (Bucciantini et al. 2002, Bucciantini et al. 2004). Cytotoxic pre-fibrillar aggregates of different proteins are recognized by the same antibody, suggesting structural and mechanistic similarities (Kayed et al. 2003, O'Nuallain and Wetzel 2002). The exact mechanism of toxicity is not known, but evidence suggests involvement of the aggregate with the cellular membrane (Anderluh et

al. 2005). Stefani and Dobson propose that the pre-fibrillar aggregates form doughnut like structures that interact with the cellular membrane forming damaging membrane pores (Stefani and Dobson 2003). Additionally, it has been proposed that the extracellular amyloid fibrils and amyloid protofibrils (i.e. smaller pre-cursor or building block to the larger amyloid fibril) interfere with extracellular receptors or block channels in discriminately (Selkoe 2003).

The implications of aggregation on neurodegenerative pathologies are numerous and, to a lesser extent, the problems with aggregation in proteins expressed and purified in laboratory or commercial setting should be addressed. Specifically, insoluble bodies present numerous problems in large-scale protein production.

TRANSIENT PROTEIN AGGREGATES

The formidably toxic aggregates may have a "weakness." There are examples of aggregation reversion, where refolding occurred. Specifically, maltose binding protein aggregates formed after unfolding in guanidine hydrochloride and dilution in refolding buffer (10 mM HEPES buffer, pH 7.3, 150 mM NaCl). Most of the aggregates spontaneously refolded within an hour (Ganesh et al. 2001). Additionally, fragments of mutant phosphoglycerate kinase from yeast were found to form transient multimeric species during refolding (Pecorari et al. 1996). Silow and Oliveberg showed that the spliceosomal protein U1A (F56W) forms short-lived transient aggregates upon refolding (Silow and Oliveberg 1997). Similarly, truncated chymotrypsin inhibitor 2 also formed short-lived protein aggregates (Silow et al. 1999).

DETECTION OF PROTEIN AGGREGATES

The method employed to detect aggregates depends on their location within or outside the cell. Specifically, analytical spectroscopy may be employed to detect purified protein aggregates, but *in vivo* intercellular aggregates require histological staining.

Purified aggregate proteins are evaluated by spectrometry and the examination of a "shift" from the native possibly monomeric protein to the aggregate or multimeric form. This may be accomplished through dynamic light scattering experiments, in which the light scattering response is proportional to the molecular weight of the multimeric species and the concentration. Alternatively, circular dichroism (CD) spectroscopy may be used to detect protein aggregates (von Bergen et al. 2000). CD measures the difference between absorption of right and left circularly polarized light, which in-turn provides the proportion of protein secondary structures (i.e. α-helices, β-sheets, etc.) present (Greenfiled 2006). The aggregate peak shifts from the native protein peak. Similarly, NMR spectroscopy may be employed to detect protein aggregates. As protein aggregates are concentration dependent, a concentration dependence of the CD and/or NMR results implies protein aggregation (Fernandez-Escamilla et al. 2004). FTIR spectrographs may be employed to detect multimeric or aggregate proteins (von Bergen et al. 2000).

Electrophoresis and chromatography (Saxena 1988) may be employed to detect aggregates or multimeric proteins. For instance, separation of species on nondenaturing acrylamide gels or separation of crosslinked species on denaturing acrylamide gel resolves monomeric from multimeric species (Kwon et al. 1995, van den Oetelaar et al. 1989).

Traditionally, amyloid fibrils are detected using electron microscopy (Shirahama and Cohen 1967), histological stains, and X-ray diffraction. Thioflavin T is used as a

histological stain to stain amyloid plaques and used *in vitro* to stain protein aggregates and amyloid fibrils in solution (LiVine and Walker 2010, LiVine 1993). Upon binding to β-sheets (and not the monomeric protein), Thioflavin T undergoes a blue shift in the emission spectrum (LiVine 1993). Similarly, Congo Red is a histological stain of amyloid fibrils that undergoes a green bifringence (i.e. refraction into two rays) when exposed to polarized light. Finally, X-ray diffraction is one of the original methods of amyloid detection, as the term "cross" β-structure/strands was derived from the X-ray diffraction patterns (Sunde et al. 1997). Specifically, cross β-structure refers to the two sets of diffraction patterns, one longitudinal and one transverse, forming the cross diffraction pattern (Pauling and Corey 1951).

REFERENCES

An S, Kumar R, Sheets ED, Benkovic SJ: Reversible compartmentalization of de novo purine biosynthetic complexes in living cells. Science 2008, 320:103-106.

Anderluh G, Gutierrez-Aguirre I, Rabzelj S, Ceru S, Kopitar-Jerala N, Macek P, Turk V, Zerovnik E: Interaction of human stefin B in the prefibrillar oligomeric form with membranes. Correlation with cellular toxicity. FEBS J 2005, 272:3042-3051.

Bajorek M, Finley D, Glickman MH: Proteasome disassembly and downregulation is correlated with viability during stationary phase. Curr Biol 2003, 13:1140-1144.

Bacher JM, de Crecy-Lagard V, Schimmel PR: Inhibited cell growth and protein functional changes from an editing-defective tRNA synthetase. Proc Natl Acad Sci U S A 2005, 102:1697-1701.

Bousset L, Thomson NH, Radford SE, Melki R: The yeast prion Ure2p retains its native alpha-helical conformation upon assembly into protein fibrils in vitro. EMBO J 2002, 21:2903-2911.

Brengues M, Teixeira D, Parker R: Movement of eukaryotic mRNAs between polysomes and cytoplasmic processing bodies. Science 2005, 310:486-489.

Breslow DK, Cameron DM, Collins SR, Schuldiner M, Stewart-Ornstein J, Newman HW, Braun S, Madhani HD, Krogan NJ, Weissman JS: A comprehensive strategy enabling high-resolution functional analysis of the yeast genome. Nat Methods 2008, 5:711-718.

Bucciantini M, Calloni G, Chiti F, Formigli L, Nosi D, Dobson CM, Stefani M: Prefibrillar amyloid protein aggregates share common features of cytotoxicity. J Biol Chem 2004, 279:31374-31382.

Bucciantini M, Giannoni E, Chiti F, Baroni F, Formigli L, Zurdo J, Taddei N, Ramponi G, Dobson CM, Stefani M: Inherent toxicity of aggregates implies a common mechanism for protein misfolding diseases. Nature 2002, 416:507-511.

Chiti F, Calamai M, Taddei N, Stefani M, Ramponi G, Dobson CM: Studies of the aggregation of mutant proteins in vitro provide insights into the genetics of amyloid diseases. Proc Natl Acad Sci U S A 2002, 99 Suppl 4:16419-16426.

Chiti F, Stefani M, Taddei N, Ramponi G, Dobson CM: Rationalization of the effects of mutations on peptide and protein aggregation rates. Nature 2003, 424:805-808.

Chiti F, Taddei N, Baroni F, Capanni C, Stefani M, Ramponi G, Dobson CM: Kinetic partitioning of protein folding and aggregation. Nat Struct Biol 2002, 9:137-143.

Choder M: A general topoisomerase I-dependent transcriptional repression in the stationary phase in yeast. Genes Dev 1991, 5:2315-2326.

de Nobel H, Ruiz C, Martin H, Morris W, Brul S, Molina M, Klis FM: Cell wall perturbation in yeast results in dual phosphorylation of the Slt2/Mpk1 MAP kinase and in an Slt2-mediated increase in FKS2-lacZ expression, glucanase resistance and thermotolerance. Microbiology 2000, 146 (Pt 9):2121-2132.

Dobson CM: Protein folding and misfolding. Nature 2003, 426:884-890.

Dobson CM: Principles of protein folding, misfolding and aggregation. Semin Cell Dev Biol 2004, 15:3-16.

Drummond DA, Wilke CO: The evolutionary consequences of erroneous protein synthesis. Nat Rev Genet 2009, 10:715-724.

Dujon B: The yeast genome project: what did we learn? Trends Genet 1996, 12:263-270.

Fernandez-Escamilla AM, Rousseau F, Schymkowitz J, Serrano L: Prediction of sequence-dependent and mutational effects on the aggregation of peptides and proteins. Nat Biotechnol 2004, 22:1302-1306.

Fuge EK, Braun EL, Werner-Washburne M: Protein synthesis in long-term stationary-phase cultures of Saccharomyces cerevisiae. J Bacteriol 1994, 176:5802-5813.

Ganesh C, Zaidi FN, Udgaonkar JB, Varadarajan R: Reversible formation of on-pathway macroscopic aggregates during the folding of maltose binding protein. Protein Sci 2001, 10:1635-1644.

Gelperin DM, White MA, Wilkinson ML, Kon Y, Kung LA, Wise KJ, Lopez-Hoyo N, Jiang L, Piccirillo S, Yu H, et al.: Biochemical and genetic analysis of the yeast proteome with a movable ORF collection. Genes Dev 2005, 19:2816-2826.

Goldsmith M, Tawfik DS: Potential role of phenotypic mutations in the evolution of protein expression and stability. Proc Natl Acad Sci U S A 2009, 106:6197-6202.

Gray JV, Petsko GA, Johnston GC, Ringe D, Singer RA, Werner-Washburne M: "Sleeping beauty": quiescence in Saccharomyces cerevisiae. Microbiol Mol Biol Rev 2004, 68:187-206.

Greenfield NJ: Using circular dichroism spectra to estimate protein secondary structure. Nat Protoc 2006, 1:2876-2890.

Haataja L, Gurlo T, Huang CJ, Butler PC: Islet amyloid in type 2 diabetes, and the toxic oligomer hypothesis. Endocr Rev 2008, 29:303-316.

Huh WK, Falvo JV, Gerke LC, Carroll AS, Howson RW, Weissman JS, O'Shea EK: Global analysis of protein localization in budding yeast. Nature 2003, 425:686-691.

Jarrett JT, Lansbury PT, Jr.: Seeding "one-dimensional crystallization" of amyloid: a pathogenic mechanism in Alzheimer's disease and scrapie? Cell 1993, 73:1055-1058.

Jona G, Choder M, Gileadi O: Glucose starvation induces a drastic reduction in the rates of both transcription and degradation of mRNA in yeast. Biochim Biophys Acta 2000, 1491:37-48.

Kayed R, Head E, Thompson JL, McIntire TM, Milton SC, Cotman CW, Glabe CG: Common structure of soluble amyloid oligomers implies common mechanism of pathogenesis. Science 2003, 300:486-489.

Kumar A, Agarwal S, Heyman JA, Matson S, Heidtman M, Piccirillo S, Umansky L, Drawid A, Jansen R, Liu Y, et al.: Subcellular localization of the yeast proteome. Genes Dev 2002, 16:707-719.

Kwon KS, Lee S, Yu MH: Refolding of alpha 1-antitrypsin expressed as inclusion bodies in Escherichia coli: characterization of aggregation. Biochim Biophys Acta 1995, 1247:179-184.

Lansbury PT, Jr.: Yeast prions: inheritance by seeded protein polymerization? Curr Biol 1997, 7:R617-619.

Laporte D, Salin B, Daignan-Fornier B, Sagot I: Reversible cytoplasmic localization of the proteasome in quiescent yeast cells. J Cell Biol 2008, 181:737-745.

Lee JW, Beebe K, Nangle LA, Jang J, Longo-Guess CM, Cook SA, Davisson MT, Sundberg JP, Schimmel P, Ackerman SL: Editing-defective tRNA synthetase causes protein misfolding and neurodegeneration. Nature 2006, 443:50-55.

LeVine H, 3rd: Thioflavine T interaction with synthetic Alzheimer's disease beta-amyloid peptides: detection of amyloid aggregation in solution. Protein Sci 1993, 2:404-410.

LeVine H, 3rd, Walker LC: Molecular polymorphism of Abeta in Alzheimer's disease. Neurobiol Aging 2010, 31:542-548.

Lewis DL, and D. K. Gattie: The ecology of quiescent microbes. ASM News 1991, 57:27-32.

Li Z, Lee I, Moradi E, Hung NJ, Johnson AW, Marcotte EM: Rational extension of the ribosome biogenesis pathway using network-guided genetics. PLoS Biol 2009, 7:e1000213.

Linding R, Schymkowitz J, Rousseau F, Diella F, Serrano L: A comparative study of the relationship between protein structure and beta-aggregation in globular and intrinsically disordered proteins. J Mol Biol 2004, 342:345-353.

Liu JL: The enigmatic cytoophidium: compartmentation of CTP synthase via filament formation. Bioessays 2010, 33:159-164.

Ludin KM, Hilti N, Schweingruber ME: The ade4 gene of Schizosaccharomyces pombe: cloning, sequence and regulation. Curr Genet 1994, 25:465-468.

Ma J, Bharucha N, Dobry CJ, Frisch RL, Lawson S, Kumar A: Localization of autophagy-related proteins in yeast using a versatile plasmid-based resource of fluorescent protein fusions. Autophagy 2008, 4:792-800.

Malinchik SB, Inouye H, Szumowski KE, Kirschner DA: Structural analysis of Alzheimer's beta(1-40) amyloid: protofilament assembly of tubular fibrils. Biophys J 1998, 74:537-545.

Martzen MR, McCraith SM, Spinelli SL, Torres FM, Fields S, Grayhack EJ, Phizicky EM: A biochemical genomics approach for identifying genes by the activity of their products. Science 1999, 286:1153-1155.

Mitchell AP, Magasanik B: Purification and properties of glutamine synthetase from Saccharomyces cerevisiae. J Biol Chem 1983, 258:119-124.

Mnaimneh S, Davierwala AP, Haynes J, Moffat J, Peng WT, Zhang W, Yang X, Pootoolal J, Chua G, Lopez A, et al.: Exploration of essential gene functions via titratable promoter alleles. Cell 2004, 118:31-44.

Nadkarni AK, McDonough VM, Yang WL, Stukey JE, Ozier-Kalogeropoulos O, Carman GM: Differential biochemical regulation of the URA7- and URA8-encoded CTP synthetases from Saccharomyces cerevisiae. J Biol Chem 1995, 270:24982-24988.

Nangle LA, Motta CM, Schimmel P: Global effects of mistranslation from an editing defect in mammalian cells. Chem Biol 2006, 13:1091-1100.

Narayanaswamy R, Levy M, Tsechansky M, Stovall GM, O'Connell JD, Mirrielees J, Ellington AD, Marcotte EM: Widespread reorganization of metabolic enzymes

into reversible assemblies upon nutrient starvation. Proc Natl Acad Sci U S A 2009, 106:10147-10152.

Noda T, Ohsumi Y: Tor, a phosphatidylinositol kinase homolog, controls autophagy in yeast. J Biol Chem 1998, 273:3963-3966.

O'Nuallain B, Wetzel R: Conformational Abs recognizing a generic amyloid fibril epitope. Proc Natl Acad Sci U S A 2002, 99:1485-1490.

Ozier-Kalogeropoulos O, Adeline MT, Yang WL, Carman GM, Lacroute F: Use of synthetic lethal mutants to clone and characterize a novel CTP synthetase gene in Saccharomyces cerevisiae. Mol Gen Genet 1994, 242:431-439.

Ozier-Kalogeropoulos O, Fasiolo F, Adeline MT, Collin J, Lacroute F: Cloning, sequencing and characterization of the Saccharomyces cerevisiae URA7 gene encoding CTP synthetase. Mol Gen Genet 1991, 231:7-16.

Pauling L, Corey RB: Configurations of Polypeptide Chains With Favored Orientations Around Single Bonds: Two New Pleated Sheets. Proc Natl Acad Sci U S A 1951, 37:729-740.

Pecorari F, Minard P, Desmadril M, Yon JM: Occurrence of transient multimeric species during the refolding of a monomeric protein. J Biol Chem 1996, 271:5270-5276.

Perutz MF, Windle AH: Cause of neural death in neurodegenerative diseases attributable to expansion of glutamine repeats. Nature 2001, 412:143-144.

Plesset J, Ludwig JR, Cox BS, McLaughlin CS: Effect of cell cycle position on thermotolerance in Saccharomyces cerevisiae. J Bacteriol 1987, 169:779-784.

Pringle JR, Hartwell LH: The Saccharomyces cerevisiae cell cycle. In Molecular biology of the yeast Saccharomyces cerevisiae: life cycle and inheritance. Edited by J. R. Broach JS, and E. Jones Cold Spring Harbor Laboratory; 1981:97-142.

Pruyne D, Legesse-Miller A, Gao L, Dong Y, Bretscher A: Mechanisms of polarized growth and organelle segregation in yeast. Annu Rev Cell Dev Biol 2004, 20:559-591.

Radonjic M, Andrau JC, Lijnzaad P, Kemmeren P, Kockelkorn TT, van Leenen D, van Berkum NL, Holstege FC: Genome-wide analyses reveal RNA polymerase II located upstream of genes poised for rapid response upon S. cerevisiae stationary phase exit. Mol Cell 2005, 18:171-183.

Roberts RL, Metz M, Monks DE, Mullaney ML, Hall T, Nester EW: Purine synthesis and increased Agrobacterium tumefaciens transformation of yeast and plants. Proc Natl Acad Sci U S A 2003, 100:6634-6639.

Ross CA, Poirier MA: Protein aggregation and neurodegenerative disease. Nat Med 2004, 10 Suppl:S10-17.

Sagot I, Pinson B, Salin B, Daignan-Fornier B: Actin bodies in yeast quiescent cells: an immediately available actin reserve? Mol Biol Cell 2006, 17:4645-4655.

Saxena AM: Phycocyanin aggregation. A small angle neutron scattering and size exclusion chromatographic study. J Mol Biol 1988, 200:579-591.

Selkoe DJ: Folding proteins in fatal ways. Nature 2003, 426:900-904.

Shirahama T, Cohen AS: High-resolution electron microscopic analysis of the amyloid fibril. J Cell Biol 1967, 33:679-708.

Silow M, Oliveberg M: Transient aggregates in protein folding are easily mistaken for folding intermediates. Proc Natl Acad Sci U S A 1997, 94:6084-6086.

Silow M, Tan YJ, Fersht AR, Oliveberg M: Formation of short-lived protein aggregates directly from the coil in two-state folding. Biochemistry 1999, 38:13006-13012.

Smolina VS, Bekker ML: [Properties of 5-phosphoryl-1-pyrophosphate amidotransferase from the yeast Saccharomyces cerevisiae wild type and mutant with altered purine biosynthesis regulation]. Biokhimiia 1982, 47:162-167.

Som I, Mitsch RN, Urbanowski JL, Rolfes RJ: DNA-bound Bas1 recruits Pho2 to activate ADE genes in Saccharomyces cerevisiae. Eukaryot Cell 2005, 4:1725-1735.

Stefani M, Dobson CM: Protein aggregation and aggregate toxicity: new insights into protein folding, misfolding diseases and biological evolution. J Mol Med 2003, 81:678-699.

Sugiyama M, Yamagishi K, Kim YH, Kaneko Y, Nishizawa M, Harashima S: Advances in molecular methods to alter chromosomes and genome in the yeast Saccharomyces cerevisiae. Appl Microbiol Biotechnol 2009, 84:1045-1052.

Sunde M, Serpell LC, Bartlam M, Fraser PE, Pepys MB, Blake CC: Common core structure of amyloid fibrils by synchrotron X-ray diffraction. J Mol Biol 1997, 273:729-739.

Thevelein JM, Cauwenberg L, Colombo S, De Winde JH, Donation M, Dumortier F, Kraakman L, Lemaire K, Ma P, Nauwelaers D, et al.: Nutrient-induced signal transduction through the protein kinase A pathway and its role in the control of metabolism, stress resistance, and growth in yeast. Enzyme Microb Technol 2000, 26:819-825.

Unno H, Uchida T, Sugawara H, Kurisu G, Sugiyama T, Yamaya T, Sakakibara H, Hase T, Kusunoki M: Atomic structure of plant glutamine synthetase: a key enzyme for plant productivity. J Biol Chem 2006, 281:29287-29296.

van den Oetelaar PJ, de Man BM, Hoenders HJ: Protein folding and aggregation studied by isoelectric focusing across a urea gradient and isoelectric focusing in two dimensions. Biochim Biophys Acta 1989, 995:82-90.

von Bergen M, Friedhoff P, Biernat J, Heberle J, Mandelkow EM, Mandelkow E: Assembly of tau protein into Alzheimer paired helical filaments depends on a local sequence motif ((306)VQIVYK(311)) forming beta structure. Proc Natl Acad Sci U S A 2000, 97:5129-5134.

Werner-Washburne M, Braun EL, Crawford ME, Peck VM: Stationary phase in Saccharomyces cerevisiae. Mol Microbiol 1996, 19:1159-1166.

Winzeler EA, Shoemaker DD, Astromoff A, Liang H, Anderson K, Andre B, Bangham R, Benito R, Boeke JD, Bussey H, et al.: Functional characterization of the S. cerevisiae genome by gene deletion and parallel analysis. Science 1999, 285:901-906.

Woods RA, Roberts DG, Friedman T, Jolly D, Filpula D: Hypoxanthine: guanine phosphoribosyltransferase mutants in Saccharomyces cerevisiae. Mol Gen Genet 1983, 191:407-412.

Zhu H, Bilgin M, Bangham R, Hall D, Casamayor A, Bertone P, Lan N, Jansen R, Bidlingmaier S, Houfek T, et al.: Global analysis of protein activities using proteome chips. Science 2001, 293:2101-2105.

Chapter 2: Aggregation Hypothesis: Mutant Design and Fitness Evaluation

INTRODUCTION

Puncta Aggregation Assembly Hypothesis

In *S. cerevisiae* stationary phase cells, the widespread reorganization of cytosolic proteins into "punctate foci" (Narayanaswamy et al. 2009) left us with more questions than answers: What are puncta (*singular* punctate, *plural* puncta)? Why do they form? How do they form? Under the right conditions, will all proteins form punctate foci?

Three early hypotheses arose: (1) Puncta are multi-enzyme complexes. (2) Puncta are storage depots. (3) Puncta are aggregation assemblies. Mounting evidence from Dr. Edward Marcotte's lab indicates that puncta from proteins in the same pathway (i.e. adenine biosynthesis pathway, uracil biosynthesis pathway) were induced under different nutrient depletion conditions (personal communication, J.D. O'Connell, University of Texas at Austin). Additionally, Ade4-GFP and Gln1-GFP punctate foci do not colocalize (Narayanaswamy et al. 2009). While these two pieces of evidence do not disprove hypotheses (1) and (2), they do not support them. However, the Marcotte lab has shown that the punctate forming proteins have an increased self-aggregation propensity (as computationally predicted by the TANGO algorithm) (Fernandez-Escamilla et al. 2004, Narayanaswamy et al. 2009). And most recently, the immunoprecipitation of Gln1-GFP puncta followed by mass spectrometry analysis identified the punctate proteins as Gln1p, GFP, and Hsc82p and/or Hsp82p (personal communication, J.D. O'Connell, University of Texas at Austin). This led us to test the puncta self-aggregation assembly hypothesis.

We hypothesize that the yeast punctate foci are the result of protein self-aggregation assemblies. Protein aggregation is both concentration and sequence dependent (Ganesh et al. 2001, Crapeau et al. 2009). Protein expression fluctuates with the growth cycle and cellular stress. If the aggregation propensity of the protein (sequence derived) is desirable, then such metabolic perturbations may cause the protein to "crash out" or aggregate *in vivo* forming punctate foci.

Difficulties in Testing Aggregation Hypothesis

There are numerous approaches to detect protein aggregation and amyloid filaments (as discussed in detail in chapter 1). Protein aggregation is traditionally detected using spectrometry. However, many of these methods require purified protein. Additionally, many techniques require *in vitro* folding or misfolding of the protein in solution and are not readily applicable to the yeast intracellular punctate foci that we seek to describe. Histological stains (such as Thioflavin T or Congo Red) are used to detect amyloid fibrils in tissues and cell. These histochemistry methods are being executed by others to examine the widespread punctate foci phenomenom in yeast. However, the histochemical techniques are not necessary straightforward, as they often require optimization and are not easily applied to single cell organisms. Therefore, we sought to test the aggregation hypothesis by taking advantage of the previously established tools used to observe the yeast punctate foci, such as GFP-tags and fluorescent microscopy.

Overview: Testing the Hypothesis

To test the aggregation hypothesis, we sought to rationally design and express proteins with an altered aggregation propensity in yeast and monitor the formation of

punctate foci. In short, amino acid mutations are introduced into the protein with a GFP-tag. This mutable protein in its original wild type form exhibits punctate foci when deprived of nutrients. These mutations are predicted to increase or decrease the aggregation propensity of the protein, while theoretically preserving the enzymatic function. We hypothesize that proteins with an increased aggregation propensity will have an increased rate of punctate formation and/or overall punctate penetrance (i.e. percentage of cells that contain puncta).

Before the punctate evaluation, it was necessary to evaluate the function of the mutant protein *in vivo*, as it pertains to the overall growth of the yeast, and fitness of the mutant strains. Precautions were made to minimize the impact of the introduced mutations on the overall function of the protein, although functional preservation is not guaranteed. Therefore, we sought to establish a functional assay, of sorts, to assess the mutants. This functional assay was in the form of OD_{600nm} growth curves, which could provide a cell-wide view of the impact of introduced mutations. However, compensatory mechanisms and cellular redundancies could obfuscate the effects of such mutations; therefore, a more sensitive method to evaluation the fitness of the organism was sought. Competitive growth experiments, involving parallel growth of two or more organisms in a single batch culture, were utilized. Such experiments tease out the competitive advantage of an organism, as cellular organisms are challenged with limited resources, increasing toxins, and aging populations of cells.

ALTERED AGGREGATION PROPENSITY: THE YEAST TANGO VARIANTS

Designing the Yeast TANGO Variants

To test the aggregration hypothesis, we sought to express mutant proteins with altered aggregation propensities. Some ground rules became apparent upon designing yeast with mutant proteins: (1) The wild type protein must demonstrate transiently forming punctate foci under controlled conditions. (2) The mutant protein must have an altered aggregation propensity (i.e. increased or decreased) relative to the wild type protein. (3) Single amino acid mutation variants are preferred in an effort to preserve protein function. (4) Preservation of protein function is desired, if not essential. (5) Modeling the yeast strain after a canonical punctate forming strain is preferred, as many of the variables involved in this phenomenon have yet to be identified. (6) The mutant protein must have a GFP fusion tag to ease the detection of the punctate foci. (7) Nonessential proteins are preferred candidates for mutation, as this simplifies the techniques necessary to introduce mutations into yeast. Once these requirements were established, we designed yeast proteins with a modified aggregation propensity.

Meeting the proposed ground rules, Ade4 protein mutants were designed, built, and evaluated using the following workflow. An algorithm ("Plost algorithm," Plost 2009) was developed that predicted the amino acid sequence of protein variants with a modified aggregation propensity. Next, gene constructs containing a GFP tag and selectable marker were built. These constructs were incorporated into the yeast genome to resemble the GFP yeast library (Huh et al. 2003), which was originally used to observe the punctate phenomenon (Narayanaswamy et al. 2009). Yeast mutants were evaluated for enzymatic function using an OD_{600nm} growth curve and batch competition

experiments tested their overall fitness. Finally, kinetic experiments were performed monitoring the formation of puncta using fluorescence microscopy.

The Plost algorithm (Plost 2009), which utilized the TANGO scoring algorithm, was employed to design proteins with a modified aggregation propensity. Developed by Luis Serrano at the European Molecular Biology Laboratory in Heidelberg, the TANGO scoring algorithm predicts protein aggregation propensity. It uses a statistical mechanics model for predicting aggregation propensities of peptides based on their amino acid sequence. The algorithm provides an aggregation "score," wherein the greater the score, the greater the aggregation propensity. The TANGO algorithm assigns the thermodynamic possibility of four conformations (i.e. cross-β-aggregate, β-sheet, α-helix, and β-turn) to a given peptide sequence. It has been used to successfully predict the aggregation of known proteins and is widely used in the literature for aggregation predictions (Fernandez-Escamilla et al. 2004).

The Plost algorithm was developed to design protein variants with altered aggregation propensities that retain their native protein function. To do this, sequences across 20 species were observed and phylogenetically nonconserved regions (or hypervariable regions) were identified as candidates for mutation, thereby maintaining the conserved sequences and theoretically preserving the protein's function (Figure 2-1). Mutations that occur in nature (mtoin), as observed in the multiple sequence alignment, were introduced and the TANGO scores were calculated (Plost 2009).

Phosphoribosylpyrophosphate amidotransferase (Ade4) was selected as the first protein candidate for mutations. Ade4p is an ideal candidate as the yeast Ade4-GFP strain forms punctate foci upon stationary phase or nutrient depletion induction and the protein is not essential in yeast, thereby simplifying the techniques required to introduce mutations. The Plost algorithm generated Ade4p variants (or "Ade4 TANGO variants")

with local maximum and minimum TANGO scores; variants contained 1 to 12 amino acid mutations (Plost 2009). Additional Ade4 TANGO variants were manually designed based on the Plost variants. Specifically, amino acid mutations that occur in nature were sampled in the already mutated sites, thereby permitting the testing of multiple mutations at a single site. The Ade4 variants' TANGO scores ranged from 1122 (48% of the original 2321 WT score) to 6005 (259% of the original 2321 WT score) (Plost 2009) (Table 2-1).

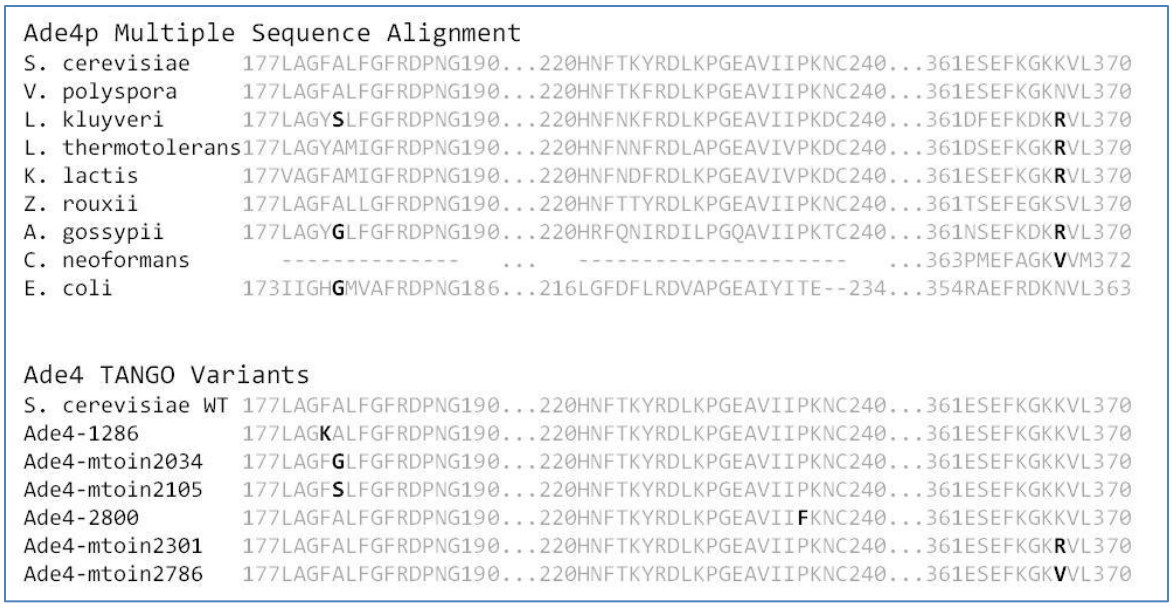

FIGURE 2-1 ADE4P MULTIPLE SEQUENCE ALIGNMENT AND TANGO VARIANTS. This is a portion of the multiple sequence alignment of the Ade4 protein from multiple species. While the *E. coli* homologous protein is shown here for reference, it was not used in the alignment when determining amino acid candidates for mutation in the design of the Ade4 variants.

Table 2-1 Yeast strains used in this work.

Yeast Strain Name (mtoin = "mutation that occurred in nature")	**Ade4p TANGO Score**	**Number of Ade4p Mutations**	**Unnaturally or Naturally occurring mutation(s)**	**Notes**
Ade4-GFP (or Ade4-GFP WT)	2321	0	N/A	Yeast strain used in the original puncta screen.
GS.Ade4-GFP	2321	0	N/A	Control strain, isogenic to TANGO variants (i.e. same parental strain as TANGO variants)
Ade4-1286	1286	1	Unnatural	Phe180Lys
Ade4-mtoin2034	2034	1	Natural	Ala181Gly
Ade4-mtoin2105	2105	1	Natural	Ala181Ser
Ade4-mtoin2301	2301	1	Natural	Lys368Arg
Ade4-mtoin2786	2786	1	Natural	Lys368Val
Ade4-2800	2800	1	Unnatural	Pro237Phe

The Ade4 TANGO variants were further evaluated using an additional aggregation propensity predicting algorithm, Zyggregator (Pawar et al. 2005). Zyggregator works similarly to the TANGO algorithm in that aggregation propensity is predicted based on physico-chemical properties (i.e. hydrophobicity, charge, and secondary protein structure preference) of the amino acid sequence (Pawar et al. 2005, Fernandez-Escamilla et al. 2004). However, the TANGO algorithm assumes aggregating amino acids are fully buried (Fernandez-Escamilla et al. 2004).

Zyggregator predicted the Ade4 TANGO variants to have a different rank order of aggregation propensity (Table 2-2). Specifically, the mutant Ade4p proteins in Ade4-mtoin2034, Ade4-mtoin2105, and Ade4-mtoin2301 have predicted aggregation propensities greater than wild type Ade4p, while the TANGO algorithm predicted these variants to have propensities less than wild type (Figure 2-2).

TABLE 2-2 ADE4 TANGO VARIANTS: AGGREGATION PROPENSITY SCORES (ascending TANGO score) (Fernandez-Escamilla et al. 2004, Pawar et al. 2005).

Strain	TANGO score	Zyggregator optimal score	Zyggregator error
Ade4-1286	1286	0.618424	0.023356
Ade4-mtoin2034	2034	0.643261	0.025344
Ade4-mtoin2105	2105	0.641536	0.0249875
Ade4-mtoin2301	2301	0.643226	0.025054
Ade4 WT	2321	0.640112	0.0250065
Ade4-mtoin2786	2786	0.646042	0.0251335
Ade4-2800	2800	0.649112	0.0249325

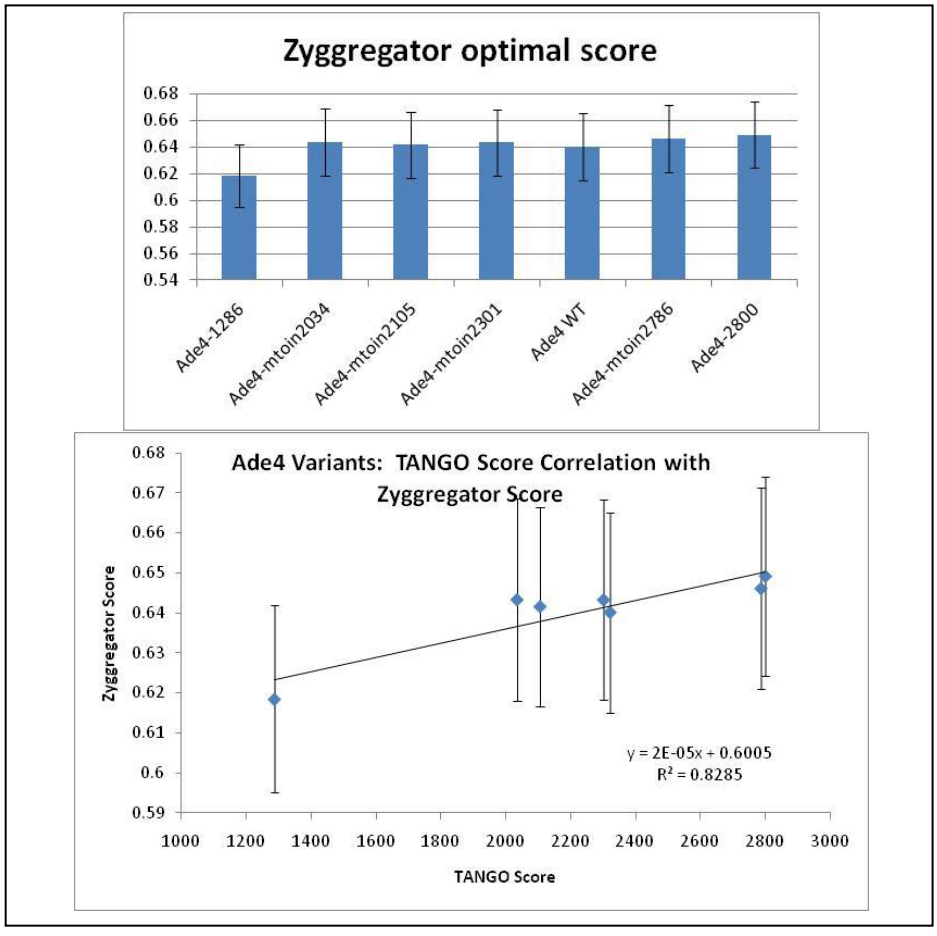

FIGURE 2-2 ZYGGREGATOR PREDICTED AGGREGATION PROPENSITIES OF ADE4 VARIANT (Fernandez-Escamilla et al. 2004, Pawar et al. 2005).

The location of the Ade4p TANGO mutations were inspected on the crystal structure of the *Escherichia coli* Ade4 homolog (glutamine phosphoribosylpyrophosphate amidotransferase, PRPP) (PDB 1ECB, Krahn et al. 1997, PDB 1ECJ, Muchmore et al. 1998). Surprisingly, the structure revealed the close structural proximity of the amino acid 180 mutation (i.e. Ade4-1286) and the 181 mutations (i.e. Ade4-mtoin2034 and Ade4-mtoin2105) to the 237 mutation (i.e. Ade4-2800) (Figure 2-3). However, the corresponding mutated amino acids in Ade4-mtoin2301 and Ade4-mtoin2786 are distant from the 180-181 and 237 sites of mutation (Figure 2-4). Notably, the *E. coli* homolog His176 (corresponding to Phe180 in *S. cerevisiae* Ade4p) is surrounded by aromatic amino acids. The Ade4-1286 variant contains a positively charged lysine at this position, which is predicted to perturb the enzyme significantly.

Inspection of the mutable positions on the *E. coli* homolog revealed the sites were only partially solvent accessible. The percentage of the amino acid surface area exposed was estimated using the DSSP program (Kabsch and Sander 1983). The values were normalized by the accessible surface area for the amino acid X side chain in the tripeptide Gly-X-Gly (Miller et al. 1987). For all 4 mutated sites, <19% of the amino acid side chain was solvent accessible. Zhou *et al.* defines buried residues as those with <25% solvent accessibility (Zhou et al. 2009), while Simpson defines buried residues as those with <5% solvent accessibility (Simpson 2003). Therefore, the amino acids were predicted to be mostly buried or just underneath the surface.

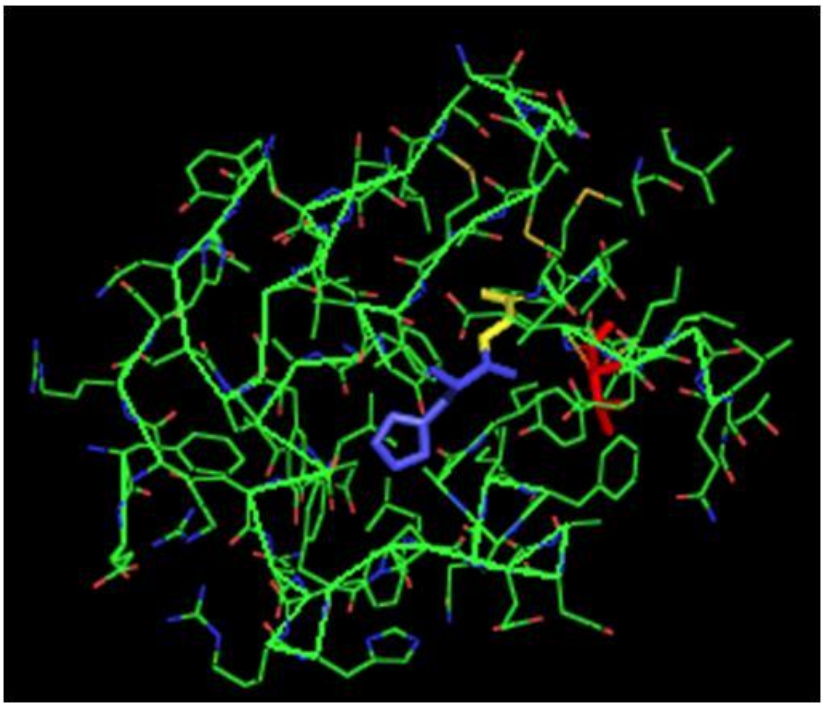

FIGURE 2-3 CRYSTAL STRUCTURE OF ADE4 HOMOLOG AND MAPPED VARIANT MUTATIONS. This is the crystal structure (partial shown) of *E. coli* glutamine phosphoribosylpyrophosphate amidotransferase (PDB 1ECB, Krahn et al. 1997). The corresponding amino acids of the Ade4 TANGO variants are highlighted. His176 (highlighted in blue) corresponds to Phe180 in *S. cerevisiae* Ade4p and Lys180 in Ade4-1286. Gly177 (highlighted in yellow) corresponds to Ala181 in *S. cerevisiae* Ade4p, Gly181 in Ade4-mtoin2034, and Ser181 in Ade4-mtoin2105. Thr233 (highlighted in red) corresponds to Pro237 in *S. cerevisiae* Ade4p and Phe237 in Ade4-2800.

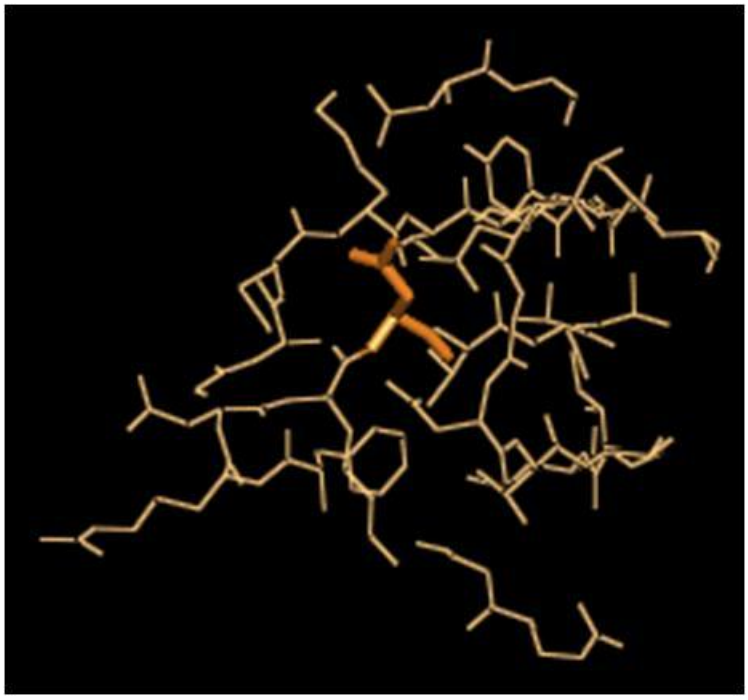

FIGURE 2-4 CRYSTAL STRUCTURE OF ADE4 HOMOLOG AND MAPPED VARIANT MUTATIONS. This is the crystal structure (partial shown) of *E. coli* glutamine phosphoribosylpyrophosphate amidotransferase (PDB 1ECB, Krahn et al. 1997). The corresponding amino acid of the Ade4 TANGO variants is highlighted. Asn361 (highlighted in light brown) corresponds to Lys368 in *S. cerevisiae* Ade4p, Arg368 in Ade4-mtoin2301, and Val368 in Ade4-mtoin2786.

The stability of the Ade4 TANGO variants was estimated using the crystal structure from the *E. coli* Ade4 homolog and the FoldX program. FoldX was designed to rapidly evaluate the stability of protein mutation(s). It draws upon the protein crystal structure to calculate the weighted energy terms and total free energy. Specifically, the ΔG is calculated as the energy difference between the folded and unfolded states and the $\Delta\Delta G$ is calculated as the energy difference between the wild type and mutant fold (Guerois et al. 2002).

Using the FoldX algorithm, the *E. coli* PRPP crystal structure (PDB 1ECJ, Muchmore et al. 1998) was initially optimized. Introducing a single mutation at a time,

the mutated structures were locally optimized. The yeast Ade4p and *E. coli* PRPP have 50% identical amino acids and 27% similar amino acids. Therefore, it was necessary to determine the free energy of the yeast wild type amino acid initially and then the free energy of the TANGO variant. The difference between the two was calculated (i.e. ΔΔG, Table 2-3) (Guerois et al. 2002).

As determined by the positive ΔΔG values, most of the Ade4 TANGO variants had destabilizing mutations. This is not unusual, as most protein mutations are destabilizing (Tokuriki et al. 2007, Goldsmith and Tawfik 2009). Only ~20% of proteins has significantly destabilizing mutations with ΔΔG > 2.0 kcal/mol (Tokuriki et al. 2007), such as the case of Ade4-mtoin2105 and Ade4-mtoin2786. Notably, the Ade4-mtoin2105 has a ΔΔG > 3.0 kcal/mol and according to Zhou et al. is considered of "structural importance," because of its significantly destabilizing effects (Zhou et al. 2009). However, negative ΔΔG values indicate that Ade4-2800 and Ade4-mtoin2034 have stabilizing mutations. The Ade4-mtoin2034 variant contains a mutation that is native in the *E. coli* homolog; therefore artificially reporting a stabilization effect (i.e. negative ΔΔG).

TABLE 2-3 ADE4 TANGO VARIANTS: STABILITY EFFECTS. The energy difference between the wild type and mutant form (ΔΔG) were calculated using the FoldX program (Guerois et al. 2002). Most of the Ade4 TANGO variants have destabilizing mutations. The Ade4-mtoin2034 variant contains a mutation that is native in the E. coli homolog (*); therefore, its predicted ΔΔG might be artificially stabilized.

Ade4 TANGO Variant	mutation (*E. coli* amino acid)	ΔΔG (kcal/mol)
Ade4-1286	F180K (H176)	1.59
Ade4-mtoin2034	A181G* (G177)	-7.34
Ade4-mtoin2105	A181S (G177)	6.39
Ade4-mtoin2301	K368R (N361)	0.33
Ade4-mtoin2786	K368V (N361)	2.39
Ade4-2800	P237F (T233)	-0.68

Building the Yeast TANGO Variants

Upon designing the Ade4p TANGO variants, six variants containing single amino acid mutations were built (see Table 2-1) using the methods discussed in this chapter. With a Longtine plasmid backbone (Longtine et al. 1998) (Figure 2-3), an *ADE4* wild type plasmid ("pFA6a-Ade4-GFPS65T-HIS3MX6") was created as a "parental plasmid" upon which all other variants were prepared (Figure 2-5). This plasmid contained the GFP fusion gene and the *Saccharomyces kluyveri HIS3* selectable marker, the same tag and selectable marker found in the yeast GFP library. It is perhaps worth noting that the original yeast GFP library paper reported that the *Schizosaccharomyces pombe HIS5*

selectable marker was used (Huh et al. 2003), but sequence verification of this strain revealed the *Saccharomyces kluyveri HIS3* gene.

The wild type *ADE4* gene with the GFP fusion gene and *HIS3* selectable marker were incorporated into an *ade4Δ* yeast strain to generate an Ade4-GFP yeast strain identical to the strain in the original GFP library screen of punctate foci (Narayanaswamy et al. 2009). The newly generated Ade4-GFP control strain ("GS.Ade4-GFP") is isogenic to the Ade4 TANGO variants, as the variants were derived from the same parental yeast strain and generated in a similar manner. All prepared yeast strains were sequenced verified using primers upstream and downstream of the insertion site.

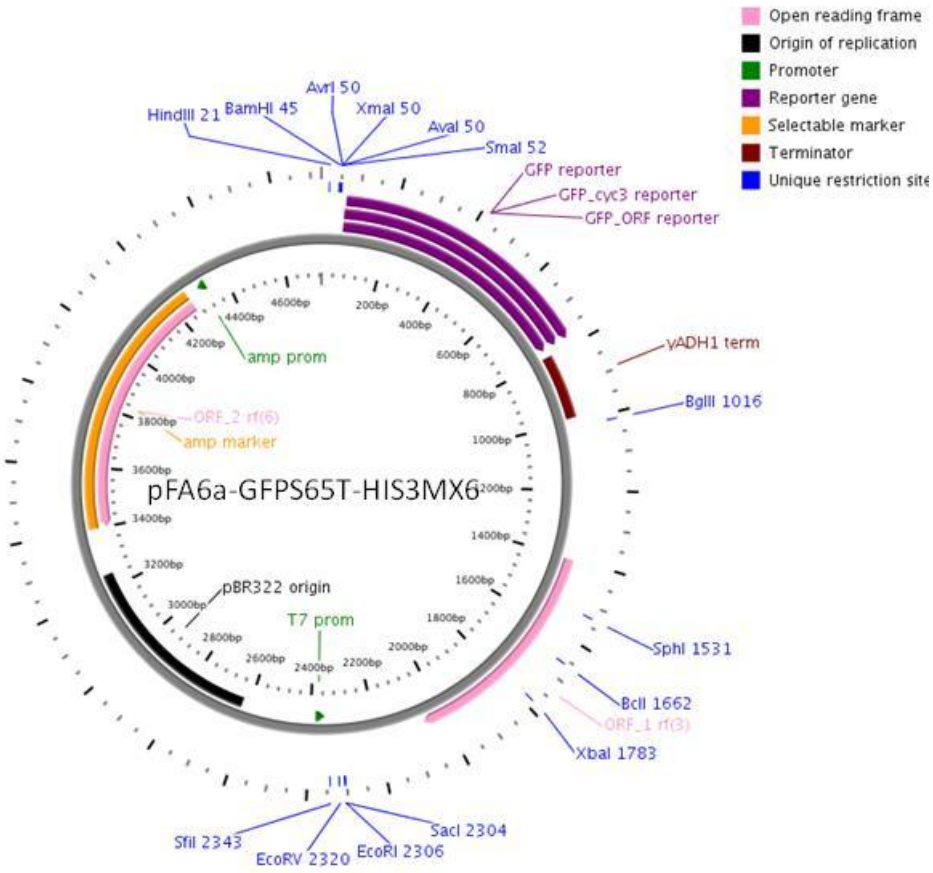

FIGURE 2-5 PFA6A-GFPS65T-HIS3MX6 PLASMID MAP. The pFA6a-GFPS65T-HIS3MX6 plasmid was used in the construction of the Ade4-GFP TANGO variant gene constructs. This Longtine plasmid (Longtine et al. 1998) was used to generate the original yeast GFP library (Huh et al. 2003). The plasmid map was generated using PlasMapper (Dong et al 2004).

During the process, it was necessary to modify the commercially available *ade4Δ* yeast strain ("*ade4Δ::KanMX*," Invitrogen, Winzeler et al. 1999), replacing the *KanMX* module with the *URA3* selectable marker and its endogenous promoter. Swapping the selectable markers was necessary to eliminate unwanted regions of homology in order to minimize unwanted crossover events between the yeast strain and the plasmid construct. This unwanted crossover between the plasmid construct and the *ade4Δ::KanMX* strain was observed, with which the genomic *KanMX* selectable module (G418 resistance) was

swapped for the *HIS3* selectable marker. Preparation of a new *ade4Δ* yeast strain ("*ade4*Δ*::URA3*") with the *URA3* selectable marker was sufficient for the parental uracil auxotroph (*ade4Δ::KanMX* yeast, ATCC # 201 388, S288C, *MATa his3*Δ*1 leu2*Δ*0 met15*Δ*0 ura3*Δ*0*).

In another attempt to circumvent unwanted crossovers, the crossover site of the *ade4Δ::KanMX* strain (i.e. 100 bp upstream and downstream of the *KanMX* module) and the *URA3* construct were checked for homology using a ClustalW multiple alignment algorithm (Thompson et al. 1994). The algorithm aligned a short 8 bp sequence (TTGATGTT), which was found in the end of the *KanMX* module in the *ade4Δ::KanMX* genome and in the middle of the *URA3* construct. The 8 bp sequence is below the 15 bp length required for homologous recombination (Manivasakam et al. 1995). The longer 40 bp homologous regions are predicted to be preferred over this shorter sequence for recombination.

FUNCTIONAL VARIANTS? GROWTH CURVE EVALUATION

The yeast TANGO variants were designed with the intent to preserve enzymatic function, while altering the aggregation propensity. It is unclear, and likely doubtful, that function and aggregation propensity may be independently assessed, for a number of reasons: (1) Conserved sequences could be indicative of functional significance, an aggregation assignment (or structural significance), or both. (2) In the case of the Ade4p enzyme, functional enzymatic assays do not exist, therefore complicating the evaluation of any introduced mutations. (3) Function and aggregation could be highly interrelated or codependent, such that altering one affects the other. As a result, we are left to creatively

use the limited "tools" available to us to predict the total impact, extrapolating function, of the mutation on the cellular system.

Without an available functional assay for Ade4p, we sought to use OD_{600nm} growth curves to evaluate the impact of the Ade4p mutations. Initially, we confirmed a growth differential between the Ade4-GFP strain the *ade4*Δ*::URA3* strain in nutritionally rich or sufficient media (Roberts et al. 2003, Li et al. 2009). Specifically, the deletion strain displayed a slower growth pattern than the Ade4-GFP strain in synthetic defined (SD) media and yeast peptone dextrose (YPD) media (Figure 2-6, 2-7, and 2-11). In the evaluation of growth differentials, *ade4Δ* yeast is an adenine auxotroph (Roberts et al. 2003). Auxotrophy was confirmed, as the *ade4*Δ*::URA3* deletion strain failed to grow in SD,-adenine media and SC,-adenine media, while the Ade4-GFP strain grew (Figure 2-6). This growth differentiation between Ade4-GFP and the deletion strain established the basis of the OD_{600nm} growth curve assay.

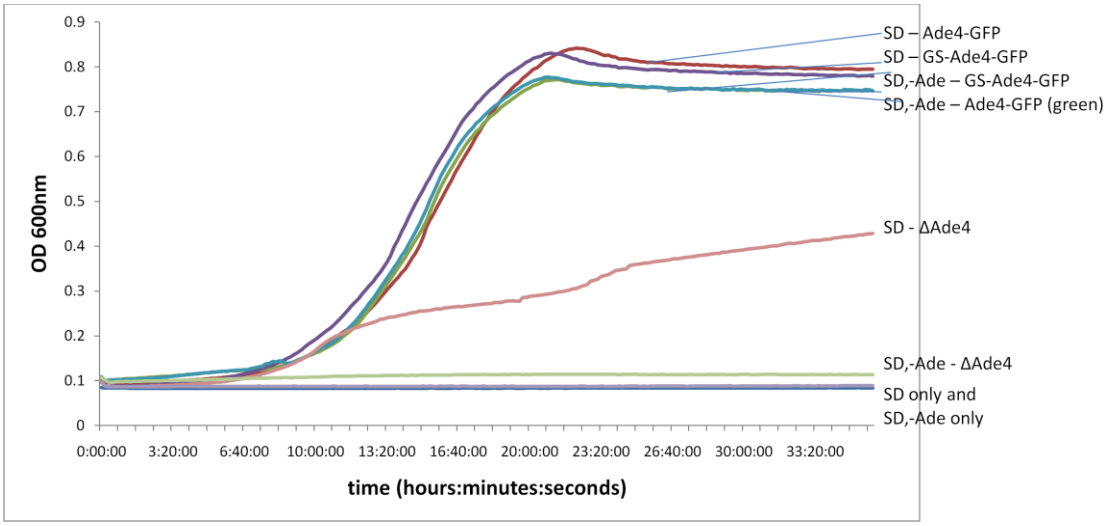

FIGURE 2-6 GROWTH CURVE OF ADE4-GFP STRAIN AND KNOCKOUT STRAIN. These are the results of the OD_{600nm} growth curve of Ade4-GFP, GS.Ade4-GFP, and *ade4*Δ*::URA3*yeast strains (average of four cultures). Overnight cultures (SD media) were diluted in either SD or SD,-adenine media to an OD_{600nm} of 0.02. Cultures were monitored for 36 hours at 30˚C. Media only controls were used, labeled as "SD only" and "SD,-Ade only."

All yeast Ade4-GFP TANGO variants were evaluated using OD_{600nm} growth curves. In general, the triplicate cultures were diluted to an OD_{600nm} of 0.02 and the OD was monitored during the 36 hour incubation at 30˚C. The average OD_{600nm} was plotted. The standard deviation between cultures was minimal (Figure 2-7a). Various growth media were examined, including SD, SD,-adenine, synthetic complete (SC), SC,-adenine, and yeast peptone dextrose (YPD).

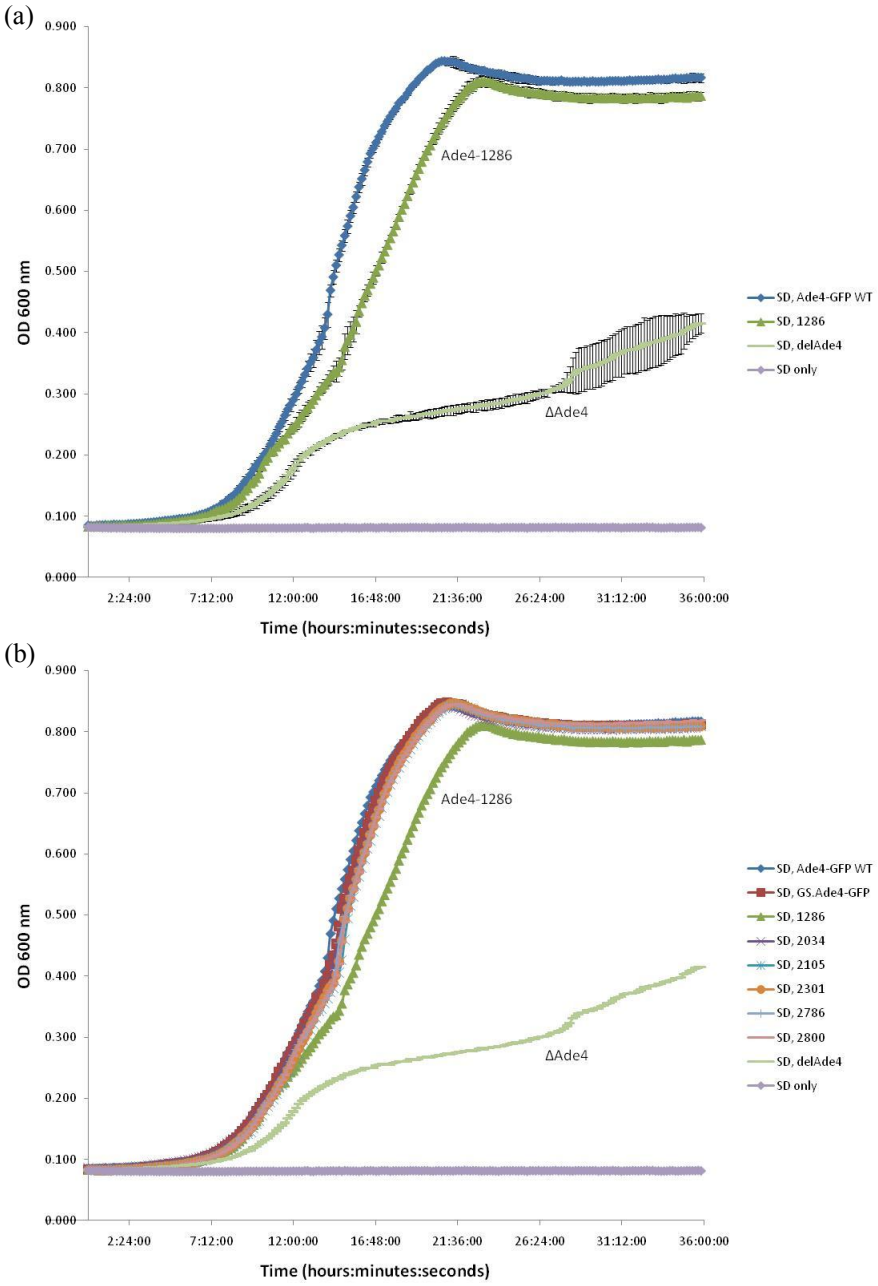

FIGURE 2-7 GROWTH CURVES OF ADE4-GFP AND TANGO VARIANTS, SD. In the SD media OD_{600nm} growth curves, the *ade4*Δ*::URA3* strain ("ΔAde4") grows slower than Ade4-GFP WT, while the Ade4-1286 TANGO variant shows only a slight growth reduction. (a) Above the average of 3 cultures with the standard deviation depicted as error bars is shown. (b) Because the standard deviation is minimal between triplicate cultures, the error bars are omitted from the growth curves and only the average value is plotted.

Although direct comparisons were not made, the cultures in SD media generally grew slower than the cultures in more nutrient rich media SC and YPD (Figures 2-6 to 2-10). In general, most of the Ade4-GFP TANGO variants grew similarly to the Ade4-GFP and GS.Ade4-GFP yeast strains, except for the Ade4p deletion strain (*ade4*Δ*::URA3*) and the Ade4-1286 variant, which grew slower. In adenine dropout media, the Ade4-1286 variant behaved as a bradytroph, having slower growth in the absence of adenine (Figures 2-8 and 2-10). Contrary to our expectations, the Ade4-1286 displayed an increase growth pattern in YPD media, where the growth curve shot up beyond the Ade4-GFP curve and the prepared strains (Figure 2-11). Based on the earlier growth curves, this behavior was not expected and the work will be repeated.

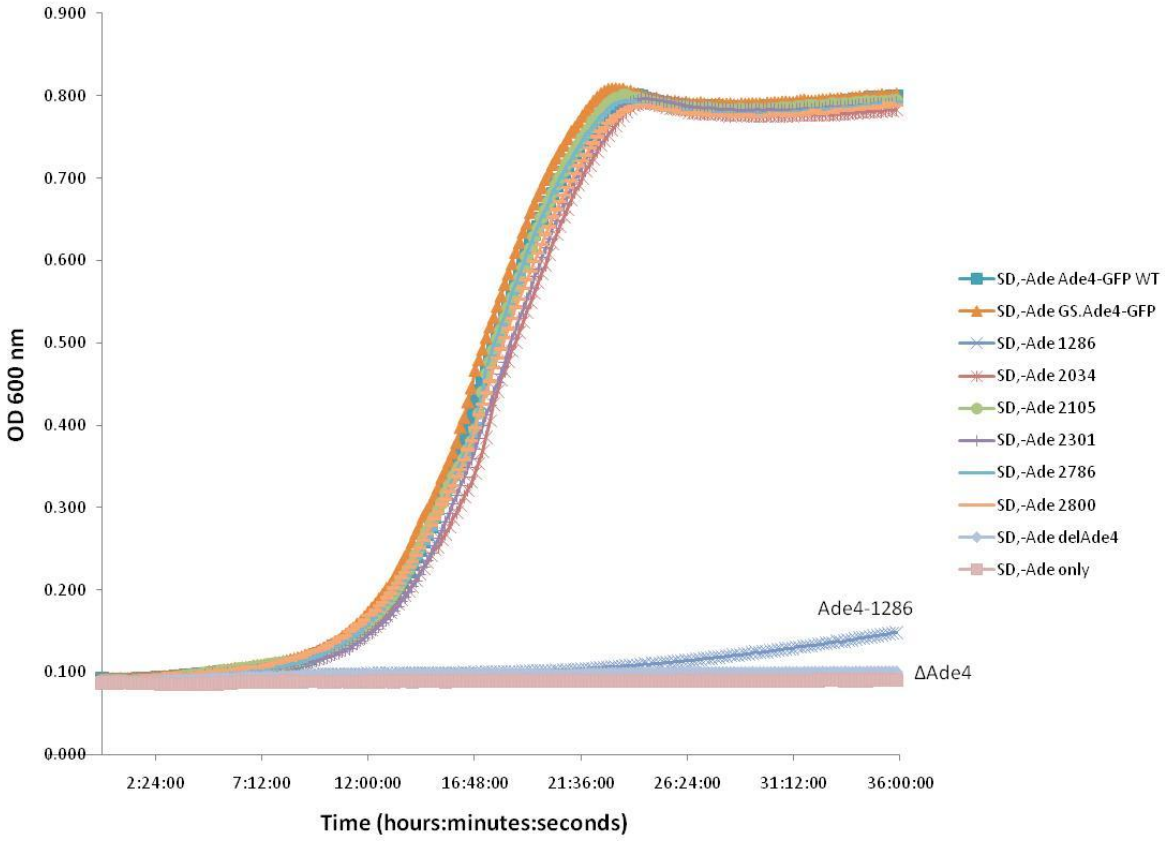

FIGURE 2-8 GROWTH CURVES OF ADE4-GFP AND TANGO VARIANTS, SD,-ADE. These are OD_{600nm} growth curves of Ade4-GFP WT and TANGO variant strains in SD,-adenine media (average of 3 cultures). The *ade4*Δ*::URA3* strain ("delAde4") and the Ade4-1286 TANGO variant show little growth over 36 hours. Overnight cultures (SD media) were diluted to an OD_{600nm} of 0.02 in SD,-adenine and monitored for 36 hours, while incubating at 30□C.

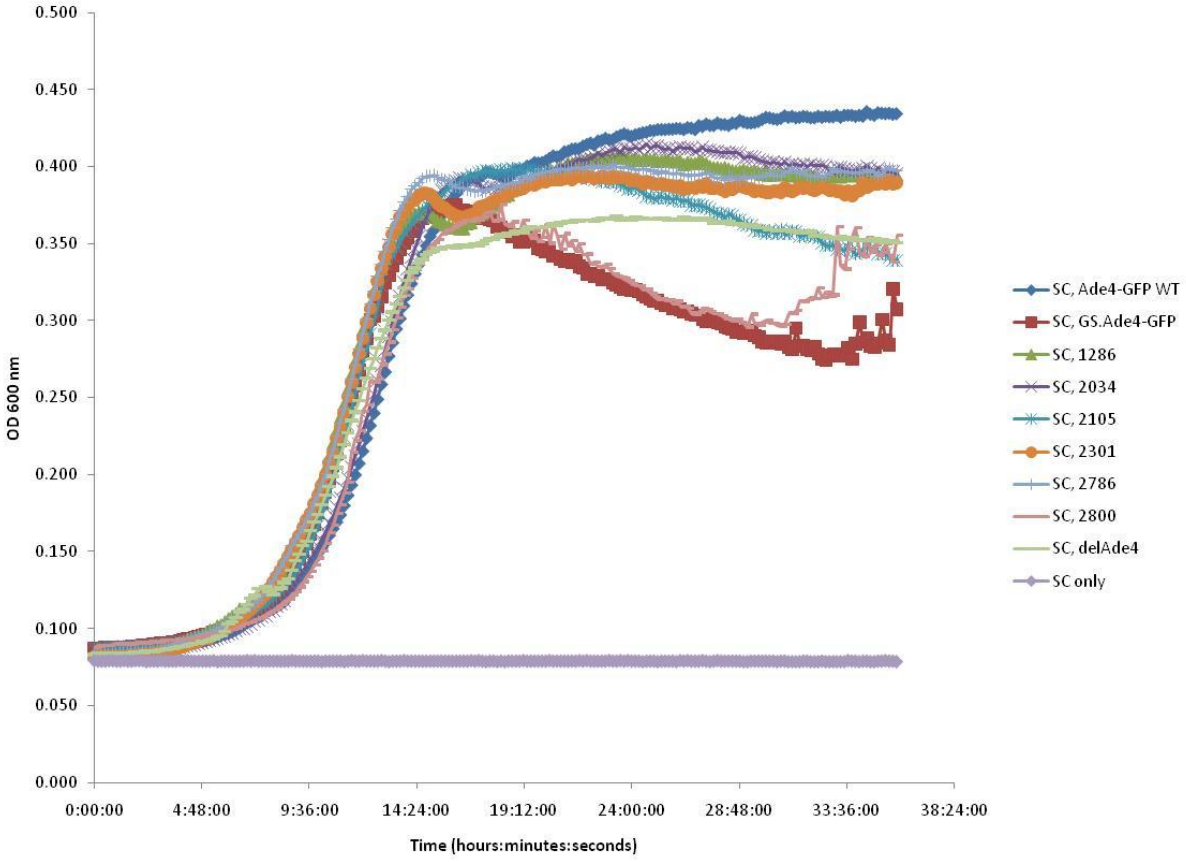

FIGURE 2-9 GROWTH CURVES OF ADE4-GFP AND TANGO VARIANTS, SC. These are OD_{600nm} growth curves of Ade4-GFP and TANGO variant strains in SC media (average of 3 cultures). All of the strains displayed similar growth rates, even the *ade4*Δ*::URA3* strain ("delAde4"). Perhaps the *ade4*Δ*::URA3* strain did not reach the degree of growth as the other strains (i.e. lower OD_{600nm}). Some of the strains (including GS.Ade4-GFP and the Ade4-2800 strains) crashed out of solution when the cultures were saturated, and therefore a decrease in OD_{600nm} was observed. Overnight cultures were diluted to an OD_{600nm} of 0.02 and monitored for 36 hours, while incubating at 30□C.

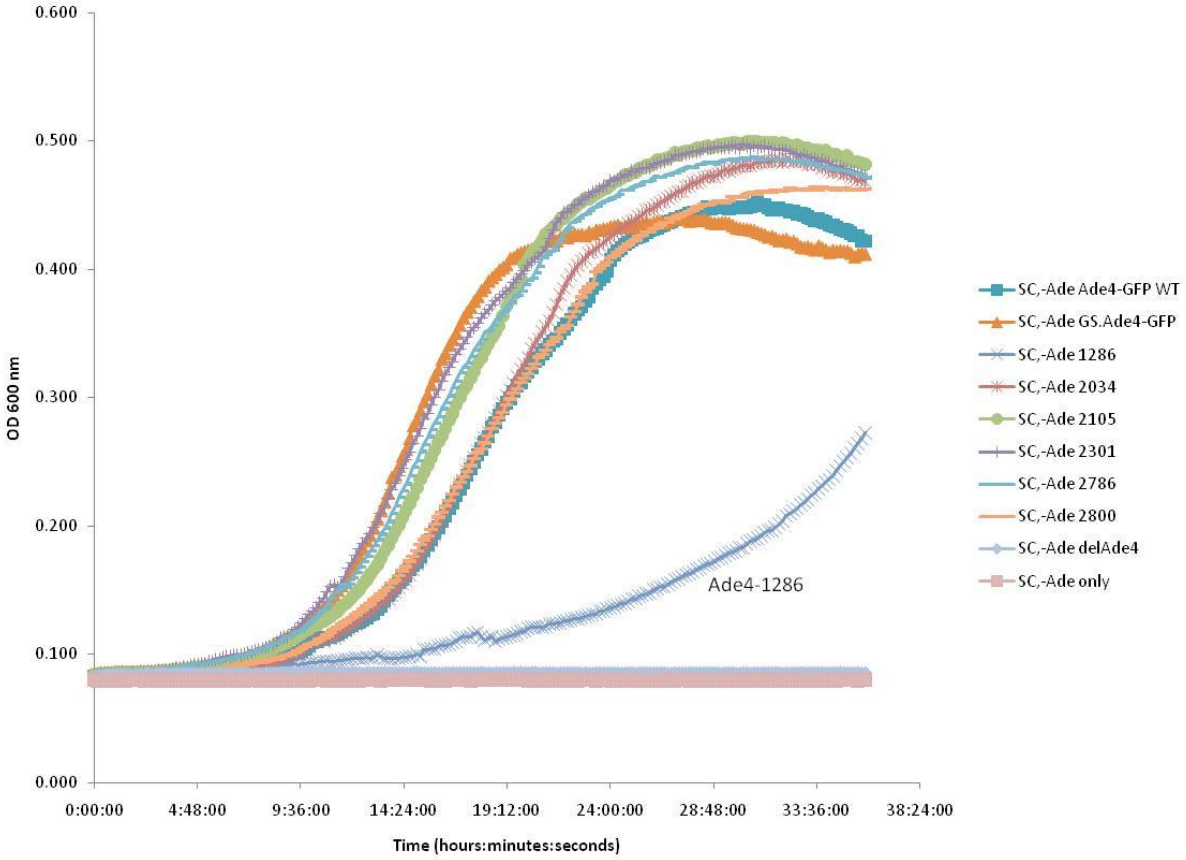

FIGURE 2-10GROWTH CURVES OF ADE4-GFP AND TANGO VARIANTS, SC,-ADE. These are OD_{600nm} growth curves of Ade4-GFP WT and TANGO variant strains in SC,-adenine media (average of 3 cultures). There was a great deal more variation between the strains, as opposed to the growth curves generated using different culture media. The cluster of growth curves, which were the most similar, included all but the Ade4-1286 and the *ade4*Δ*::URA3* curves. The Ade4-1286 strain again (as with the SD,-adenine curves) displayed a slower growth than the other strains, while the *ade4*Δ*::URA3* did not grow in SC,-adenine media. Overnight cultures were diluted to an OD_{600nm} of 0.02 and monitored for 36 hours, while incubating at 30□C.

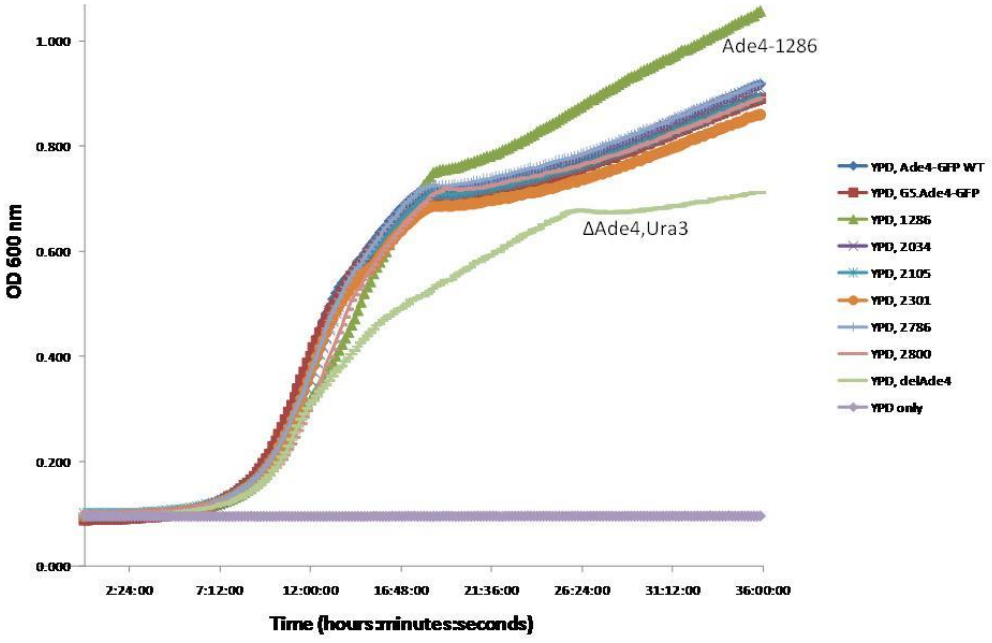

FIGURE 2-11GROWTH CURVES OF ADE4-GFP AND TANGO VARIANTS, YPD. These are OD_{600nm} growth curves of Ade4-GFP WT and TANGO variant strains in YPD media (average of 3 cultures). The *ade4*Δ*::URA3*("ΔAde4,Ura3") strain grows slower than Ade4-GFP WT and the Ade4 TANGO variants. The Ade4-1286 strain exhibits an odd growth curve, in that previously this strain exhibited a slower growth pattern, but in YPD it appears to have a second growth spurt, out growing the other strains. The Ade4-1286 growth curve should be further evaluated. Overnight cultures were diluted to an OD_{600nm} of 0.02 and monitored for 36 hours, while incubating at 30□C.

Based on these growth curves, it was concluded that the GS.Ade4-GFP strain and all of the Ade4 TANGO variants, except for Ade4-1286, grew similarly to the Ade4-GFP strain. These results suggest the Ade4 TANGO variants (except the Ade4-1286 strain) contain enzymatically active Ade4p. Therefore, these strains were used in all downstream analyses, including competition experiments and kinetic punctate foci evaluation.

The retarded growth patterns of the Ade4-1286 were likely due to a defective Ade4p. Structural perturbation caused by the replacement of an aromatic phenylalanine

with a basic lysine residue at position 180 could significantly alter the catalytic activity of the protein. The result was not unexpected when considering the magnitude of the amino acid mutation (i.e. nonpolar replaced with basic amino acid) and the introduction of a non-native mutation (i.e. mutation was not seen in other species in the multiple sequence alignment).

FUNCTIONALLY EQUIVALENT? COMPETITIVE GROWTH EXPERIMENTS

Designed and built to test the aggregation hypothesis, the Ade4 TANGO variants were evaluated for function and more stringently evaluated for functional equivalency to the wild type strain. The growth curves suggested functional Ade4 activity, although it is unclear to the extent of this activity or the similarity to the wild type strain. Therefore, the Ade4 TANGO variants were further evaluated using competitive growth experiments. These sensitive co-culture experiments involve the simultaneous growth of one or more yeast strains in a batch culture. The competition for nutrients and survival, pitting one strain against another, allow for the observation of a competitive advantage in the form of increased or dominating strain composition. The advantage of such a technique is the sensitivity, testing functional equivalence to the wild type strain.

Multiple batch culture experiments were performed. In general, one or more of the Ade4 TANGO variants were grown in a co-culture containing either Ade4-GFP or GS.Ade4-GFP (isogenic to variants). The batch cultures were grown for 7-14 days. Every 24 hours, glycerol stocks were prepared and the cultures were diluted to a 0.02 OD_{600nm}. All cultures were grown in a 30˚C shaking incubator. Strain composition was determined by PCR amplification of the area of mutation and restriction digestion, as restriction sites were unique to the gene encoding wild type Ade4p.

Three TANGO variants were identified as candidates for co-culture experimentation, because their Ade4 mutations eliminated restriction sites present in the wild type *ADE4* gene. The three TANGO variants are Ade4-mtoin2034 (Ala181Gly), Ade4-mtoin2105 (Ala181Ser), and Ade4-2800 (Pro237Phe) (Table 2-1). Compared to the wild type Ade4p (TANGO score 2321), Ade4-mtoin2034 and Ade4-mtoin2105 mutant proteins have a TANGO predicted decreased aggregation propensity, while the Ade4-2800 mutant protein has a TANGO predicted increased aggregation propensity.

Two different medias were selected for the competition experiments: SD and SD,-adenine. SD media was selected because it is a minimal media and permits a more rapid competition for nutrients than more nutrient rich media. And, the SD,-adenine media was selected because it forces the *de novo* synthesis of adenine in yeast, further tasking the Ade4p enzyme.

While the observation of puncta is outside the scope of the competition experiment, it is interesting to note the differences in punctate induction between the SD media and SD,-adenine media. SD,-adenine media induces Ade4-GFP puncta (~50-60% maximum penetrance) within 2 h (Narayanaswamy et al. 2009). Perhaps contrary to what was reported in the original description of the punctate phenomenon (Narayanaswamy et al. 2009), SD media does not induce Ade4-GFP puncta in early log phase. However, after 24 hours of growth in SD media the culture enters early stationary phase, resulting in~12% punctate penetrance.

Binary Competition Experiments: Ade4-GFP vs. TANGO Variant

Continuous binary co-culture experiments were performed pitting the Ade4-GFP strain against an Ade4-TANGO variant: Ade4-mtoin2034, Ade4-mtoin2105, or Ade4-

2800. Parallel SD and SD,-adenine co-cultures were grown for 7 days and then analyzed using the PCR-restriction digestion described above.

The SD media Ade4-GFP co-cultures containing Ade4-mtoin2034 or Ade4-mtoin2105 had a slight increase in the Ade4-GFP strain composition over the course of 7 days (Figure 2-12). However, the SD,-adenine media co-culture of Ade4-GFP and Ade4-mtoin2034 (also referred to as Ade4-GFP/Ade4-mtoin2034) had a greater increase in Ade4-GFP concentration over 7 days. At the end of the experiment, the culture contained 77% Ade4-GFP and 23% Ade4-mtoin2034. Unfortunately, the results of the other co-cultures were not as definitive, as the SD,-adenine media Ade4-GFP/Ade4-mtoin2105 co-culture was not started at an equivalent concentration and the Ade4-GFP/Ade4-2800 co-cultures were inadequately digested and analyzed. The results of the SD,-adenine media Ade4-GFP/Ade4-2800 co-cultures do offer themselves to interpretation, though not quantitatively. This co-culture was almost completely comprised of Ade4-GFP after 7 days, although the beginning ($t = 0$) concentrations of Ade4-GFP and Ade4-2800 are unclear (results not shown).

Perhaps the best explanation of these competition results is that the Ade4 TANGO variants (i.e. Ade4-mtoin2034, Ade4-mtoin2105, and possibly Ade4-2800) are not functionally equivalent to the wild type Ade4-GFP, although this does not necessarily preclude aggregation induced effects. It was necessary to reproduce the result in triplicate, before concluding the advantage of the Ade4-GFP in competitive growth experiments.

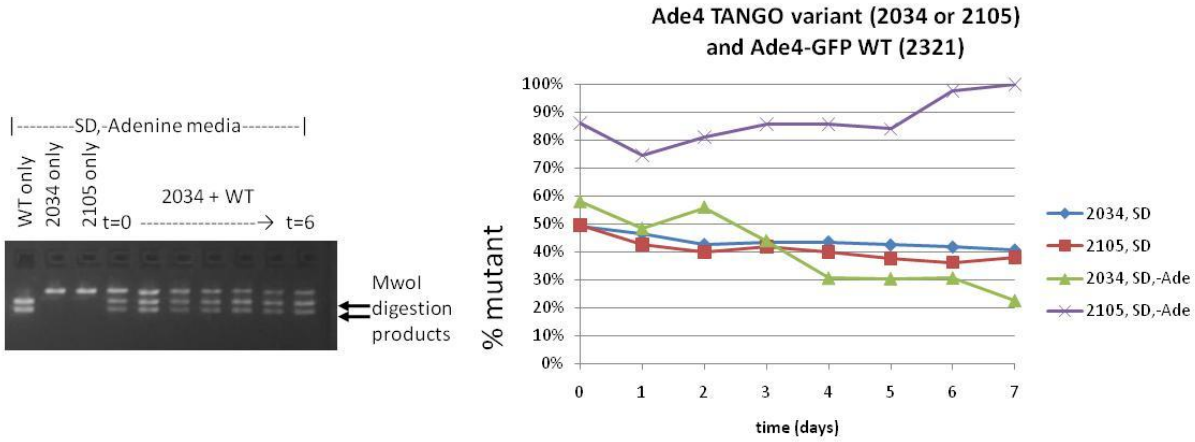

FIGURE 2-12BINARY COMPETITION EXPERIMENT RESULTS. These are the binary competition experiment results, including a representative agarose gel image of the digestion products from the Ade4-GFP and Ade4-mtoin2034 co-culture. The two SD cultures drifted slightly from their initial ~1:1 ratio to a slight increase in the Ade4-GFP strain. Alternatively, the SD,-adenine co-culture containing Ade4-GFP and Ade4-mtoin2034 had a greater shift in strain composition, 77% Ade4-GFP WT: 23% Ade4-mtoin2034 after 7 days. The initial SD,-adenine Ade4-GFP WT and Ade4-mtoin2105 co-culture was skewed toward Ade4-mtoin2105, instead of the intended 50:50 starting ratio.

The Ade4-mtoin2034 co-culture was reexamined by performing the competition experiment in triplicate and pitting the strain against the isogenic GS.Ade4-GFP strain. As previously discussed, the GS.Ade4-GFP strain was designed and constructed to be equivalent to the Ade4-GFP strain, while the GS.Ade4-GFP and the Ade4 TANGO variants were prepared from the same parental strains (i.e. identical backgrounds). The results from this 14 day competition experiment (performed in triplicate) were in line with the previous 7 day experiment (Figure 2-13). Specifically, the SD media co-cultures slightly increased in GS.Ade4-GFP concentration over the course of 14 days. However, the SD,-adenine media co-culture results were more pronounced, as the culture was

primarily comprised of GS.Ade4-GFP after 7 days. The GS.Ade4-GFP strain out-competed the Ade4-mtoin2034 strain.

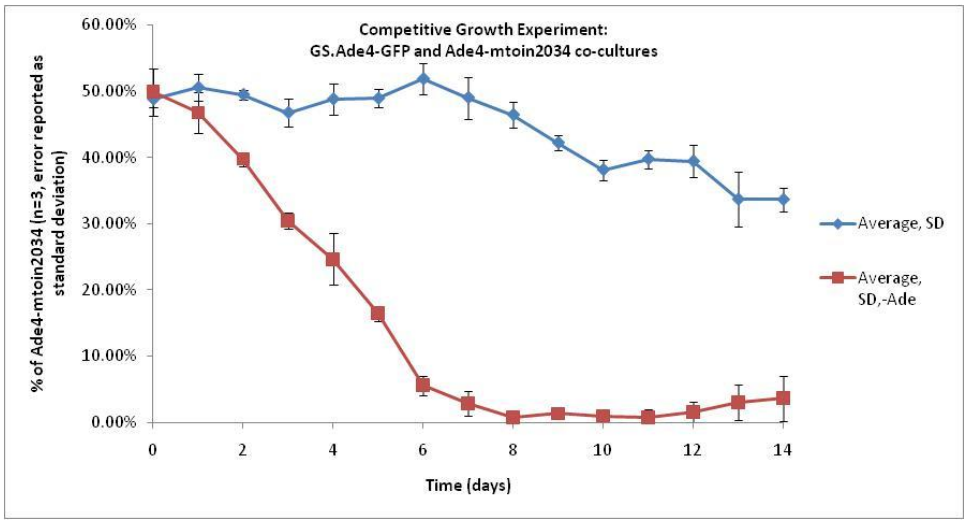

FIGURE 2-13 COMPETITION EXPERIMENT: GS.ADE4-GFP VS. ADE4-MTOIN2034. GS.Ade4-GFP and Ade4-mtoin2034 co-cultures were competed against one another in SD media and SD,-adenine media. Co-cultures were passaged every 24 hours for 14 days. The graph shows the average of 3 replicates, with error reported as standard deviation.

The error introduced in the competition experiments results with the possible underestimation of the digested population PCR product (i.e. GS.Ade4-GFP). Further discussion of the error involved and the subsequent impact on the results is reserved for the following section.

While we originally predicted the strain with the decreased aggregation propensity would outcompete a strain with a greater propensity, this clearly is not what was observed. The Ade4-mtoin2034 strain has a lower aggregation propensity than the GS.Ade4-GFP strain, but the culture was predominately GS.Ade4-GFP at the end of the experiment.

Again, the most accessible conclusion to these results is that the TANGO mutant is not functionally equivalent to the wild type Ade4-GFP. However, results from Chen

and Dokholyan suggest the interrelatedness between function and aggregation. That is - essential proteins were found to have a lower TANGO score than nonessential proteins (Chen and Dokholyan 2008). But given the results of the competitive experiment, it seems most appropriate to conclude inequivalent function and to save the aggregation discussion for later experiments.

4 strains in a pot: GS.Ade4-GFP vs. 3 TANGO mutants

The results of the binary competition experiments left us asking "why" and "what if." Why did the Ade4 TANGO variants drop-off? If we stressed the system in other ways, such as using glycerol (instead of glucose) as the primary carbon source, will the TANGO variants still "die off" in the co-culture? Or, would a continuous co-culture that is rarely passaged or not passaged end with the same results?

Perhaps, though, instead of asking why the TANGO variants "died," the real interesting work would come finding a "winner" or variant that is functionally equivalent or even at an advantaged when compared to wild type. Although the binary competition experiments could offer the answer to such inquiries, the experiments are extremely time consuming and laborious. This led us to ask if we could more rapidly resolve a competitive "winner" by co-culturing multiple strains together.

In one big competition experiment, the GS.Ade4-GFP strain was competed against three Ade4 TANGO variants: Ade4-mtoin2034, Ade4-mtoin2105, and Ade4-2800. All four strains were added at equal concentrations to the co-culture (i.e. 25% GS.Ade4-GFP, 25% Ade4-2800, 25% Ade4-mtoin2034, and 25% Ade4-mtoin2105). Triplicate co-cultures were passaged and sampled every 24 h for 14 days. Co-cultures were analyzed using PCR and digestion reactions (described previously). Because both

the Ade4-mtoin2034 and Ade4-mtoin2105 strains contained mutations at amino acid 181, the MwoI restriction enzyme site (native in *ADE4* wild type gene) was eliminated. Therefore, Ade4-mtoin2034 and Ade4-mtoin2105 were unable to be discerned from each other using the demonstrated techniques. If deemed necessary, the strains could be discriminated via Southern blots or real-time PCR.

The results of the "4 strains in a pot" competition experiment (Figure 2-14) were similar to those results obtained previously. The SD media co-culture strain composition somewhat fluctuated over the course of the 14-day experiment; although in the end, the final concentrations drifted little from the initial concentrations. However, the SD,-adenine media co-cultures predominately contained the GS.Ade4-GFP strain by the end of the experiment.

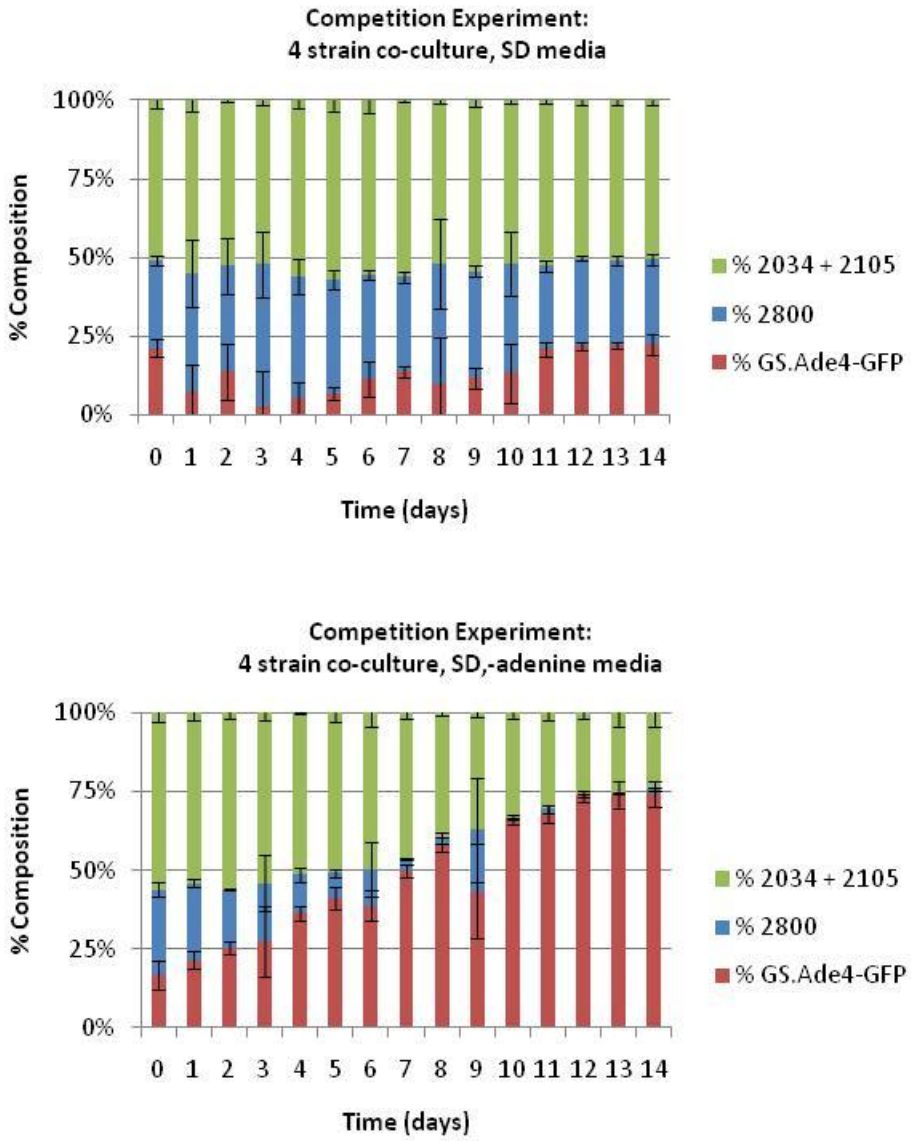

FIGURE 2-14COMPETITION EXPERIMENT: 4 STRAINS IN A POT. These are the results of the competition experiment with the co-culture containing 4 yeast strains: GS.Ade4-GFP, Ade4-mtoin2034, Ade4-mtoin2105, and Ade4-2800. With the SD media co-culture, the initial and final culture strain compositions were approximately the same, although there were some composition fluctuations towards the beginning and the middle of the experiment. However, the SD,-adenine media co-culture was predominately the GS.Ade4-GFP strain by the end of the experiment. The competition experiment was performed (described above) and analyzed by population PCR and restriction digestion of the strain(s).

The error introduced in this experiment results in the underestimation of the GS.Ade4-GFP concentration. Specifically, the concentration of GS.Ade4-GFP is determined by quantifying the digested population PCR product on an agarose gel, assuming the PCR product is completely digested. As per the "strain only" controls, the digestion efficiencies are typically near 100%, but the BtsCI digestion efficiency has been low on a couple of occasions (i.e. 42% and 86% efficient). Additionally, it is necessary to have complete band separation on the agarose gel to assure proper quantification. In running agarose gels out, we run the risk of diluting the ethidium bromide in the DNA. That is, the ethidium bromide migrates contrary to the DNA and this may result with fainter bands toward the bottom of the gel, again resulting in the underestimation of the digested product (GS.Ade4-GFP). And, finally, the calculated concentrations are all relative, therefore an errant concentration perpetuates subsequence errant concentrations.

In conclusion, the results of this experiment further support the notion that the Ade4 variants are not functionally equivalent to the wild type strain. Again, the effects of this are most evident when the yeast has to make its own adenine (i.e. in adenine dropout media).

CONCLUSIONS

In conclusion, we successfully generated multiple yeast strains by introducing mutant *ADE4* genes and further modifying an *ade4*Δ knockout strain. These strains include the *ade4*Δ*::URA3* strain, the GS.Ade4-GFP strain, and six Ade4 TANGO variant yeast strains. All strains were sequence verified.

After growth curve evaluation, it was concluded that the GS.Ade4-GFP strain and all of the Ade4 TANGO variants, except for Ade4-1286, grew similarly to the Ade4-GFP strain. These results suggest that all of the Ade4 TANGO variants (except for the Ade4-1286 strain) contain functional Ade4p, at least to some extent.

The co-culture competition experiments revealed a preference for the wild type Ade4p present in the Ade4-GFP strain and the control GS.Ade4-GFP strain over the Ade4 TANGO variants. This strongly suggests the Ade4 TANGO variants are not functionally equivalent to the wild type Ade4p strains (i.e. Ade4-GFP and GS.Ade4-GFP). The effects of this are most evident when the yeast must make their own adenine.

While the Ade4 TANGO variants were designed with the intent to preserve function, this may not have been the end result. Instead, the deleterious mutations likely destabilized a majority of the variants, resulting in decrease fitness in the form of slow growth (at worse) and not functionally equivalent to wild type (at best). The mutations were introduced into two locations on the protein: N-terminal domain mutations and C-terminal domain mutations (Figures 2-3 and 2-4). Examination of the *E. coli* homolog revealed the N-terminal domain mutation sites (i.e. *S. cerevisiae* amino acids 180, 181, and 237) were within close proximity on the crystal structure and it was these Ade4 TANGO variants (1286, 2034, 2105, and 2800) containing the neighboring mutation sites that had a decrease in fitness. Of the mutations in the 1286, 2034, 2105, and 2800 strains, free energy estimates predict 2 of these 4 mutations to have destabilizing effects, while one of the free energy estimates favored the *E. coli* model (identical to Ade4 variant mutation), reporting a significantly stabilizing effect (i.e. -7.34 kcal/mol) (Table 2-3). This evidence suggests mutations introduced to this area of the protein have a destabilizing effect, resulting in a decrease in fitness. The Ade4 TANGO variants (2301 and 2786) containing the C-terminal mutations grew similarly to the wild type strain and

were not stringently tested in competition experiments. Free energy estimates predict the C-terminal mutations to be destabilizing, with the Lys368Val more destabilizing than the Lys368Arg mutation. Such mutation induced protein instability is not rare and instead most protein mutations result in a reduction of protein stability (Tokuriki et al. 2007, Goldsmith and Tawfik 2009).

Destabilized proteins require additional folding machinery in the form of chaperone proteins rescuing the stabilized proteins from misfolding. The expression of this quality control machinery has a fitness cost (Drummond and Wilke 2009), thus offering a plausible explanation how the Ade4 TANGO variants were outcompeted in the competitive growth experiments, but grew similarly to the wild type strain in single cultures.

These results illustrate the importance in mutant functional evaluation. That is – when examining function, competition experiments are more sensitive than other means (such as growth curves), offering the "best" evaluation of function.

MATERIALS AND METHODS

Building the *ade4Δ::URA3*Strain

URA3 Insertion

To minimize unwanted crossover events, a new *ADE4* deletion (*ade4Δ*) strain was prepared, replacing the *KanMX* selectable module in the *ade4Δ::KanMX* strain (Open Biosystems) with the *URA3* gene and its endogenous promoter (yeast chromosome V: 116011:117048). The *URA3* selectable marker was sufficient for the *ade4Δ::KanMX*

parental uracil auxotroph (ATCC # 201 388, S288C, *MATa his3Δ1 leu2Δ0 met15Δ0 ura3Δ0*). *URA3* and its endogenous promoter were PCR amplified from a BG1805 plasmid, isolated from an *E. coli* strain in the Yeast ORF Collection (Open Biosystems, Gelperin 2005). The *URA3* construct was flanked by 40 bp homologous to the upstream and downstream regions of the *KanMX* module on the *ade4Δ::KanMX* yeast genome. The *URA3* PCR product was transformed into *ade4Δ::KanMX* strain from the Yeast Knockout Library (Open Biosystems, Winzeler et al. 1999), therefore generating the *ade4Δ::URA3* strain. The *ade4Δ::URA3* strain was confirmed by PCR and colony PCR product was sequence verified using flanking genomic primers.

Yeast Transformation

The yeast transformation protocol was adapted from the "Saccharomyces Genome Deletion Project" website (www-sequence.stanford.edu/group/yeast_deletion_project/).

Log phase cells were prepared by growing a yeast culture for ~8 h at 30˚C in a shaking incubator. An overnight culture was prepared from the 8 h culture, such that the overnight culture would have an OD_{600nm} of 1.5-2.0 in the morning. Cells were pelleted by centrifugation (1620 xg for 4 min) at room temperature and supernatant was discarded. Cells were washed twice with 0.5 volumes of 100 mM LiAcetate and pelleted by centrifugation (1620 xg spin for 3 min). Cells were resuspended in 1/100 vol of 100 mM LiAcetate and concentration was adjusted to an OD_{600nm} of 1.0. Carrier DNA (1/9 vol), which had been boiled for 10 min and cooled, was added to the cells. To 25 uL carrier DNA/cell mixture, 5 uL of PCR product was added. Cells were incubated for 15 min at 30˚C and then 150 uL of a LiAcetate/PEG solution (~50% (w/v) PEG-3350, 100 mM LiAcetate) was added. Cells were again incubated for 0.5-1.5 h at 30˚C, followed by

the addition of 17 uL of DMSO. Cells were heat shocked for 15 min in a 42˚C water bath. Upon pelleting the cells by centrifugation (1000 xg for 5 min), the supernatant was carefully removed. The cells were resuspended in 200 uL of YPD and incubated at 30˚C for 0.5-3 h, depending on the selectable marker used. The entire transformation reaction was plated on selective plates and incubated at 30˚C for 36-48 h in a shaking incubator. SD,-uracil selective plates were used when generating the *ade4*Δ*::URA3* strain and SD,-histidine plates for Ade4 TANGO variants.

Building the GS.Ade4-GFP Strain

The GS.Ade4-GFP yeast strain was built to resemble the Ade4-GFP strain (Invitrogen, Huh et al. 2003), which was initially used to observe the punctate foci phenomenon. It was necessary to build the GS.Ade4-GFP strain to perfect the techniques necessary to build the Ade4-TANGO variants and prepare a control strain with a background identical to the Ade4 TANGO variants.

The pFA6a-Ade4-GFPS65T-HIS3MX6 plasmid was generated as a master template upon which all future Ade4 TANGO variant gene constructs would be prepared. The plasmid was prepared by cloning the *ADE4* gene into the pFA6a-GFPS65T-HIS3MX6 plasmid (Longtine et al.1998). Using the commercially available Ade4-GFP yeast strain (Invitrogen) as template, the *ADE4* gene was PCR amplified using primers containing BamHI restriction digestion sites. The *ADE4* gene construct was non-directionally cloned using a BamHI (NEB) digestion and subsequent ligation. The generated "pFA6a-Ade4-GFPS65T-HIS3MX6" plasmid contained a single G to A mutation. This mutation was corrected using the "mega primer" whole plasmid PCR method described in the generation of the Ade4 TANGO variant gene constructs.

To generate the GS.Ade4-GFP strain, the "Ade4-GFP-His3" construct was PCR amplified from the pFA6a-Ade4-GFPS65T-HIS3MX6 plasmid described above. The construct encodes the Ade4-GFP fusion protein (containing wild type *ADE4*), yADH1 transcription terminator, as well as the *Saccharomyces kluyveri HIS3* gene under the *Ashbya gossypii* TEF promoter and terminator sequences (Longtine et al. 1998). The construct is flanked with regions homologous to the genome upstream and downstream of *URA3* in the *ade4*Δ*::URA3*(i.e. genomic DNA flanking *ADE4* site).

It is perhaps worth noting that the original yeast GFP library paper (Huh et al. 2003) reported the *Schizosaccharomyces pombe HIS5* selectable marker was used, but sequence verification of this strain revealed the *Saccharomyces kluyveri HIS3* gene.

Using the transformation described above, the Ade4-GFP-His3 PCR product was transformed into the *ade4*Δ*::URA3* strain, thus generating the "GS.Ade4-GFP" strain. The strain was PCR verified using colony PCR product generated from genomic flanking primers.

Generation of Ade4 TANGO variants

Mega Primer Whole Plasmid PCR

To introduce single nucleotide (nt) or 1-3 neighboring nt changes/mutations into a plasmid, the mega primer whole plasmid PCR method was utilized. This method was used to fix an unwanted mutation that occurred in the pFA6a-Ade4-GFPS65T-HIS3MX6 plasmid and to create Ade4 TANGO gene constructs. To perform this method, PCR reactions using primers containing the sequence change and the plasmid template (such as pFA6a-Ade4-GFPS65T-HIS3MX6) were used to generate 0.5-1.0 kb products. A high fidelity DNA polymerase is required. The resulting PCR products are spin-column

purified (Qiagen) and then used as primers in a subsequent PCR reaction with the plasmid template (500 ng "primers" and ~100 ng plasmid template per 50 uL reaction). An initial denaturation step of 95˚C for 2 min was performed, followed by 18 thermocycler cycles of the following program: 95˚C – 30 sec, 55˚C – 30 sec, 68˚C – 10 min. A subsequent DpnI (NEB) reaction (1 uL DpnI/50 uL PCR reaction and incubate at 37˚C for 1 h) digested the methylated plasmid template containing the unwanted sequence. Sampling of the pre-PCR reaction, pre-DpnI digestion, and post-DpnI digestion aid in the identification of products on an agarose gel. Once digestion is completed, 2 uL of the fixed linear plasmid are transformed into *E.coli* cells. *E.coli* are plated on selective media. Colonies are prepped and plasmids are later purified and sequence verified.

Transformation of Ade4 TANGO DNA Constructs into ade4Δ::URA3 Strain Genome

Upon generating the pFA6a plasmids with the Ade4 TANGO constructs, the "Ade4-[TANGO score]-GFP-His3" linear constructs are generated using PCR, thereby encoding the Ade4 TANGO GFP-fusion protein with the *HIS3* selectable marker. These constructs were transformed into the *ade4Δ::URA3* yeast strain using the transformation method described previously. Colony PCR products from all yeast Ade4 TANGO variants were sequence verified.

OD_{600nm} Growth Curves

OD_{600nm} growth curves were performed to evaluate the function of the yeast Ade4 TANGO variants.

Cultures (3 mL) were generated selecting colonies from plates and growing cultures overnight in media in a 30˚C shaking incubator. Overnight cultures were diluted to an OD_{600nm} of 0.02. Cultures, in 100 uL aliquots, were distributed to the wells of clear 96-well plates. The OD_{600nm} was read every 10 min for 36 h at 30˚C on a BioTek Synergy HT-I plate reader. The plate was shaken for 9 min and then rested for 1 min prior to each reading. Media only controls were monitored for contamination or spillover.

Competitive Growth Experiments

To generate the starting cultures, overnight cultures grown in SD media or SD,-adenine media seeded new 3 mL cultures (OD_{600nm} 0.2). Cultures were grown for 4 h at 30˚C. Glycerol stocks (17% glycerol) of individual strains were prepared.

Co-cultures were generated, mixing equal parts of each culture (final OD_{600nm} 1.0). Glycerol stocks (17% glycerol) using these concentrated "t = 0" cultures were prepared. Cultures were diluted to an OD_{600nm} of 0.02 or 0.04 and incubated cultures for 24 hours in a 30˚C shaking incubator. Every 24 hours, glycerol co-culture stocks were prepared, cultures were diluted to an OD_{600nm} of 0.02, and cultures were returned to a 30˚C shaking incubator.

The strain composition reactions were designed as follows. Initially, restriction sites unique to either the TANGO variant or the Ade4 WT strain were identified. PCR reactions were designed maximizing product size, while limiting the restriction site to the area of the mutation. For the co-cultures containing Ade4-mtoin2034 and/or Ade4-mtoin2105, a 689 bp PCR product was generated for a MwoI restriction enzyme digestion. The MwoI restriction site was unique to the wild type *ADE4* gene. After

digestion with MwoI, the wild type *ADE4* gene was detected by the presence of 278 bp and 411 bp bands. For the Ade4-2800 competitive growth experiments, a 395 bp PCR product was generated for a BtsCI restriction enzyme digestion. The BtsCI restriction site was unique to the wild type ADE4 gene. After digestion with BtsCI, the wild type ADE4 gene was detected by the presence of 112 bp and 283 bp bands.

Strain composition of co-cultures was determined as follows. Glycerol stocks served as template for population PCR reactions. Speroplasted cells were generated by mixing an ice chip from a glycerol stock with 75 units (30 uL) Zymolase and incubating at 37˚C for 30 min. Population PCR (50 uL reactions) was performed on speroplasted cells, amplifying the region around the site of mutation. PCR products were purified using Qiagen spin-columns. Purified DNA (44 uL) was digested by the appropriate digestion enzymes, MwoI (5 U, NEB) at 60˚ for 16 h or BtsCI (20 U, NEB) at 50˚ for 16 h. Digestion products were run on 2% (w/v) agarose gels (NuSieve 3:1) in TBE. Gels were analyzed and band intensity was quantitated using the ImageJ program (1.43u, NIH).

REFERENCES

Chen Y, Dokholyan NV: Natural selection against protein aggregation on self-interacting and essential proteins in yeast, fly, and worm. Mol Biol Evol 2008, 25:1530-1533.

Crapeau M, Marchal C, Cullin C, Maillet L: The cellular concentration of the yeast Ure2p prion protein affects its propagation as a prion. Mol Biol Cell 2009, 20:2286-2296.

Dong X, Stothard P, Forsythe IJ, Wishart DS: PlasMapper: a web server for drawing and auto-annotating plasmid maps. Nucleic Acids Res 2004, 32:W660-664.

Drummond DA, Wilke CO: The evolutionary consequences of erroneous protein synthesis. Nat Rev Genet 2009, 10:715-724.

Fernandez-Escamilla AM, Rousseau F, Schymkowitz J, Serrano L: Prediction of sequence-dependent and mutational effects on the aggregation of peptides and proteins. Nat Biotechnol 2004, 22:1302-1306.

Ganesh C, Zaidi FN, Udgaonkar JB, Varadarajan R: Reversible formation of on-pathway macroscopic aggregates during the folding of maltose binding protein. Protein Sci 2001, 10:1635-1644.

Gelperin DM, White MA, Wilkinson ML, Kon Y, Kung LA, Wise KJ, Lopez-Hoyo N, Jiang L, Piccirillo S, Yu H, et al.: Biochemical and genetic analysis of the yeast proteome with a movable ORF collection. Genes Dev 2005, 19:2816-2826.

Goldsmith M, Tawfik DS: Potential role of phenotypic mutations in the evolution of protein expression and stability. Proc Natl Acad Sci U S A 2009, 106:6197-6202.

Guerois R, Nielsen JE, Serrano L: Predicting changes in the stability of proteins and protein complexes: a study of more than 1000 mutations. J Mol Biol 2002, 320:369-387.

Huh WK, Falvo JV, Gerke LC, Carroll AS, Howson RW, Weissman JS, O'Shea EK: Global analysis of protein localization in budding yeast. Nature 2003, 425:686-691.

Kabsch W, Sander C: Dictionary of protein secondary structure: pattern recognition of hydrogen-bonded and geometrical features. Biopolymers 1983, 22:2577-2637.

Krahn JM, Kim JH, Burns MR, Parry RJ, Zalkin H, Smith JL: Coupled formation of an amidotransferase interdomain ammonia channel and a phosphoribosyltransferase active site. Biochemistry 1997, 36:11061-11068.

Li Z, Lee I, Moradi E, Hung NJ, Johnson AW, Marcotte EM: Rational extension of the ribosome biogenesis pathway using network-guided genetics. PLoS Biol 2009, 7:e1000213.

Longtine MS, McKenzie A, 3rd, Demarini DJ, Shah NG, Wach A, Brachat A, Philippsen P, Pringle JR: Additional modules for versatile and economical PCR-based gene deletion and modification in Saccharomyces cerevisiae. Yeast 1998, 14:953-961.

Manivasakam P, Weber SC, McElver J, Schiestl RH: Micro-homology mediated PCR targeting in Saccharomyces cerevisiae. Nucleic Acids Res 1995, 23:2799-2800.

Miller S, Janin J, Lesk AM, Chothia C: Interior and surface of monomeric proteins. J Mol Biol 1987, 196:641-656.

Muchmore CR, Krahn JM, Kim JH, Zalkin H, Smith JL: Crystal structure of glutamine phosphoribosylpyrophosphate amidotransferase from Escherichia coli. Protein Sci 1998, 7:39-51.

Narayanaswamy R, Levy M, Tsechansky M, Stovall GM, O'Connell JD, Mirrielees J, Ellington AD, Marcotte EM: Widespread reorganization of metabolic enzymes into reversible assemblies upon nutrient starvation. Proc Natl Acad Sci U S A.

Pawar AP, Dubay KF, Zurdo J, Chiti F, Vendruscolo M, Dobson CM: Prediction of "aggregation-prone" and "aggregation-susceptible" regions in proteins associated with neurodegenerative diseases. J Mol Biol 2005, 350:379-392.

Plost B: Protein Aggregation Optimization: An Algorithmic Approach [Undergraduate Honors Thesis]. Austin: University of Texas at Austin: 2009.

Roberts RL, Metz M, Monks DE, Mullaney ML, Hall T, Nester EW: Purine synthesis and increased Agrobacterium tumefaciens transformation of yeast and plants. Proc Natl Acad Sci U S A 2003, 100:6634-6639.

Simpson RJ: Proteins and proteomics: a laboratory manual. Cold Spring Harbor, NY: Cold Spring Harbor Laboratory Press; 2003.

Thompson JD, Higgins DG, Gibson TJ: CLUSTAL W: improving the sensitivity of progressive multiple sequence alignment through sequence weighting, position-specific gap penalties and weight matrix choice. Nucleic Acids Res 1994, 22:4673-4680.

Tokuriki N, Stricher F, Schymkowitz J, Serrano L, Tawfik DS: The stability effects of protein mutations appear to be universally distributed. J Mol Biol 2007, 369:1318-1332.

Winzeler EA, Shoemaker DD, Astromoff A, Liang H, Anderson K, Andre B, Bangham R, Benito R, Boeke JD, Bussey H, et al.: Functional characterization of the S. cerevisiae genome by gene deletion and parallel analysis. Science 1999, 285:901-906.

Zhou T, Weems M, Wilke CO: Translationally optimal codons associate with structurally sensitive sites in proteins. Mol Biol Evol 2009, 26:1571-1580.

Chapter 3: Method Development: Punctate Quantification

INTRODUCTION

Examples of Punctate Foci and Types of Quantification

Punctate foci or intracellular "spots" come in many forms. Immunofluorescently labeled histone γ-H2AX foci accumulate at the site of DNA double stranded breaks upon exposure to ionizing radiation (Das et al. 2007, Redon et al. 2010). Alternatively, mice challenged with B16OVA melanoma tumor cells form black metastatic foci on lung tissue (Krishnan et al. 2003). Likewise, in *in* situ hybridization colorimetric assays, *Cryptosporidium parvum* infections are detected using an 18S rRNA specific probe and quantifying the foci (Rochelle et al. 2001). In the examples provided here, foci quantification (manually obtain) was essential to the work.

An accurate quantification of the foci (specifically, transiently forming foci) is essential for the evaluation of the phenomenon. This evaluation may take the form of (1) identification of punctate foci, (2) kinetics of formation or dissolution of punctate foci, (3) punctate foci penetrance (or the percentage of cells containing puncta), (4) punctate foci size and/or fluorescence intensity, (5) punctate foci cellular localization, and/or (6) intracellular count of puncta foci, as well as other features that may be employed to characterize the phenomenon.

The Problem with Counting Puncta

Counting puncta is an inherently simple problem to understand. Then why can it be so complicated? Humans are biased, leading to inconsistencies in punctate

identification and variations of counts between people. For instance, the "intermediate" punctate appear as neither completely diffuse protein, nor discrete punctate foci. The designation between the two groups varies widely. Additionally, oftentimes puncta are not visible using brightfield microscopy, therefore fluorescence microscopy must be employed. The overall fluorescence intensity fluctuates as GFP-tagged protein expression can vary from culture-to-culture or even cell-to-cell. Additionally, focusing on a single plane can obscure puncta in distant planes and obfuscates the overall cellular puncta count. The problem is further complicated when trying to quantify the puncta penetrance (or percentage of cells containing puncta) in a yeast culture. Perhaps one of the most challenging aspects of quantifying puncta is that puncta are transient bodies, i.e. they form or dissipate over time. Lastly, a modestly large number of yeast cells must be counted to precisely represent the puncta penetrance of a population. We have found it necessary to manually count at least 200 yeast Ade4-GFP cells to precisely represent the population (Patel 2010). This population sample number could vary from strain to strain, but the necessary cell count illustrates the time intensive and laborious nature of the process.

Manually Counting Puncta

Manual inspection of fluorescence microscopy images has become the method of choice when quantifying punctate penetrance in yeast. Typically, to manually count cells from a single culture, 200 cells are imaged in a minimum of 4 fluorescence and 4 brightfield images (Patel 2010). Total cell number is determined and then the cells containing puncta (or "puncta positive" cells) are counted to determine the punctate

penetrance or percentage of cells containing puncta. To standardize the manual counting practices, a number of rules or guidelines were established:

1. A cell containing one or more puncta was considered "puncta positive."
2. Cells containing more than four puncta were not "puncta positive" and instead not counted for belief that another phenomenon was occurring.
3. If a majority of the cell was included in the microscopy image, then it was counted.
4. Out-of-focus cells were counted at the discretion of the observer, if the observer believed he/she could discern puncta, if present.
5. As with the case of budding cells or attached cells, if the budding or attached cell appeared large enough to contain potential puncta, then it was counted.
6. All identified fluorescent puncta had to be located within a cell. This was accomplished by overlaying the fluorescence image on the brightfield image and verifying the localization of the puncta.
7. To determine punctate penetrance (i.e. percentage of cells containing puncta), it was necessary to count both the "punctate positive" cells and the total cells using the rules listed here.

Automated image analysis in the form of intensity thresholding techniques was evaluated to mitigate the manual counting problems. Using this method, punctate penetrance was determined by finding the ratio of puncta to total cells. An image intensity threshold was determined and all objects above that threshold intensity were counted, thus determining total puncta. The total number of cells was determined one of two ways: manually counting cells or using Calcofluor white to fluorescently stain the outer membrane of the cell. Cell quantification, using the Calcofluor staining method, involved intensity thresholding to identify and count the cells. Utilizing such techniques

was at best clumsy and the settings derived for one set of experiments rarely transferred to other experiments. This left the observer regularly adjusting the punctate threshold range and manually validating the counting practice. There may have been a slight time advantage when using such image analytical tools, but this advantage was overshadowed by the manual validation requirements of such tools. Additionally, the analytical method only counted a fraction of the cells as cells were regularly omitted, because of cell clustering or improper staining. Ultimately, it was found that the automated image analysis offered few if any advantages over the manual counting techniques and the automated image thresholding analysis was abandoned.

QUANTIFYING PUNCTA USING TRADITIONAL FLOW CYTOMETRY

Given the different fluorescent properties of punctate and non-punctate cells, we asked if puncta could be quantified using flow cytometry. Initial work began with the Gln1-GFP strain. 48 hours of growth in YPD media was sufficient for stationary phase induction of Gln1-GFP puncta, while incubating cells (starting OD_{600nm} of 0.2) for 2 hours at 30˚C generated log phase cells that were free of puncta. Examination of stationary phase cells and log phase cells on a BD FACS Calibur revealed a shift of green fluorescence (Figure 3-1). The results were recapitulated with the punctate forming CTP synthase isozyme, Ura7-GFP cells (Figure 3-2). Additionally, puncta could be dissipated in punctate positive Gln1-GFP stationary phase cells by replacing the spent media with fresh YPD media and incubating the cells for 2 hours at 30 ˚C. FACS examination of these recovered cells revealed a broad peak, shifted between the stationary phase peak and the log phase peak (occasionally more resembling the log phase peak).

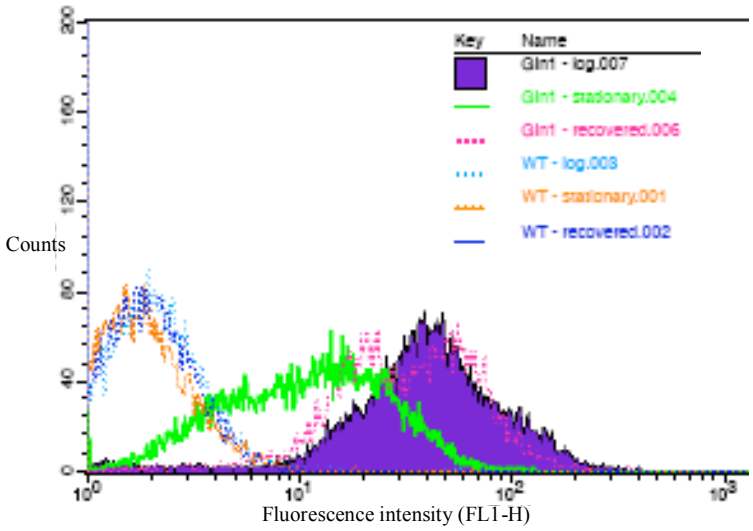

FIGURE 3-1 FLOW CYTOMETRY: GLN1-GFP CELLS. These are the flow cytometry results of Gln1-GFP and wild type (WT, without GFP tag) stationary phase, log phase, and recovered cells. The punctate positive stationary phase cells had a peak shift (decreased fluorescence intensity) when compared to the log phase cells. Punctate positive stationary phase cells were generated after 2 days of growth at 30˚C. Non-punctate log phase cells were generated from these cells after diluting the culture to an OD_{600nm} of 0.2 (45-fold dilution) and incubating the culture at 30˚C for 2 hours. Non-punctate "recovered" cells were prepared from stationary phase cells; media was removed and replaced with fresh YPD, while diluting the cells 2-fold. Recovered cells were incubated at 30˚C for 2 hours. The WT cells were used as a control to identify the GFP specific signal. 10,000 events were collected on the flow cytometer.

Perhaps diffuse Gln1-GFP or Ura7-GFP protein or an increased protein concentration caused the increased fluorescence shift of the log phase cells. Western blot analysis confirmed an approximately 2-fold increase of Gln1-GFP in log phase cells compared to stationary phase cell (data not shown).

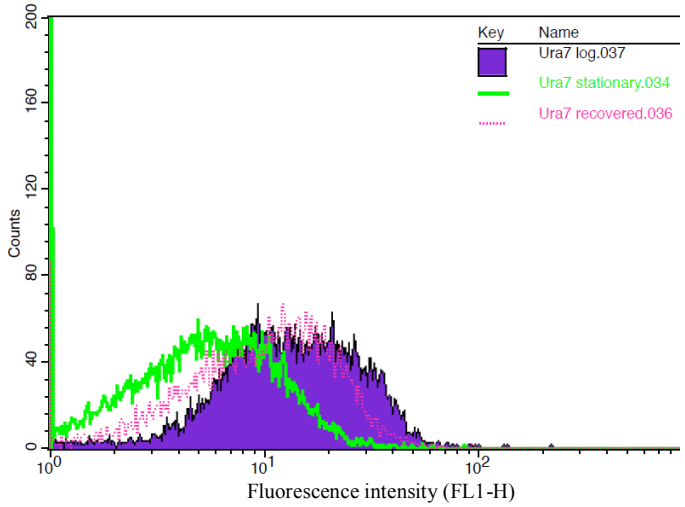

FIGURE 3-2 FLOW CYTOMETRY: URA7-GFP CELLS. These are the flow cytometry results of Ura7-GFP stationary phase, log phase, and "recovered" cells. The punctate positive stationary phase cells had a peak shift (decreased fluorescence intensity) when compared to the log phase cells. Punctate positive stationary phase cells (~25% punctate penetrance) were generated after 2 days of growth at 30˚C. Non-punctate log phase cells were generated from these cells after diluting the culture to an OD_{600nm} of 0.3 and incubating the culture at 30˚C for 2.5 hours. Non-punctate "recovered" cells were prepared from stationary phase cells; media was removed and replaced with fresh YPD. Recovered cells were incubated at 30˚C for 2.5 hours.

To address concerns of varying cell age and other conditions, FACS experiments were performed using Gln1-GFP cells harvested from the same parental culture and compared punctate induced cells to non-punctate cells. Puncta were induced using glucose depleted synthetic complete media (SC,-glucose media). After SC,-glucose induction, the punctate positive cells had a peak shift (decreased fluorescence) (Figure 3-3). More work was necessary to determine the cause of such a FACS shift.

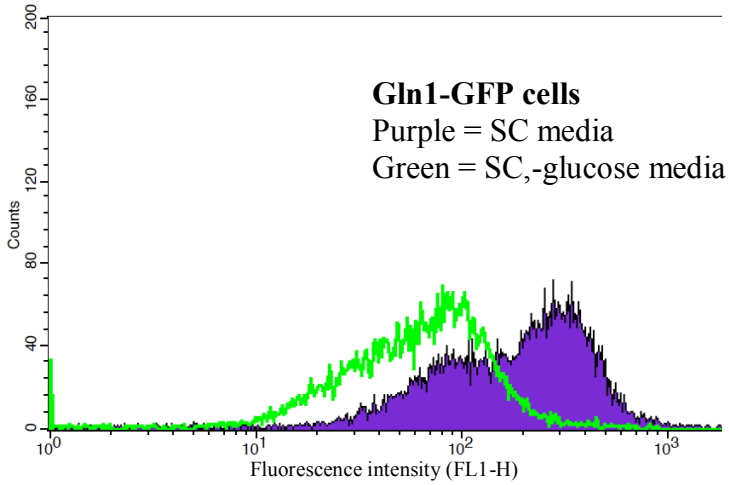

FIGURE 3-3 FLOW CYTOMETRY: GLN1-GFP CELLS. These are the flow cytometry results of Gln1-GFP cells in SC media and SC,-glucose media. The punctate positive cells induced in SC,-glucose provided a FACS peak shift (decreased fluorescence) compared to the non-punctate cells in SC media. Cells were generated by diluting a 48 hour SC culture to an OD_{600nm} of ~0.3 and growing for 2 hours at 30˚C to an OD_{600nm} of ~0.5. Cells were split and media was replaced with either SC or SC,-glucose media. Cultures grew for an additional 2 hours at 30˚C, then obtained microscopy images immediately before running cells on flow cytometer.

To evaluate the cause of the flow cytometry peak shift, the flow cytometry work was repeated on a BD FACS Aria machine, which has cell sorting capabilities. Analysis of the Gln1-GFP stationary phase cells with punctate foci revealed a broad peak, possibly containing multiple populations of cells (Figure 3-4). The broad peak was sorted into two populations: P1 gated cells (less fluorescence) and P2 gated cells (greater fluorescence). Both populations of sorted cells were viewed using fluorescence microscopy and punctate penetrance was estimated. By visual inspection, the less intense P1 sorted cells appeared to have a greater punctate penetrance than the more intense P2 sorted cells. Likewise, log phase Gln1-GFP cells, which were mostly void of GFP-tagged puncta, were analyzed on the BD FACS Aria. Using the gating parameters established using the stationary phase cells, the single peak of log phase cells appeared in

the more intense P2 gate (Figure 3-4). The P2 gated cells were collected and inspected using fluorescence microscopy, which revealed that the previously non-punctate cells were now in a punctate state. The results were not completely surprising, as the Gln1-GFP cells, which were in YPD media, were being passed through the flow cytometer surrounded by a phosphate buffered saline environment. The yeast Gln1-GFP cells will form puncta when suspended in water (Narayanaswamy et al. 2009). Therefore, the punctate state of the FACS sorted cells might be expected. In subsequent work, glutaraldehyde cellular fixative (4%) was utilized, but did not preserve the non-punctate state of the log phase Gln1-GFP cells. Punctate quantitation using traditional flow cytometry techniques were abandoned for an advanced flow cytometer with fluorescence and brightfield imaging capabilities, which will be discussed in the following section.

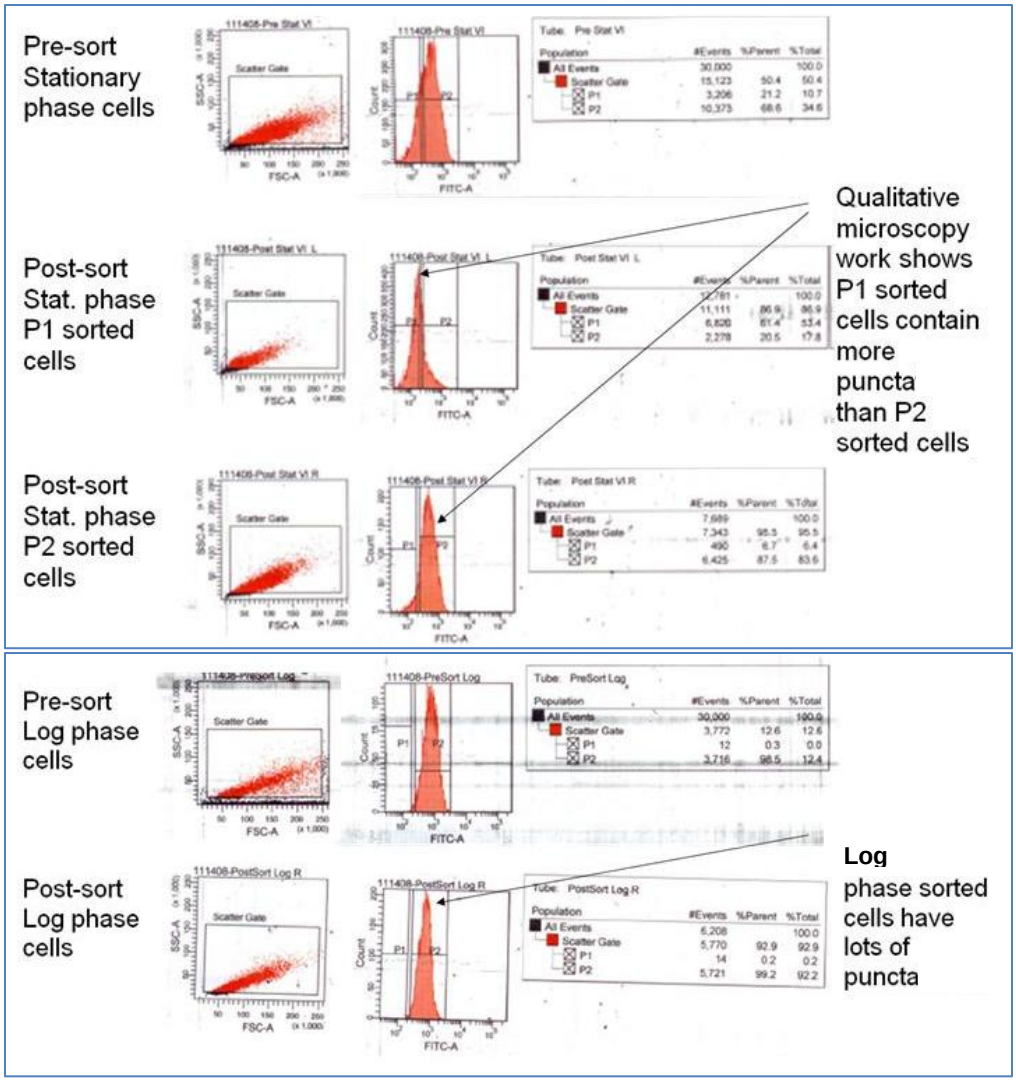

FIGURE 3-4 FLOW CYTOMETRY CELL SORTING: GLN1-GFP CELLS. Populations of Gln1-GFP stationary phase and log phase cells were sorted using the BD FACS Aria. Stationary phase cells were sorted into two bins: P1 and P2. Post-sort examination of the cells revealed that the P1 bin contained more puncta than the P2 bin. The log phase cells were contained in the P2 bin and the post-sort examination of these cells revealed many puncta. Punctate positive stationary phase cells were generated after 2 days of growth at 30˚C. Non-punctate log phase cells were generated from these cells after diluting the culture to an OD_{600nm} of 0.3 (41-fold dilution) and incubating the culture at 30˚C for 2 hours. Non-punctate "recovered" cells were prepared from stationary phase cells; media was removed and replaced with fresh YPD, while diluting the cells 2-fold. Recovered cells were incubated at 30˚C for 2 hours.

AMNIS IMAGESTREAM QUANTITATION

Analytical Scheme Development

The ImageStream (Amnis, Seattle, WA) imaging flow cytometer was utilized to mitigate the manual foci quantification problems. The ImageStream combines the capabilities of a flow cytometer with high resolution brightfield and fluorescence microscopy. At 40x magnification, Amnis reports flow cytometry speeds of 1,000 cells/second, with the use of up to 5 lasers and 12 images per a cell (https://www.amnis.com).

The *S. cerevisiae* Ade4-GFP (phosphoribosylpyrophosphate amidotransferase-GFP) yeast strain forms GFP-tagged punctate foci through nutrient depletion, such as through stationary phase induction or in the presence of synthetic defined media lacking adenine (SD,-ade). The Ade4-GFP strain reaches maximum punctate penetrance of ~50-60% within 2 hours in SD,-ade media. This rapid reorganization of protein may be observed using the ImageStream technology, and therefore a time course experiment sampling the yeast over a 2 hour period after SD,-ade induction was used to train the analytical scheme. Specifically, the punctuate count of the samples, as determined by visual inspection, were used to generate the analytical scheme.

To quantify the punctate foci, Brian Hall at Amnis (Seattle, WA) developed an ImageStream data analytical scheme, using the accompanying IDEAS software. All data files were batch processed through the four step gating regime to assure consistency of gating. Initially, single cells were separated from debris and multi-cellular aggregates in the Brightfield channel using the IDEAS features Aspect Ratio and Area. The Aspect Ratio feature is a measure of object roundness (i.e. width divided by height). A perfect circle will have an Aspect Ratio of 1; doublets typically have an Aspect Ratio of ~0.5. Area was calculated by multiplying the pixels in the image by 0.5 um^2 at 40x

magnification or 0.33 um^2 at 60x magnification. The Area of cell clumps is usually three or more times the Area of single cells. Additionally, cell debris may be partitioned from the single cells, as the debris typically has a smaller Area and varied Aspect Ratio.

Upon identification of single cells, the focused cells were selected using the Gradient Root Mean Square (RMS) feature. This feature measures the change in pixel intensity across the edge of an image. Focused cells have a steep edge gradient, while unfocused cells with a blurry edge have less of an edge gradient. Typically ~50% of the events were dismissed in this step of the gating regime, although the flow cytometry settings could be better optimized to focus on the cells at the expense of the flow rate.

GFP positive cells were selected in the next step of the analytical scheme. These GFP positive events are identified by generating a histogram of Channel 2 (480-560 nm spectral band) intensity. Typically, less than 1% of the cells were lost in this step of the analysis.

The final step of the gating regime involved the identification of the punctate foci using the Area of the 30% Threshold Mask and the Bright Detail (BD) Intensity features. The 30% Threshold Mask identifies the most intense 30^{th} percentile of the pixels in the image; therefore, the Area of this Mask measures the size of the brightest pixels. Cells containing diffuse GFP have a greater Area of the 30% Threshold Mask, while cells containing punctate foci have a smaller Area of the 30% Threshold Mask. Specifically, in the diffuse state, more pixels qualify as the brightest 30^{th} percentile, because the pixel intensity values tend to be low and similar to each other. However, fewer pixels are indentified as the brightest 30^{th} percentile when the GFP is condensed into punctate foci. The Bright Detail Intensity identifies small spots within the cell (~3 um in diameter at 40x magnification) and then measures the overall pixel intensity of these spots (i.e. diffuse GFP has low BD intensity and GFP punctate foci have high BD intensity).

Testing and Validation

Inspection of the Ade4-GFP punctate foci counts revealed the manually obtained counts to be similar to the automated IDEAS counts (analytical scheme described above, Figure 3-5). This was expected, as manually obtained punctate counts were used to train the algorithm. A small-scale validation of the analytical scheme was obtained by performing a "blind test" on a newly prepared Ade4-GFP yeast strain (GS.Ade4-GFP) and a mutant Ade4-GFP yeast strain (Ade4-mtoin2786). The manual punctate counts were not revealed before the automated IDEAS punctate counts were reported and vice versa. Correlation between the manual counts and the automated IDEAS counts of the trained and blind test sets revealed R-squared values of 0.98 or better (Figure 3-6).

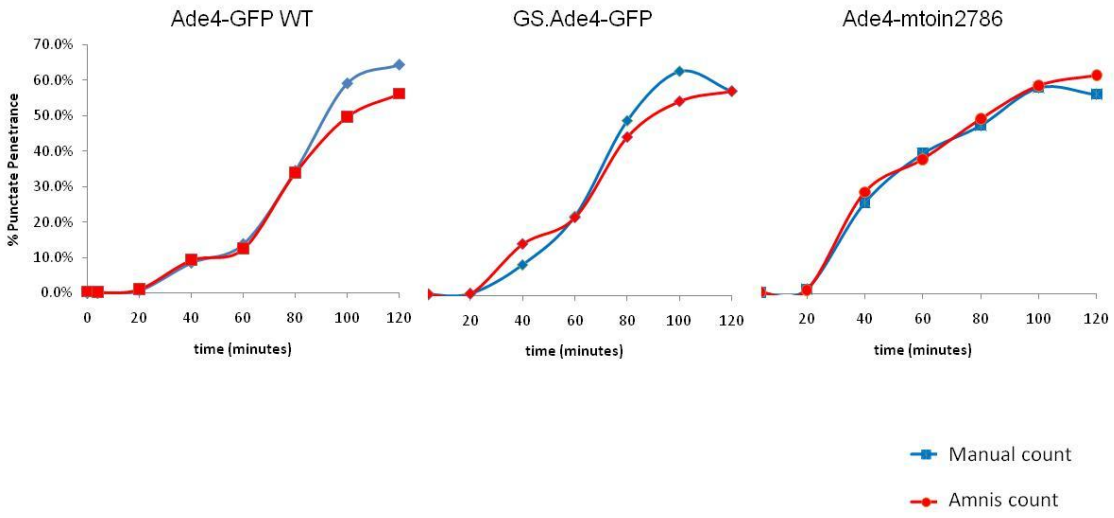

FIGURE 3-5 AMNIS IMAGESTREAM/IDEAS PUNCTATE FOCI QUANTIFICATION. These are the results of the training and validation of the Amnis ImageStream/IDEAS punctate foci quantification scheme. The time course samples from the Ade4-GFP WT strain and the manual punctate foci counts were used to train the IDEAS analytical scheme. Validation tests were performed using the time course samples from the GS.Ade4-GFP strain and the Ade4-mtoin2786 strain and comparing the manual punctate foci counts with the automated IDEAS punctate counts. The time course samples were prepared using a SD,-adenine punctate induction method (manuscript in preparation).

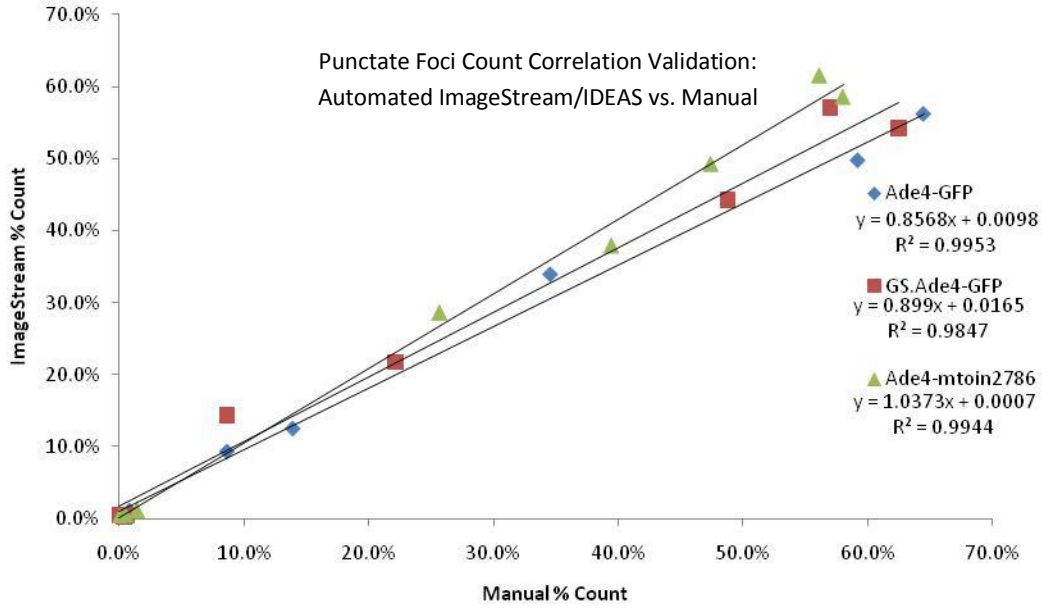

FIGURE 3-6 CORRELATION VALIDATION OF THE AUTOMATED IMAGESTREAM COUNT. A correlation validation of the punctate foci was preformed, comparing the automated Amnis ImageStream/IDEAS count to the manual count. The time course samples from the Ade4-GFP strain were used to train the automated IDEAS foci count scheme. A "blind" validation test was performed using the time course samples from the GS.Ade4-GFP strain and the Ade4-mtoin2786 strain. In this test, the manual punctate counts were not revealed before the automated IDEAS punctate counts were reported or vice versa (manuscript in preparation).

A large-scale validation test was performed to compare the manual punctate counts to the automated IDEAS count (Figure 3-7). The Ade4-GFP strains as well as multiple mutant Ade4-GFP strains (1286-2800) were examined both by visual inspection and using the automated IDEAS analytical scheme described above. Again, the counts were very similar, with the most obvious differences occurring when technical difficulties occurred while obtaining the fluorescent images for the manual counts. These images were "blurry" (i.e. large RMS gradients), therefore obscuring the intracellular features, including puncta, and presumably reduced the reported puncta count.

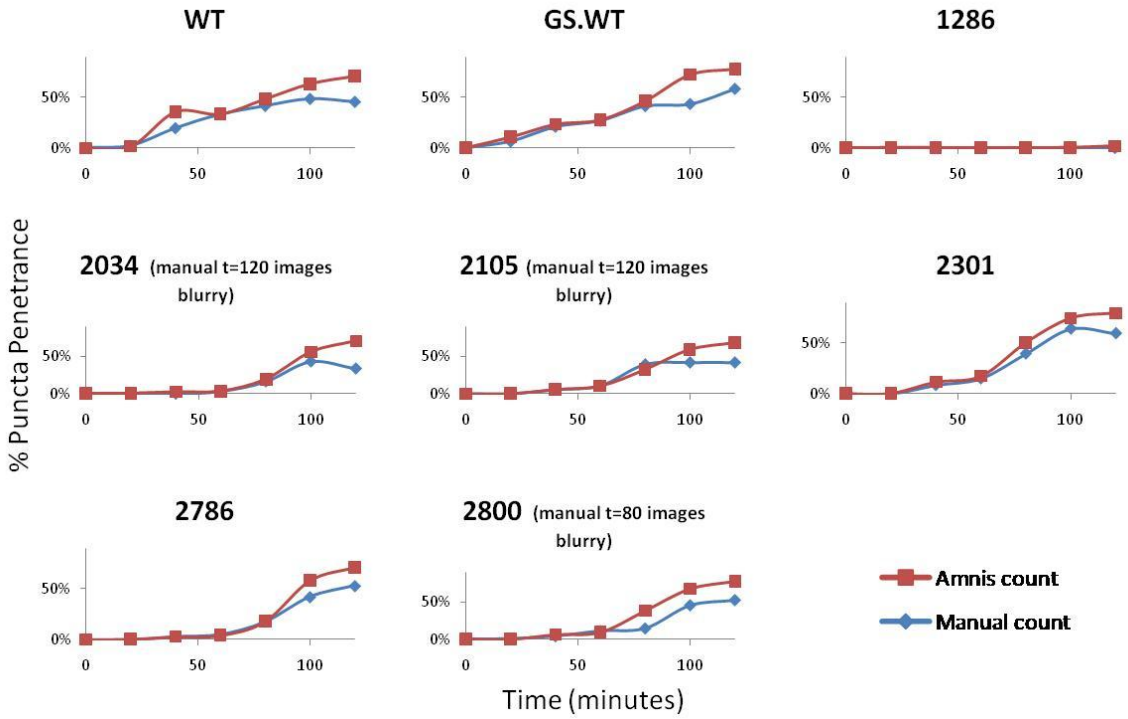

FIGURE 3-7 COMPARISON BETWEEN AUTOMATED AND MANUAL COUNTS. The automated Amnis ImageStream/IDEAS punctate foci counts were compared to the manual punctate foci counts. Ade4-GFP WT (WT), GS.Ade4-GFP (GS.WT), Ade4-1286 (1286), Ade4-mtoin2034 (2034), Ade4-mtoin2105 (2105), Ade4-mtoin2301 (2301), Ade4-mtoin2786 (2786), and Ade4-2800 (2800) cells fixed and counted using the automated IDEAS method and manual method described previously. Time course samples were prepared using a SD,-adenine punctate induction method.

Method Refinement

The IDEAS analytical scheme was adapted to a newly acquired ImageStream and we used the opportunity to refine the method to the new instrument's parameters and for use with other GFP labeled yeast strains. Designed by Jeremy O'Connell, the sequence of gating events was reordered by stringency from coarse to fine, thereby further optimizing the order, while essentially maintaining the purpose of the scheme. Initially,

focused cells, single cells, and then GFP positive cells were gated using the same features described previously. The final step of the refined analytical scheme, selecting cells with punctate foci, involved the Area of the 30% Threshold Mask (as described previously) and the Intensity of the 30% Threshold Mask. The Intensity of the 30% Threshold Mask feature, much like the Bright Detail Intensity feature used previously, separates events to permit the selection and gating of punctate positive cells. While the Intensity of the 30% Threshold Mask feature uses the same intensity threshold to identify the brightest pixels, the Bright Detail is specific to the pixels within in the small spots (~3 uM wide at 40x magnification). The increased range of separation permits better partitioning of the intermediate states.

Thus, another refinement was made in the final binning of the cells into "punctate," "nonpunctate," and "granular" (or intermediate) groups. Previously, just two bins were used (i.e. punctate and nonpunctate bins). Inspection of the gated cells in the IDEAS program revealed that there were three cells types and we sought to classify these intermediate cells as such. Instead of making a distinction at this point, we sought to keep the three bins of cells and see how these bins compared to the manually obtained punctate count.

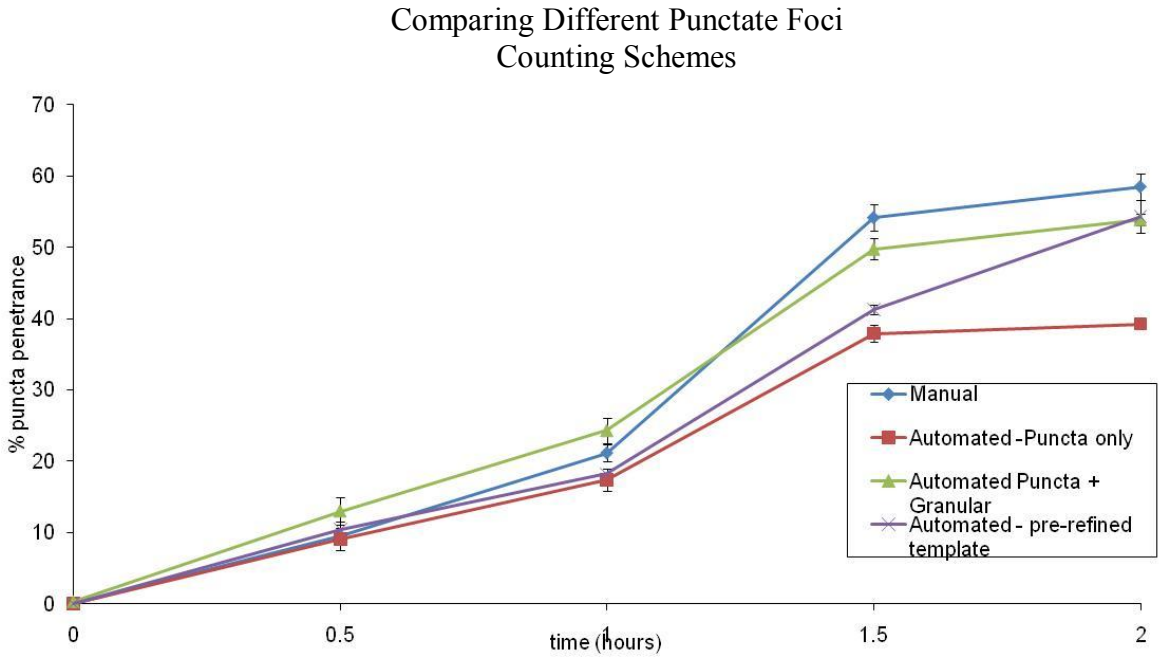

FIGURE 3-8 COMPARISON OF DIFFERENT AUTOMATED PUNCTATE FOCI COUNTING SCHEMES. The Ade4-GFP cell samples (n=3) were counted using the manual counting scheme and 3 different automated IDEAS counting schemes. The "Automated – pre-refined template" count were generating using the original automated analytical scheme. Using the refined automated analytical schemes, the "Automated – Puncta only" count included only the "punctate" bin of the analytical scheme, while the "Automated Puncta + Granular" count included "punctate" and "granular" bins of the analytical scheme. Time course samples were prepared using a SD,-adenine punctate induction method.

Comparison of Analytical Methods

The original and refined IDEAS analytical schemes were compared using Ade4-GFP cells in punctate inducing SD,-adenine media. The automated punctate foci counts were similar to the manual counts. The "punctate" only count from the refined analytical scheme underestimated the foci count, as compared to the manual count. Alternatively, the sum of the "punctate" count and the "granular" count from the same scheme better

resembled the manual foci count. These counts could indicate that the manual counts included both bins in the punctate counts, as an intermediate classifier was not used in the manual count. Alternatively, this could be indicative of the difference in the quality of images between the microscopes and the ImageStream, as images of poor quality may hinder punctate identification. Or – an adjustment of the punctate-positive bin may be necessary to include these "granular" containing cells. All IDEAS analytical schemes provided punctate foci counts that correlated to the manual counts with R-squared values of 0.97 or better (Figure 3-9). The refined schemes provided the best correlation with R-squared values greater than 0.99.

The comparison of the analytical methods involved the use of the original scheme, which was initially developed and tested on another ImageStream. Laser intensities and settings may vary slightly between machines. Therefore, independent gating regimes are necessary from cytometer-to-cytometer, although the same gating strategy may be used.

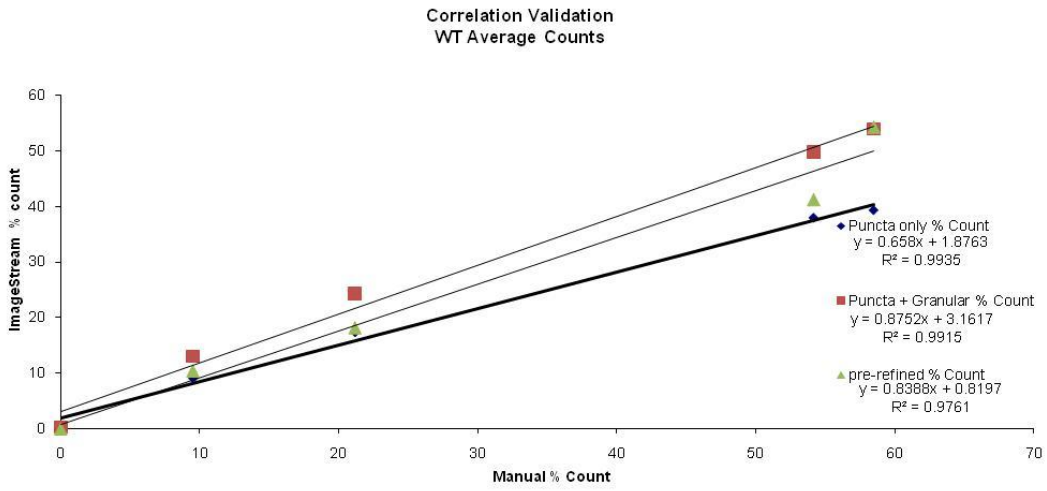

FIGURE 3-9 CORRELATION VALIDATION OF THE AUTOMATED IMAGESTREAM COUNT. A correlation validation of the punctate foci was preformed, comparing the automated Amnis ImageStream/IDEAS count to the manual count. The Ade4-GFP cell samples (n=3) were counted using the manual counting scheme and 3 different automated IDEAS counting schemes. The refined analytical schemes better recapitulated the manual puncta counts than the original ("pre refined") scheme. Time course samples were prepared using a SD,-adenine punctate induction method.

CONCLUSIONS

The time intensive and laborious nature of manually quantifying punctate foci necessitated the search for better quantification techniques. Traditional flow cytometery techniques appeared promising, but the validation of such work was complicated by the transient formation of punctate bodies, which were induced upon introduction into PBS in the cytometer, and the analysis based solely on fluorescence intensity. Changes in fluorescence intensity may be skewed by condensation or dissipation of protein, protein concentration, or photo bleaching and therefore always draws into question what was actually observed in the flow cytometry peak shifts. This work was abandoned, replaced instead by a newer tool on the market, the Amnis ImageStream imaging flow cytometer.

The combination of a flow cytometery with brightfield and fluorescence imaging capabilities, in addition to the readily available IDEAS image analytical tools, facilitated the design of multiple analytical schemes to quantify puncta. Every event generated a fluorescence and brightfield image, therefore gating schemes were easily assigned based on inspection of the images. Large scale comparisons between the automated punctate foci counts and the manual punctate counts validated the use of the equipment in punctate quantification.

In conclusion, the ImageStream imaging flow cytometer and IDEAS analytical software are capable of quantitating the punctate penetrance of yeast cells. The ImageStream is capable of counting thousands of cells (instead of the hundreds traditionally manually counted), thereby improving the precision and confidence. In a single day, the ImageStream and accompanying IDEAS software counts and analyzes thousands of cells or ~60 time course samples. It would normally take three to four days, at best, to manually obtain these fluorescence images and quantify the punctate penetrance. Perhaps one of the greatest advantages of this technique is that it removes much of the human subjectivity from the interpretation of a punctate and provides another method for the detection for this new phenomenon. Therefore, the ImageStream imaging flow cytometer will propel research into the yeast punctate phenomenon, analyzing cells in a fraction of the time, standardizing the definition of punctate foci without need for human interpretation, and improving precision far past what is feasible by manual quantification methods. While many researchers before us manually quantified foci by visual inspection (Das et al. 2007, Redon et al. 2010, Krishnan et al. 2003, Rochelle et al. 2001), this may be a way of the past. The benefits of the imaging flow cytometer may be widespread, as the technology allows researchers to move beyond the traditional manual foci quantification into automated quantification.

MATERIALS AND METHODS

Time Course: Stationary Phase Induction of Gln1-GFP and Ura7-GFP Puncta

Using Gln1-GFP or Ura7-GFP yeast strains (Invitrogen, Huh et al. 2003), punctate positive stationary phase cells were generated after 2 days of growth in YPD at 30˚C in a shaking incubator. Non-punctate log phase cells were generated from these stationary phase cells after diluting the culture to an OD_{600nm} of 0.2-0.3 and incubating the culture at 30˚C for 2-2.5 hours (1-1.5 population doublings).

Non-punctate "recovered" cells were prepared from stationary phase cells; media was removed by pelleting cells with centrifugation (3,700 xg for 2 min, 4˚C) and aspirating media. Cells were resuspended in fresh YPD to a concentration of 0.5x - 1x the stationary phase concentration. Recovered cells were incubated at 30˚C for 2-2.5 hours.

For the traditional flow cytometry, cells were examined using epifluorescence and brightfield microscopy immediately prior to running the cells on the cytometer. Sorted cells were examined on the microscope post-sort, as well.

Time Course: SC,-Glucose Media Induction of Gln1-GFP GFP Puncta

Early log phase Gln1-GFP cells (Invitrogen, Huh et al. 2003) were generated by diluting a 48 hour SC culture to an OD_{600nm} of ~0.3 and growing for 2 hours at 30˚C to an OD_{600nm} of ~0.5. Cells were split and media was replaced with either SC or SC,-glucose media. Cultures were incubated for an additional 2 hours at 30˚C, then microscopy images were obtained immediately before running cells on flow cytometer.

Time Course: SD,-Adenine Media Induction of Ade4-GFP Puncta

Early log phase yeast Ade4-GFP cells (Invitrogen, Huh et al. 2003) were prepared as follows. 3 mL starting cultures were grown in synthetic defined media lacking histidine (SD,-his, Sunrise Science) for 8 hours at 30˚C. Cultures were diluted in SD media (5 mL total volume, Sunrise Science) and grown overnight (~16 h) to an OD_{600nm} of 1.5. Cultures were again diluted in SD media (3-5 mL total volume) and grown for 4 hours to an OD_{600nm} of 0.5.

Ade4-GFP puncta were induced by replacing media of early log phase cells with SD,-adenine media (SD,-ade, Sunrise Science). Specifically, cells were pelleted by centrifugation (i.e. spun at 1,000 xg for 5 min). Media was aspirated and replaced with SD,-adenine media. For 2 hours, 0.5 mL cell aliquots were removed and fixed every ~20-30 minutes using the 4% formaldehyde fixation method described below. Cells were returned to the shaking 30˚C incubator in-between time points.

Cells were fixed in 4% formaldehyde (SPI Supplies) for 20 min at room temperature. Fixed cells were washed 3 times in 0.5 mL PBS (Invitrogen) by spinning cells at 10,000 rpm (12,400 xg) for 3 minutes, aspirating media, and resuspending cell pellet in PBS.

All OD measurements were performed at 600 nm. All cultures were grown at 30˚C in a shaking incubator.

Western Blot: Estimating Gln1-GFP Concentrations in Log Phase, Stationary Phase, and Recovered Cells

Gln1-GFP stationary phase, log phase, and recovered cells were prepared as described previously. Based on OD_{600nm}, cell equivalents (equivalent to 2.3 mL of 1

OD_{600nm} cells) were concentrated in 200 uL of YPD by centrifuging at 3,700 xg for 2 min, 4˚C and aspirating media. Roche protease inhibitor was added to cells and beads were lysed with glass beads and a BeadBeater. 10 uL of cell lysate was added to 4 uL of 4x LDS Loading Dye (Invitrogen) and lysates were denatured for 10 min at 70˚C. Lysates were run on a 4-12% NuPAGE Bis-Tris gel (Invitrogen) using MOPS running buffer (Invitrogen). Gel proteins were transferred to a PVDF membrane. The western was performed using rabbit α-GFP primary antibody (Sigma) and Goat α-rabbit-IR dye 680 secondary antibody (LiCore Odyssey). The blot was analyzed using the LiCor Odyssey.

REFERENCES

Das AK, Chen BP, Story MD, Sato M, Minna JD, Chen DJ, Nirodi CS: Somatic mutations in the tyrosine kinase domain of epidermal growth factor receptor (EGFR) abrogate EGFR-mediated radioprotection in non-small cell lung carcinoma. Cancer Res 2007, 67:5267-5274.

Huh WK, Falvo JV, Gerke LC, Carroll AS, Howson RW, Weissman JS, O'Shea EK: Global analysis of protein localization in budding yeast. Nature 2003, 425:686-691.

Krishnan L, Sad S, Patel GB, Sprott GD: Archaeosomes induce enhanced cytotoxic T lymphocyte responses to entrapped soluble protein in the absence of interleukin 12 and protect against tumor challenge. Cancer Res 2003, 63:2526-2534.

Narayanaswamy R, Levy M, Tsechansky M, Stovall GM, O'Connell JD, Mirrielees J, Ellington AD, Marcotte EM: Widespread reorganization of metabolic enzymes into reversible assemblies upon nutrient starvation. Proc Natl Acad Sci U S A 2009, 106:10147-10152.

Patel A: Generating Mutant Yeast and Measuring the Rate of Ade4 Punctate Foci Formation [Undergraduate Honors Thesis]. Austin: University of Texas at Austin: 2010.

Redon CE, Nakamura AJ, Gouliaeva K, Rahman A, Blakely WF, Bonner WM: The use of gamma-H2AX as a biodosimeter for total-body radiation exposure in non-human primates. PLoS One 2010, 5:e15544.

Rochelle PA, Ferguson DM, Johnson AM, De Leon R: Quantitation of Cryptosporidium parvum infection in cell culture using a colorimetric in situ hybridization assay. J Eukaryot Microbiol 2001, 48:565-574.

Chapter 4: Characterization and Manipulation of Puncta

PUNCTA KINETIC EXPERIMENTS USING TANGO MUTANTS

Introduction

We seek to understand the widespread reorganization of *S. cerevisiae* cytosolic proteins into "punctate foci" that occurs during starvation, originally described by Narayanaswamy et al (2009). We hypothesize that puncta are the result of self-aggregation or misfolded oligomers (described in Chapter 2). In support of the hypothesis, punctate forming proteins were computationally predicted using the TANGO algorithm (Fernandez-Escamilla et al. 2004) to have an increased self-aggregation propensity (Narayanaswamy et al. 2009). Most recently, the immunoprecipitation of Gln1-GFP puncta followed by mass spectrometry analysis identified the punctate proteins as Gln1p, GFP, and Hsc82p and/or Hsp82p (personal communication, J.D. O'Connell, University of Texas at Austin), further supporting the hypothesis of self-aggregation assemblies.

To test this hypothesis, yeast Ade4 TANGO variants were designed with predicted non-native aggregation propensities (described in Chapter 2). These yeast variants were built and their fitness was evaluated (described in Chapter 2). The Ade4 TANGO variants were used in kinetic experiments, comparing the rates of puncta formation. Punctate coverage was reported as puncta penetrance or the percentage of cells containing punctate foci. We predict the Ade4 TANGO variants with a predicted aggregation propensity greater than the wild type Ade4p aggregation propensity will form puncta faster and the Ade4 TANGO variants with a predicted aggregation propensity less than the wild type aggregation propensity will form puncta slower.

Time Course: Evaluation of Control Strain GS.Ade4-GFP and Ade4-mtoin2786 TANGO Variant

Initially, we sought to compare the kinetic curve of Ade4-GFP punctate formation to the control strain, GS.Ade4-GFP. The yeast GS.Ade4-GFP strain was designed to be identical to the Ade4-GFP strain (Invitrogen, Huh et al. 2003), which was in the library originally used to observe the phenomenon (Narayanaswamy et al. 2009). The GS.Ade4-GFP and the Ade4 TANGO variants were generated from the same parental strain (isogenic) and built using the same methodology (Chapter 2).

One of the first time course experiments compared Ade4-GFP, GS.Ade4-GFP, and the TANGO variant Ade4-mtoin2786. The design and the construction of the Ade4-mtoin2786 and all of the TANGO variants were described previously in Chapter 2. The time course was performed with early log phase cells. Puncta were induced using SD,-adenine media and cells were fixed at regular time intervals. Punctate penetrance of the fixed cell samples was quantitated manually by visual inspection using fluorescent microscopy (Figure 4-1) and quantitated using the Amnis ImageStream/IDEAS automated counting scheme (Chapter 3, Figure 3-5).

The wild type Ade4p strains (i.e. Ade4-GFP strain and the GS.Ade4-GFP strain) had similar kinetic curves in the time course experiment. However, the Ade4-mtoin2786 kinetic curve somewhat varied from the Ade4-GFP kinetic curve (Ade4p WT TANGO score 2321). At most, the wild type Ade4p yeast strains differed by ~15% punctate penetrance at a single time point. Alternatively, the Ade4-mtoin2786 TANGO variant differed as much as ~17% punctate penetrance for two time points (Figure 4-1). These initial results support the hypothesis that the Ade4 TANGO variants with greater aggregation propensity form puncta faster than the wild type Ade4p yeast. Interestingly,

and perhaps contrary to what was reported in the original description of the punctate phenomenon (Narayanaswamy et al. 2009), we found that SD media does not induce Ade4-GFP puncta in early log phase.

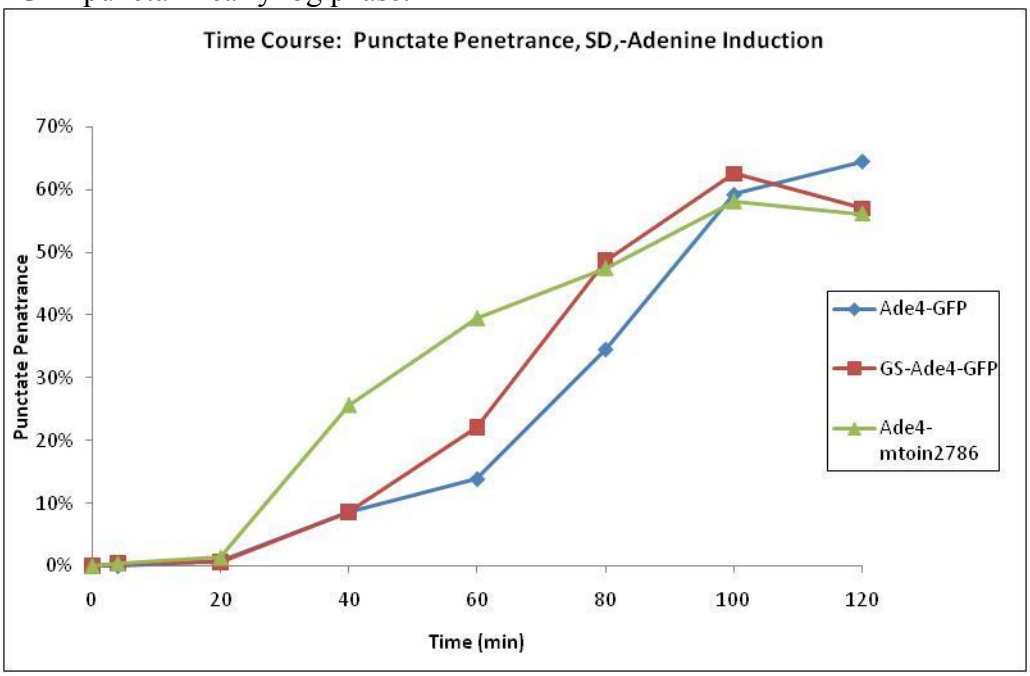

FIGURE 4-1 TIME COURSE: ADE4-GFP, GS.ADE4-GFP, AND ADE4-MTOIN2786. Shown here are the results of the time course comparison of the Ade4-GFP, GS.Ade4-GFP, and Ade4-mtoin2786 strains using SD,-adenine media punctate induction. The Ade4-GFP strain and the GS.Ade4-GFP strain may show similar kinetic trends. However, the TANGO variant Ade4-mtoin2786 results may vary from the Ade4-GFP trend. Puncta were induced in early log phase cells using SD,-adenine media. Aliquots were removed from the cultures every 20 minutes and fixed in 4% formaldehyde. Punctate penetrance was quantified manually and using the Amnis ImageStream/IDEAS automated counting scheme (refer to Figure 3-5 for automated counts)

Time Course: Evaluation of All Ade4 TANGO Variants

The punctate forming kinetics of all of the Ade4 TANGO variants were evaluated using a two hour time course experiment. Puncta were induced using SD,-adenine media

and cells were fixed at regular time intervals. Punctate penetrance of the fixed cell samples was quantitated manually (Figure 4-2) and using the Amnis ImageStream/IDEAS automated counting scheme (Chapter 3, Figure 3-7).

Relative to the Ade4-GFP WT and the GS.Ade4-GFP strains, two of the yeast strains with decreased TANGO scores, Ade4-mtoin2034 strain and Ade4-mtoin2105 strain, had a slight decrease in the rate of punctate formation. Alternatively, two of the strains with an increased TANGO score, Ade4-mtoin2786 and Ade4-2800, had a slight increase in the rate of punctate formation, when compared to the Ade4-GFP strains. In growth curve comparison studies, the Ade4-1286 yeast did not grow similarly to the Ade4-GFP strains, indicating a poorly functioning mutant Ade4p enzyme (Chapter 2, Figure 2-5 and 2-6). However, the strain was casually examined in the time course studies. The Ade4-1286 strain contained only a few puncta after two hours in SD,-adenine induction. The Ade4-mtoin2301 strain puncta kinetics revealed the strain pulled-away from the kinetic "group" and the rate of punctate formation exceeded all the other strains examined (Figure 4-2). With the exception of the Ade4-mtoin2301 and the Ade4-1286 results, the kinetic results suggested support of the hypothesis that variants with a greater aggregation propensity formed puncta faster and the variants with a reduced aggregation propensity formed puncta slower.

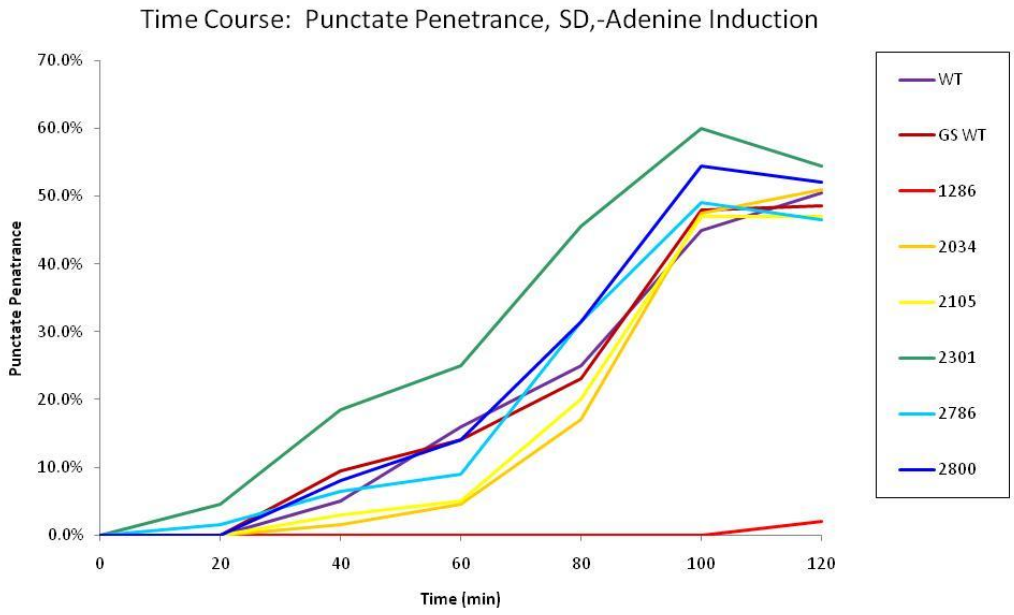

FIGURE 4-2 TIME COURSE: ADE4 TANGO VARIANTS, SD,-ADENINE. Shown here are the results of the time course comparison of the Ade4-GFP, GS.Ade4-GFP, and Ade4 TANGO variants using SD,-adenine media punctate induction. Two strains with increased TANGO scores (2301 and 2786) more rapidly formed puncta than Ade4-GFP (WT) and GS.Ade4-GFP (GS WT), while two strains with decreased TANGO scores (2034 and 2105) more slowly formed puncta than the WT and GS WT. The Ade4-GFP and GS.Ade4-GFP have Ade4 TANGO scores of 2321. Puncta were induced in early log phase cells using SD,-adenine media. Aliquots were removed from the cultures every 20 minutes and fixed in 4% formaldehyde. Punctate penetrance was quantified manually and using the Amnis ImageStream/IDEAS automated counting scheme (refer to Chapter 3, Figure 3-7 for automated counts).

The time course experiment was repeated two more times and the averages of the three experiments are shown in Figure 4-3. The punctate formation kinetics of most of the Ade4 TANGO variants overlap with the GS.Ade4-GFP curves, except for a couple of notable results: Ade4-1286 and Ade4-mtoin2301. The Ade4-1286 variant has an average puncta penetrance of only 1.3% at 2 hours. As described previously in Chapter

2, compared to the wild type yeast the Ade4-1286 variant has a retarded growth pattern, inferring a reduction in functional capacity and available to only a "casual inspection" in punctate formation kinetics. The Ade4-mtoin2301 variant resulted with ~60% punctate penetrance at 100 minutes, while the GS.Ade4-GFP curve depicts only ~44% punctate penetrance. This Ade4-mtoin2301 differential was not observed using the Amnis ImageStream automated quantification scheme described in Chapter 3 (Figure 3-7). In its current form, the Ade4-mtoin2301 single point "outlier" is interesting, but testing further describing the punctate penetrance between 80-120 minutes is necessary to determine the validity of this bulge in punctate formation kinetics.

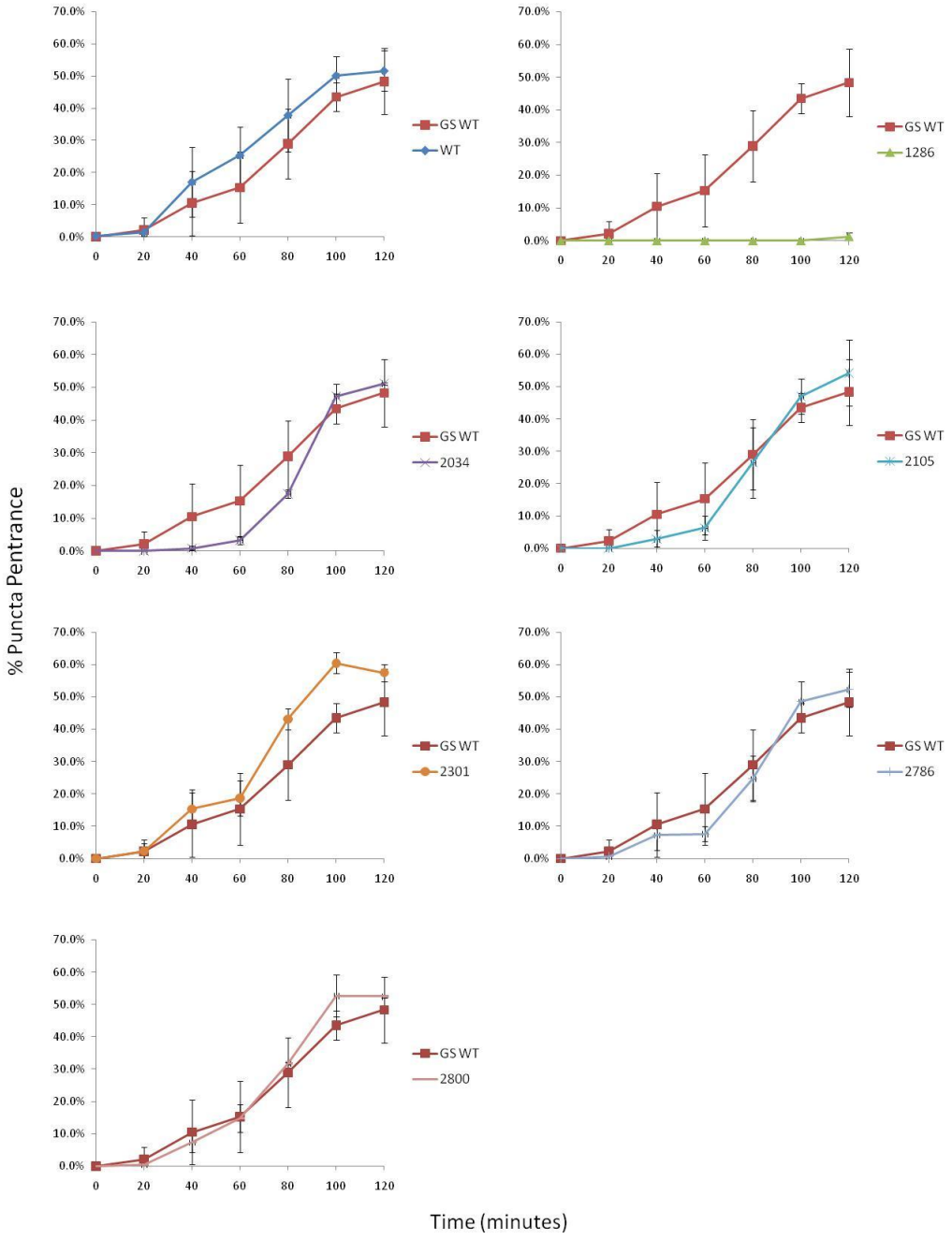

FIGURE 4-3 TIME COURSE: ADE4 TANGO VARIANTS, SD,-ADENINE. These are the average of the time course comparisons of the Ade4-GFP ("WT"), GS.Ade4-GFP ("GS WT"), and Ade4 TANGO variants ("1286" – "2800") using SD,-adenine media punctate induction (n=3, manually quantified). Three time points from a single experiment were omitted, due to blurred microscopy images (2034 t=120, 2105 t=120, and 2800 t=80).

Slow Kinetics: Evaluation of Media and Induction Methodologies

Kinetic variation between experiments was detected, but the ~50-60% maximum puncta penetrance was typical. The variation occurred when attempting to capture cells as they quickly changed from their non-punctate state to a punctate state in ~60-80 minutes.

We sought to better understand the variation between the experiments and perhaps slow down the rate of punctate formation. To better understand the variation between the experiments, time course cultures were prepared in triplicate. These tests are explained in the following section. In an effort to slow down the rate of punctate formation and possibly tease out the differences between strain kinetics, different media and punctate induction methods were examined.

To slow down the puncta forming kinetics, adenine dropout synthetic complete (SC,-ade) media was used to induce puncta in time course evaluations of the Ade4 TANGO variants. The more nutrient rich synthetic complete media contains all amino acids, unlike SD media, which only contains essential amino acids. With the exception of L-aspartic acid, L-threonine, and L-valine, the amino acid concentrations are greater in SC media (Sigma dropout mix) than SD media (Sunrise Science). Therefore, SC media was predicted to slow down the rate of puncta formation, such that the differing puncta forming kinetics (if present) may be better observed.

The punctate forming kinetics of the Ade4 TANGO variants were evaluated using a SC,-adenine punctate induction time course. Cells were fixed at regular time intervals and punctate penetrance of the fixed cell samples was quantitated manually (Figure 4-4). A cursory evaluation of the results indicated a slight overall decrease in the rate of

punctate formation, as the usual Ade4 maximal penetrance ~50-60% puncta was not achieved within 2 hours and only a single strain showed puncta at the 40 minute time point. Trends between rate of puncta formation and TANGO score were not observed. The results appeared as varied as previous results.

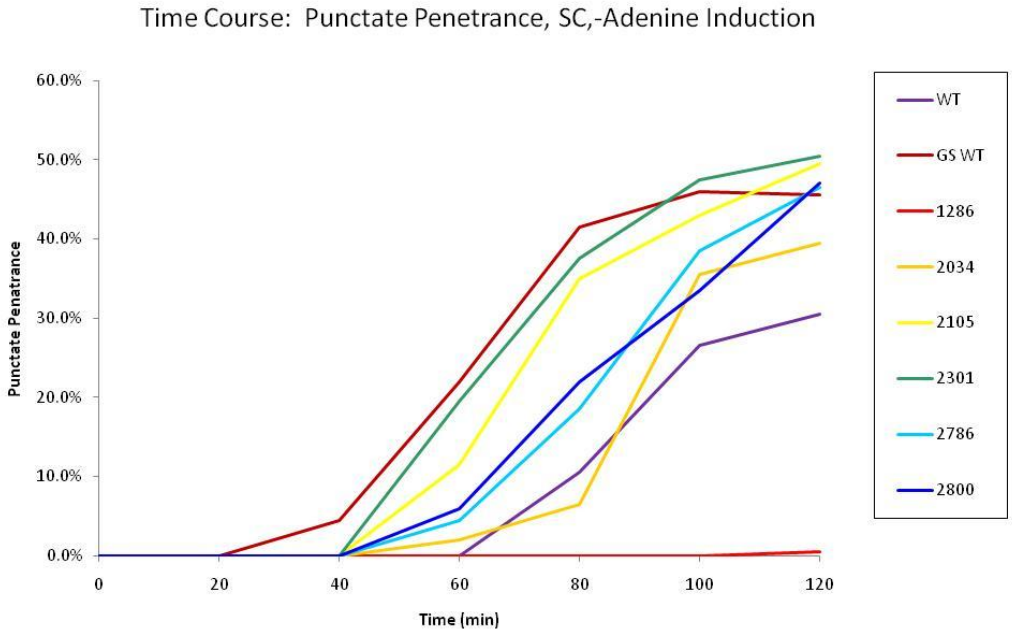

FIGURE 4-4 TIME COURSE: ADE4 TANGO VARIANTS, SC,-ADENINE. Shown here are the results of the time course comparison of the Ade4-GFP, GS.Ade4-GFP, and Ade4 TANGO variants using SC,-adenine media punctate induction. The time course revealed great variation between strain puncta kinetics. The puncta were induced in early log phase cells using SC,-adenine media. Aliquots were removed from the cultures every 20 minutes and fixed in 4% formaldehyde. Punctate penetrance was quantified manually.

Although it is perhaps worth noting that variation between cultures grown in SC media is not unheard of, as Minois et al. observed death rate variations in SC media (Minois et al. 2009). Likewise, the OD_{600nm} yeast growth curves in SC media (Figures 2-8 and 2-9) were more varied than the tight SD media yeast curves (Figures 2-6 and 2-7), which prompted us to seek another growth and punctate induction media.

In another attempt to further slow down punctate formation and tease out the kinetic differences between strains, a time course experiment with a stationary phase punctate induction was performed. Stationary phase punctate onset is predicted to take longer than the typical 2 hours necessary for adenine dropout punctate induction. Therefore, small differences between the strains, if present, should be easily detected. This method had the added benefit of evaluating another induction methodology. Multiple mechanisms may be implicated in puncta formation; as such, the adenine dropout mechanism may offer different kinetics than the stationary phase mechanism. The observation of the stationary phase mechanism may be more applicable to the global aggregation hypothesis, as stationary phase induced many cytoplasmic proteins to punctate.

The punctate forming kinetics of the Ade4 TANGO variants were evaluated using the time course methodology and stationary phase punctate induction in nutrient rich YPD media. The YPD cultures were incubated at 30˚C and culture aliquots were removed and fixed with 4% formaldehyde. Similar YPD media stationary phase induction time course experiments were performed by members of Edward Marcotte's laboratory in the evaluation of multiple strains from the yeast GFP library (personal communication, M. Tsechansky, University of Texas at Austin).

The results of the time course revealed spiking penetrance at t = 8 h. This was likely due to mishandling or inadequately fixing the cell aliquot, as the culture returned to a lower penetrance at later time points (Figure 4-5). After 48 hours, examination of the time course results revealed very little difference across strains. That is, there was ≤10% penetrance difference aside of the spiking t = 8 h and disregarding the casual examination of the malfunctioning Ade4-1286 (discussed in Chapter 2). While maximal penetrance

was not obtained during this time, the early to mid-kinetics of punctate formation were very similar for all yeast strains tested.

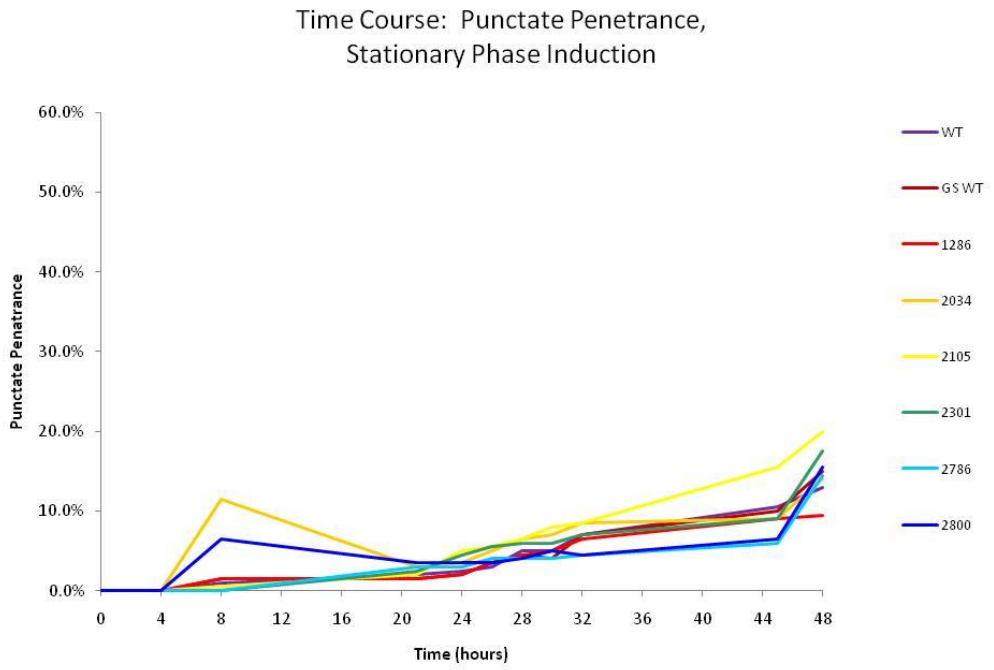

FIGURE 4-5 TIME COURSE: ADE4 TANGO VARIANTS, YPD. Shown here are the results of the time course comparison of the Ade4-GFP, GS.Ade4-GFP, and Ade4 TANGO variants using stationary phase punctate induction. With the exception of a couple of spiking points at t = 8 h and the malfunctioning Ade4-1286, the results between strains were very similar and varied by ≤10% penetrance. The YPD cultures were grown at 30˚C. Aliquots were removed from the cultures and fixed in 4% formaldehyde. Punctate penetrance was quantified manually.

Conclusions: Ade4 TANGO Variants and Punctate Kinetics

At least three likely conclusions can be made from this body of work: (1) the time course methodology is unable to distinguish similar kinetic curves with rapidly forming puncta (i.e. less than 2 hours), and/or (2) there may be very little difference in

the punctate formation kinetics of the Ade4 TANGO variants. (3) In consideration of the fitness evaluation (Chapter 2) in conjugation with the puncta formation kinetics, the Ade4 TANGO protein variants appear to be destabilized and lack significant alteration to their aggregation propensity.

The inability of the methodology to distinguish similar punctate formation kinetic curves is most apparent in some of the earlier SD,-adenine induction curves. Comparison of these curves clearly shows the reordering of the strains from experiment to experiment (Figures 4-2 example). While the maximum punctate penetrance (~50-60%), relative onset (t = ~20-40 minutes), or onset of penetrance maximum (t = 100 minutes) of the strains does not change, the kinetic curves between experiments change (standard deviation recorded in Figure 4-3).

There are a number of possible sources of variation stemming from the methodology. For instance, in the SD,-adenine inductions, the Ade4 strains could reasonably form puncta at a rate of 10% penetrance increase in 10 minutes. Sampling and fixing 8 strains (i.e. Ade4-GFP, GS.Ade4-GFP, and Ade4 TANGO variants) could take as long as 10 minutes, thus introducing variation (~10%) from the first to the last sample. Measures were taken to minimize the impact of sampling induced variation by maintaining the order of the sampled strains through the experiments. Additionally, cell cultures were passaged multiple times to generate early log phase cells of similar age. We sought to generate time course cultures at an OD_{600nm} of 0.5 before beginning the experiments, although this was not always the case and instead cultures were at an OD_{600nm} of 0.2-0.7 for the SD,-adenine induction time course and OD_{600nm} of 0.1-0.3 for the SC,-adenine induction. Some of these cultures may have still been maturing in lag phase growth and therefore responded differently than the actively budding log phase cells. Additional sources of error include manual quantification, as discussed in Chapter

2. Guidelines have been implemented to mitigate these errors, although reported count variation as much as 3% puncta may occur (Patel 2010). And, finally, while steps were made to standardize the preparation of media, the aging and subsequent deterioration of nutrients or improper charring of glucose within the media could alter puncta kinetics and be a source of variation between experiments.

Using the information learned here, all future punctate formation kinetic experiments will incorporate the following procedural changes: (1) Duplicate or triplicate cultures will be evaluated to establish the variation of penetrance within the experiment. (2) Sample number will be minimized (such as through binary comparison experiments) to reduce the sample prep time for time points, therefore better capturing the cells at the targeted time point. (3) The number of time points collected will be reduced to further simplify the workload, until it is deemed necessary to increase the kinetic points. (4) Time course experiments will be quickly repeated with the same materials (i.e. media, culture plates, etc.) Additionally, different induction conditions and media will be evaluated for their ability to reduce the rate of punctate formation, such that we may better observe the kinetics.

Aside from or in addition to the methodology conclusion, there may be very little difference in the puncta kinetics of the Ade4 TANGO variants. Perhaps the results from the SD,-adenine induction (Figure 4-3) and YPD stationary phase induction time course best exemplify this (Figure 4-5). In the case of the YPD stationary phase induction experiment, the cultures were monitored for 48 hours and during that time, with the exception of the spiking points at t =8 h and the casual observation of the malfunctioning Ade4-1286 strain, the puncta penetrance varied 10% or less between strains. The similar penetrance values and the changing of the rank order of the strains throughout the experiment, suggest similar punctate formation kinetics.

While the TANGO algorithm offered a first estimate of protein aggregation propensity, perhaps the TANGO algorithm does not best estimate the aggregation propensity of the Ade4-GFP strain and related mutants. For example, the TANGO algorithm failed to predict the aggregation nuclei of yeast Sup35 and Ure2 prion-forming domains (Linding et al. 2004). Such glutamine/asparagine-rich (Q/N-rich) amyloid domains are not easily detected by aggregation propensity predicting algorithms (Toombs et al. 2010). While the Ade4p is not particularly Q/N-rich, there may be other such properties that make their aggregation propensity difficult to predict.

Perhaps other aggregation propensity predicting algorithms would better predict the aggregation propensity of the Ade4 TANGO variants. The Zyggregator (Pawar et al. 2005), another aggregation propensity predicting algorithm, was also used to predict the aggregation propensity of the Ade4 variants. Zyggregator works similarly to the TANGO algorithm in that aggregation propensity is predicted based on physico-chemical properties of the amino acid sequence (Pawar et al. 2005, Fernandez-Escamilla et al. 2004). However, the TANGO algorithm assumes aggregating amino acids are fully buried (Fernandez-Escamilla et al. 2004).

Zyggregator predicted (1) the Ade4 TANGO variants to have a different rank order of aggregation propensity and predicted (2) little difference in the predicted aggregation propensities between strains (Table 2-2). Specifically, the mutant Ade4p proteins in Ade4-mtoin2034, Ade4-mtoin2105, and Ade4-mtoin2301 have Zyggregator predicted aggregation propensities greater than wild type Ade4p, while the TANGO algorithm predicted these variants to have propensities less than wild type (Table 2-2). In consideration of the Zyggregator error, the Ade4-GFP predicted aggregation propensity is similar to the Ade4 TANGO variants. Only the Ade4-1286 variant's predicted aggregation propensity noticeably shifts below and away from the others (Figure 2-2).

A final conclusion may be made in consideration of the results from the fitness evaluation (Chapter 2) in conjugation with the puncta formation kinetics: the Ade4 TANGO protein variants appear to be destabilized and lack significant alteration to their aggregation propensity. In short, we got what we designed. We designed the protein variants using a multiple sequence alignment to select nonconserved amino acids as mutable candidates. Nonconserved regions flanked by conserved peptides are typically external loops and/or areas of transition between secondary structures (Lesk 2001, Blouoin et al. 2004). Inspection of the *E. coli* Ade4p homolog confirmed that the sites of mutated amino acids just buried beneath the surface and usually in areas transitioning between secondary structures (Chapter 2). Protein folding is in part driven by the "hydrophobic effect" in which hydrophobic residues sequester to form the core of a globular protein due to favorable inter-residue interactions and unfavorable water-residue interactions (discussed in Voet and Voet 2004). Therefore, small changes in the form of single amino acid mutations near the surface are less likely to disrupt the folding of the protein. Alternatively, mutations in a protein's interior, shielded from solvent, tend to have negative structural and possibly functional implications (Matthews 1993, Tokuriki et al. 2007). Although the mutations likely failed to alter the aggregation propensity of the variants, none of the variants stringently tested in the competition experiments (tested 3 of 6 variants) were functionally equivalent to the wild type strain. The amino acid mutations in the Ade4 variants, like most mutations (Tokuriki et al. 2009, Goldsmith and Tawfik 2009), might have been destabilizing. The fitness cost of this type of destabilization might have been in the form of reduced protein function or in the need to increase the production of protein folding machinery such as chaperone proteins. Thus, the fitness penalty for the Ade4 TANGO variants was best observed in the batch culture experiments, which resulted with the wild type yeast out-competing the variants.

While the Ade4 TANGO variants were designed with the intent of preserving function, this was not the end result. Instead, the deleterious mutations destabilized a majority of the variants, resulting in decrease fitness in the form of slow growth (at worst) and not functionally equivalent to wild type (at best). The reduction in fitness was not accompanied by a change in aggregation, as observed by punctate formation kinetics.

CHAPERONE KNOCKOUT: ADE4-GFP

Introduction

In an effort to further explore the yeast punctate foci as an aggregation phenomenon, we sought to examine how the deletion of chaperone proteins alters punctate foci formation. We hypothesize that knocking out this protein folding machinery will increase the number of misfolded proteins and therefore influence the rate and/or total punctate penetrance in the cells.

Initially, four chaperone knockout strains were designed using the yeast Ade4-GFP background, with each strain lacking a single chaperone protein. The chaperone protein encoding genes *HSP104* (YL026W), *HSP82* (YPL240C), *HSC82* (YMR186W), and *SSA1* (YAL005C) were selected as candidates for deletion. Hsp104p targets former protein aggregates and is involved in their refolding and reactivation (Parsell et al 1994, Parsell et al. 1991). Additionally, Hsp104p has the traditionally unlikely involvement in yeast prion-like factor psi+ propagation (Chernoff et al. 1995), which makes it an interesting choice for this work. Hsp82 and Hsc82 were selected, because they are Hsp90 proteins, which are highly abundant and protect against self-aggregation (Miyata and Yahara 1992). The simultaneous deletion of these Hsp90p encoding genes is not viable, although a single deletion is viable (Nathan et al. 1997). Ssa1p was selected, because it is

in the Hsp70 family of proteins. The Hsp70 proteins prevent aggregation by binding exposed hydrophobic amino acids as the nascent protein emerges from the ribosome (Hartl and Hayer-Hartl 2002) and they have been implicated as "modulators of misfolding disease" (reviewed in Broadley and Hartl 2009). Additionally, the four selected deletion candidates also have the advantage of being non-essential, which simplifies the techniques necessary to knock them out from the yeast genome.

There are at least two methods to generate the chaperone knockout, Ade4-GFP yeast strains: (1) Using the *chaperoneΔ::KanMX* strain (Invitrogen, Winzeler et al. 1999), the GFP encoded tag and selectable marker are genomically integrated to the end of *ADE4*. (2) Using the Ade4-GFP yeast strain (Invitrogen, Huh et al. 2003), the chaperone encoded gene is knocked out, replacing it with a selectable marker. We opted to use the Ade4-GFP yeast strain and knockout the chaperone encoding genes, instead of adding the GFP tag to the *ADE4* gene in the deletion strain. Use of the *chaperoneΔ::KanMX* background would require promoter modifications/swaps to prevent unwanted crossover events with the *ADE4* tag (i.e. GFP-*HIS3* construct tag, construct described previously in Chapter 2). Additionally, the yeast deletion library (Winzeler et al. 1999) contains compensatory mutations, rearrangements, as well as unwanted deletions (reviewed in Scherens and Goffeau 2004). It is estimated that up to 8% of the strains in the deletion library may contain a form of the gene that was deleted and is therefore not a suitable background for this work (Hughes et al. 2000).

The chaperone knockouts were prepared by replacing the chaperone genes with the *URA3* gene and its endogenous promoter, thus restoring uracil synthesis to the former auxotroph. The knockouts were generated using a protocol similar to that used to generate the *ade4*Δ*::URA3* strain described in Chapter 2.

Results and Discussion

Clones were generated in the *hsc82*Δ*::URA3, ssa1*Δ*::URA3,* and *hsp82*Δ*::URA3* transformations in the Ade4-GFP strain, but we were unable to knockout the *HSP104* gene. Three clones from the *hsc82*Δ*::URA3* transformation, one clone from the *ssa1*Δ*::URA3* transformation, and three clones from the *hsp82*Δ*::URA3* transformation were tested for insertion of *URA3* using colony PCR (Figure 4-6). All clones tested generated correctly sized *URA3* colony PCR products.

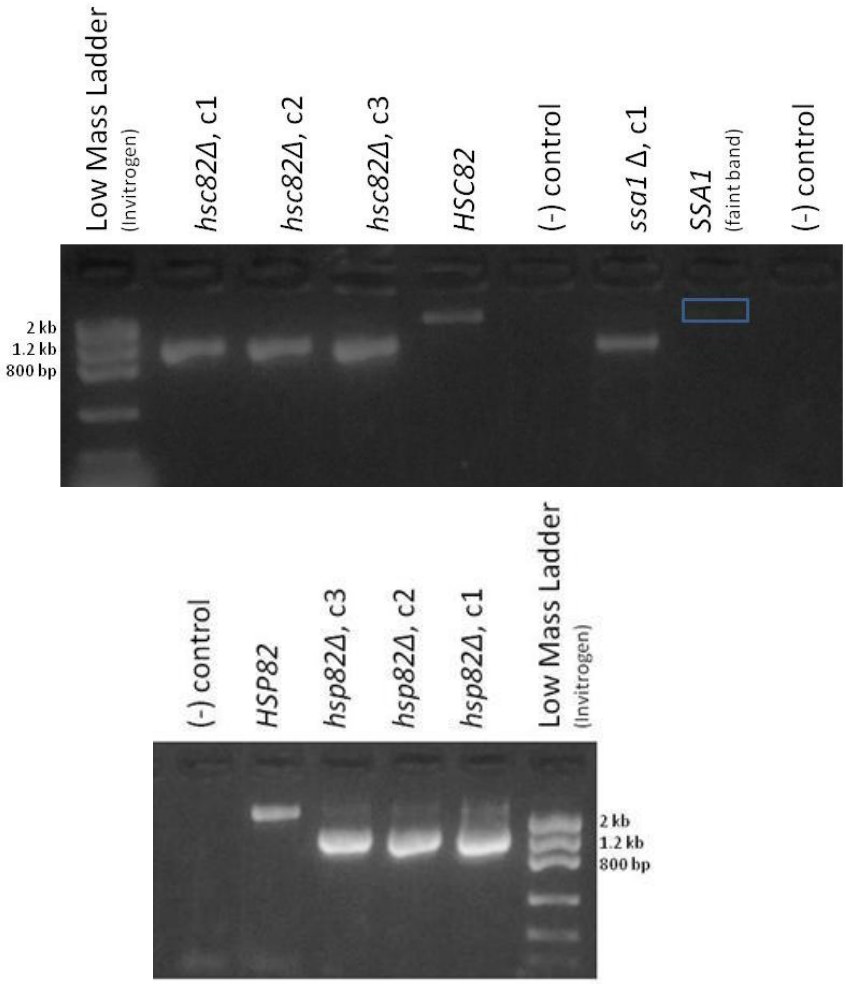

FIGURE 4-6 VERIFICATION OF CHAPERONE GENE DELETIONS. Show here are the agarose gels used to verify the deletion of the chaperone protein genes in the Ade4-GFP yeast strain. Three clones from the *hsc82*Δ*::URA3* transformation, one clone from the *ssa1*Δ*::URA3* transformation, and three clones from the *hsp82*Δ*::URA3* transformation were tested for insertion of *URA3* using colony PCR. PCR products were run on an agarose gel for size verification. PCR primers flanking the chaperone genes were used to verify the deletion of the chaperone gene. The deletion (i.e. *URA3*) PCR product was 1117 bp, while the intact chaperone gene products were 2009 bp, 2198 bp, and 2210 bp for *SSA1, HSC82*, and *HSP82* respectively. The *hsp82*Δ*::URA3* colony PCR reactions were slightly over PCR-amplified, thereby generating a faint smear of larger products.

The chaperone knockouts were evaluated for growth by generating an OD_{600nm} growth curve. All of the chaperone knockouts behaved similarly to the Ade4-GFP WT strain in SD media (Figure 4-7). However, the *hsc82Δ::URA3*, Ade4-GFP strains grew slightly slower than the Ade4-GFP strain and the other chaperone knockout strains in SD,-adenine (see Figure 4-8). Such a decrease in growth rate might be explained by the reported decline in replicative life span upon the deletion of the chaperone protein (Kaeberlein et al. 2005), although it is unclear why the growth rate reduction was not evident in the SD media growth curve.

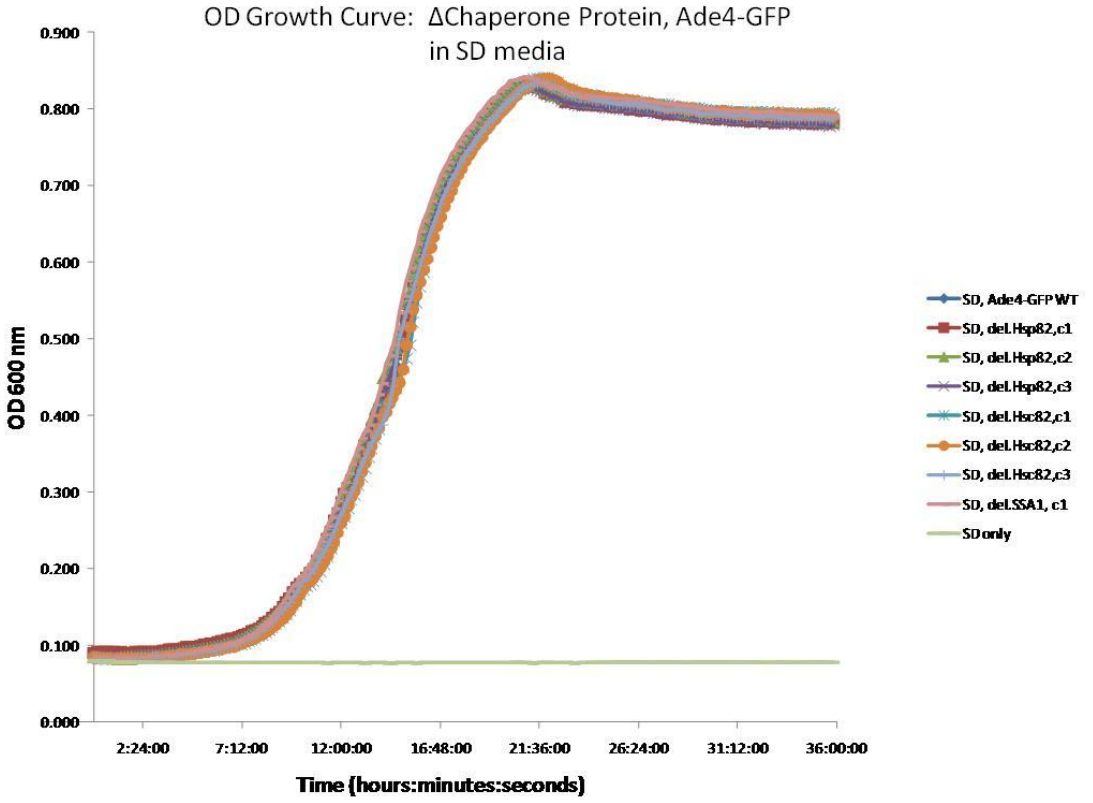

FIGURE 4-7 GROWTH CURVE CHAPERONE KNOCKOUT, ADE4-GFP, SD. Shown above are the results of the OD_{600nm} growth curves of chaperone knockout, Ade4-GFP strains in SD media (average of 3 cultures). All of the chaperone knockout strains grew similarly to the parental Ade4-GFP strain. OD_{600nm} growth curves were prepared by diluting overnight cultures to an OD_{600nm} of 0.02 and monitoring growth for 36 hours at 30˚C.

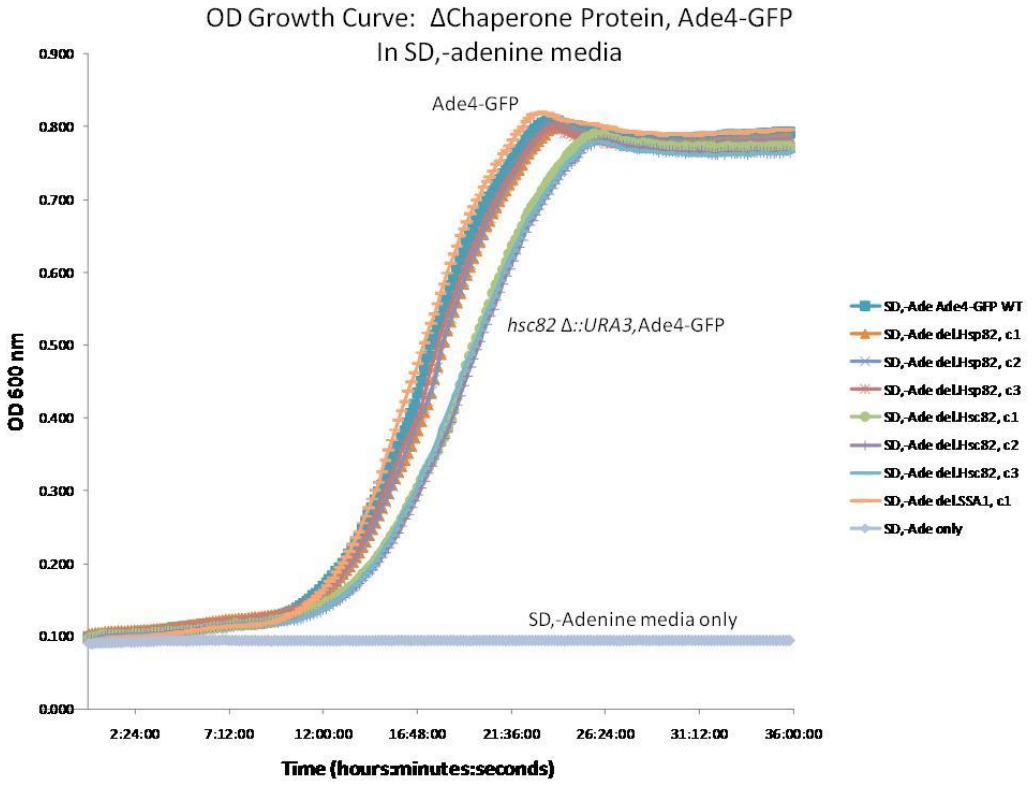

FIGURE 4-8 GROWTH CURVE OF CHAPERONE KNOCKOUT, ADE4-GFP, SD,-ADE. Shown above are the OD_{600nm} growth curves of chaperone knockout, Ade4-GFP strains in SD,-adenine media (average of 3 cultures). The *hsc82Δ::URA3* strain grew slower than the Ade4-GFP strain and other chaperone knockout strains. OD_{600nm} growth curves were prepared by diluting overnight cultures to an OD_{600nm} of 0.02 and monitoring growth for 36 hours at 30˚C.

The punctate forming kinetics of theAde4-GFP chaperone knockout strains were evaluated using a cursory time course experiment with an SD,-adenine media induction. Single cultures (instead of replicate cultures) were used in the cursory time course, to obtain a feel for how the newly generated strains would behave. Once the conditions were evaluated, the time course procedure (such as induction time) could be adjusted to accommodate the new strains, if necessary. To perform the first cursory time course

evaluation, early log phase cells were induced with SD,-adenine media. Cells were fixed at regular time intervals and GFP-tagged puncta were manually counted.

The time course resulted with the chaperone knock-out strains having a slight increase in the rate of punctate formation when compared to the Ade4-GFP and GS.Ade4-GFP strains (Figure 4-9). The Ade4-GFP strain did not reach maximum penetrance of 50-60%, which is typical at 2 hours. If disregarding the Ade4-GFP curve, then most divergence between the strains occurs at t = 0.5 h with only a ~19% puncta difference, with the curves drawing closer to each other as the experiment proceeded.

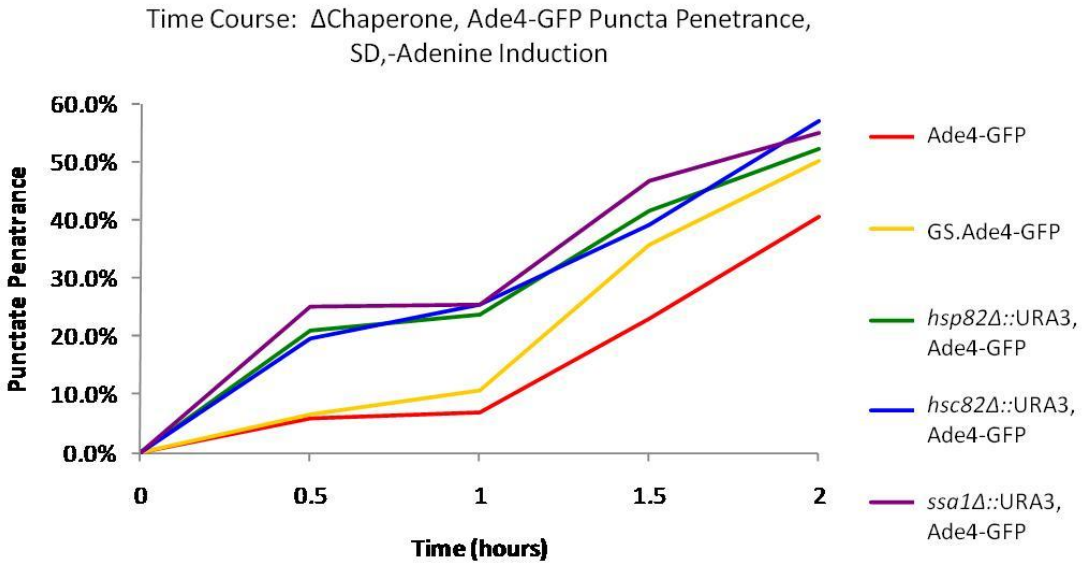

FIGURE 4-9 CURSORY TIME COURSE: CHAPERONE KNOCK, ADE4-GFP. Shown above are the results the cursory time course experiment of the knockout chaperone, Ade4-GFP strains with a SD,-adenine punctate induction. This work was performed to get a feel for the overall performance of these strains, so that future kinetic experiments could be tailored to best observe the rate of punctate formation. Perhaps at first glance, the knock-out chaperone strains appear to have a faster rate of punctate formation, although the curves only differ by 19% puncta at most (see explanation above), which may not be a significant shift. The time course was performed by inducing puncta in early log phase cells, fixing culture aliquots at regular intervals, and quantifying the punctate penetrance manually.

Based on the results of this cursory examination of the chaperone strains, the time course procedure in its current state was deemed appropriate, as the chaperone knockouts reached maximum GS.Ade4-GFP punctate penetrance (~50-60% puncta), which is typical after two hours of induction.

Further examination of the Ade4-GFP chaperone knock-out strain took the form of binary time course experiments in triplicate and quantification of puncta penetrance

using an automated Amnis ImageStream/IDEAS analytical scheme (described in Chapter 3). Specifically, triplicate cultures of a chaperone knockout strain and its Ade4-GFP parental strain were compared using the time course methodology. In an effort to minimize the number of samples and subsequent sample prep time, only the Ade4-GFP strain and the *hsp82*Δ*::URA3*, Ade4-GFP strain were examined.

The time course results indicated similar kinetics between the *hsp82*Δ*::URA3*, Ade4-GFP strain and the Ade4-GFP strain (Figure 4-10). Although all of the error bars do not overlap, the similarity between the puncta formation kinetics suggested very little difference in the rate of puncta formation. The results of this work were reproduced in a subsequent kinetic experiment comparing the two strains (Figure 4-11), therefore further supporting the similarities between the puncta formation kinetics.

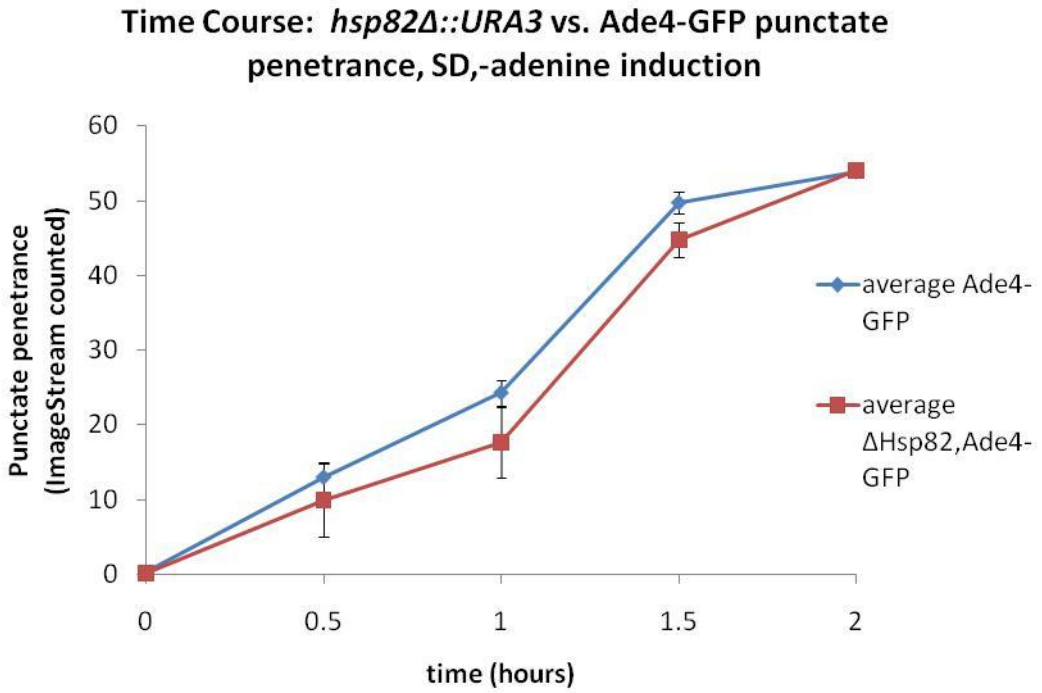

FIGURE 4-10TIME COURSE: *HSP82Δ::URA3*, ADE4-GFP STRAIN. These are the results of the time course of the *hsp82Δ::URA3*, Ade4-GFP strain and theAde4-GFP strain with a SD,-adenine induction (average of triplicate cultures). The time course experiment was performed by inducing puncta in early log phase cells with SD,-adenine media. Culture aliquots were fixed every 30 minutes with formaldehyde and punctate penetrance was quantified using the Amnis ImageStream/IDEAS automated counting scheme.

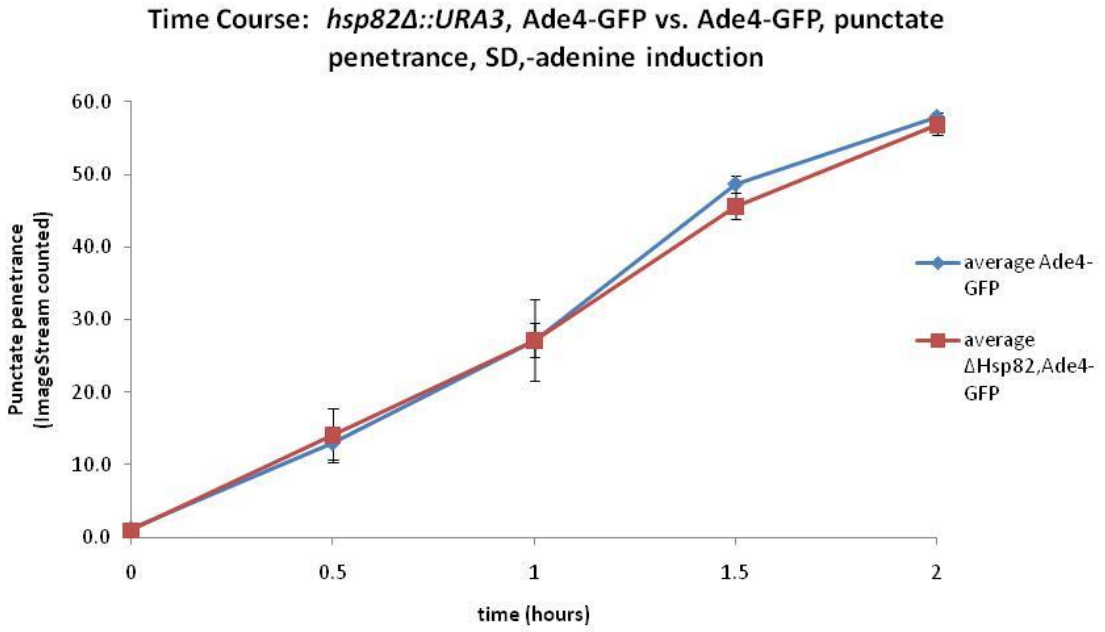

FIGURE 4-11TIME COURSE: *HSP82Δ::URA3*, ADE4-GFP STRAIN. These are the results, reproducing the previous results, of the time course of the *hsp82Δ::URA3*, Ade4-GFP strain and the Ade4-GFP strain with a SD,-adenine induction (average of triplicate cultures). These and the previous results indicate very little variation in puncta formation kinetics between the two strains. The time course experiment was performed as described previously.

Conclusions

In an effort to describe the involvement of chaperone proteins in the formation of punctate foci, we successfully generated chaperone knockouts using the Ade4-GFP parental strain. The kinetics of punctate formation were observed in time course experiments. An initial cursory experiment suggested kinetic similarities between the three Ade4-GFP knockout strains (*hsc82*Δ, *ssa1*Δ, and *hsp82*Δ) (Figure 4-9). Subsequent experiments focusing on the *hsp82Δ::URA3* strain and the parental Ade4-GFP strain revealed almost overlapping kinetic curves, reaching of maximum penetrance of 54-58% puncta in two hours.

The similarities between the *hsp82Δ::URA3*, Ade4-GFP strain and the Ade4-GFP strain might be expected. There is some evidence Hsc82p compensates for the deletion of *hsp82* (Cox and Miller 2003), perhaps masking any aggregation and/or punctate foci effects. The deletion of both *hsp82* and *hsc82* is not viable (Nathan et al. 1997), but examination of the deletion of one and the reduction of the other might be possible, such as through use of a titratable promoter (such as the Tet promoter), and should be consider for future work.

CHAPERONE KNOCKOUT: GLN1-GFP

Introduction

Pull-down experiments isolated Gln1-GFP puncta and, mass spectrometry analysis, revealed the presence of Hsp82p and/or Hsc82p, as well as Gln1p and GFP (personal communication, J.D. O'Connell, University of Texas at Austin). *HSP82* and *HSC82* have 97% protein sequence identity, which complicates the identification of the co-precipitating protein(s). Fortuitously, the *HSP82* and *HSC82* genes were deleted from the Ade4-GFP strain and just prior to hearing of the Gln1-GFP pull down results.

We sought to knockout chaperone proteins, thereby inducing protein misfolding events, which we hypothesize will increase the number of puncta foci. The three chaperone proteins deleted from the Ade4-GFP strain, described previously, were selected as candidates for deletion from the Gln1-GFP strain. Specifically, the chaperone proteins Hsp82 (YPL240C), Hsc82 (YMR186W), and Ssa1 (YAL005C) were selected as candidates for deletion from the Gln1-GFP yeast strain. The proteins' involvement in the prevention of aggregation, as well as the identification of 1 or 2 of these proteins as co-precipitates with Gln1-GFP puncta made these chaperone protein interesting candidates

for deletion. We predict the deletion of a chaperone protein (especially Hsp82p or Hsc82p) will alter the punctate forming kinetics of the Gln1-GFP strain.

Results and Discussion

The Gln1-GFP *hsp82Δ::URA3*, *hsc82Δ::URA3*, and *ssa1Δ::URA3* yeast strains were generated using homologous recombination with the *URA3* gene construct flanked by regions homologous to upstream and downstream of the chaperone gene (described previously). The gene knockouts were confirmed by colony PCR (Figure 4-12).

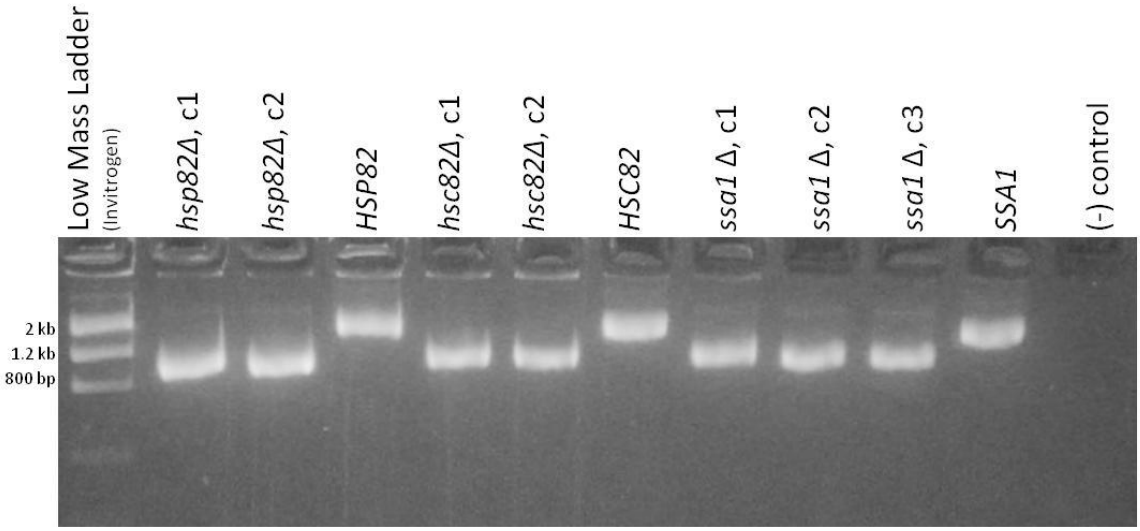

FIGURE 4-12VERIFICATION OF CHAPERONE GENE DELETIONS. Shown here are the agarose gels used to verify the deletion the chaperone protein genes in the Gln1-GFP yeast strain. Two clones from the hsp82Δ::URA3 transformation, two clones from the hsc82Δ::URA3 transformation, and three clones from the ssa1Δ::URA3 transformation were tested for insertion of URA3 using colony PCR. PCR products were run on an agarose gel for size verification. PCR primers flanking the chaperone genes were used to verify the deletion of the chaperone gene. The deletion (i.e. *URA3*) PCR product was 1117 bp, while the intact chaperone gene products were 2009 bp, 2198 bp, and 2210 bp for *SSA1*, *HSC82*, and *HSP82* respectively.

The Gln1-GFP chaperone knockouts were evaluated using a time course experiment with SC,-glucose media punctate induction. We found it necessary to optimize the cellular fixation methods and the automated Amnis ImageStream analytical scheme. We again verified that the harsh conditions of a flow cytometer (i.e. Amnis ImageStream) could induce puncta of unfixed Gln1-GFP cells. The Gln1-GFP yeast cells required more stringent fixatives than the Ade4-GFP strain to preserve the non-punctate state of log phase cells. Although 4% formaldehyde (20 minute incubation) fixed the Ade4-GFP cells, this method was not sufficient to preserve the non-punctate state of log phase cells. Additionally, "over fixing" cells diminished the fluorescence signal, therefore hindering puncta quantification. And, lastly, the Amnis ImageStream analytical scheme, though validated for the Ade4-GFP punctate foci, required refinement. While optimizing these methods, we returned to manual quantification of puncta.

The chaperone knockouts were evaluated for growth by generating an OD_{600nm} growth curve. All of the chaperone knockouts behaved similarly to the Ade4-GFP WT strain in SC media (Figure 4-13). Glucose is the usual carbon source of yeast. But, when grown in media lacking glucose, yeast grew much slower as they are forced to catabolize amino acids for energy (Figure 4-14).

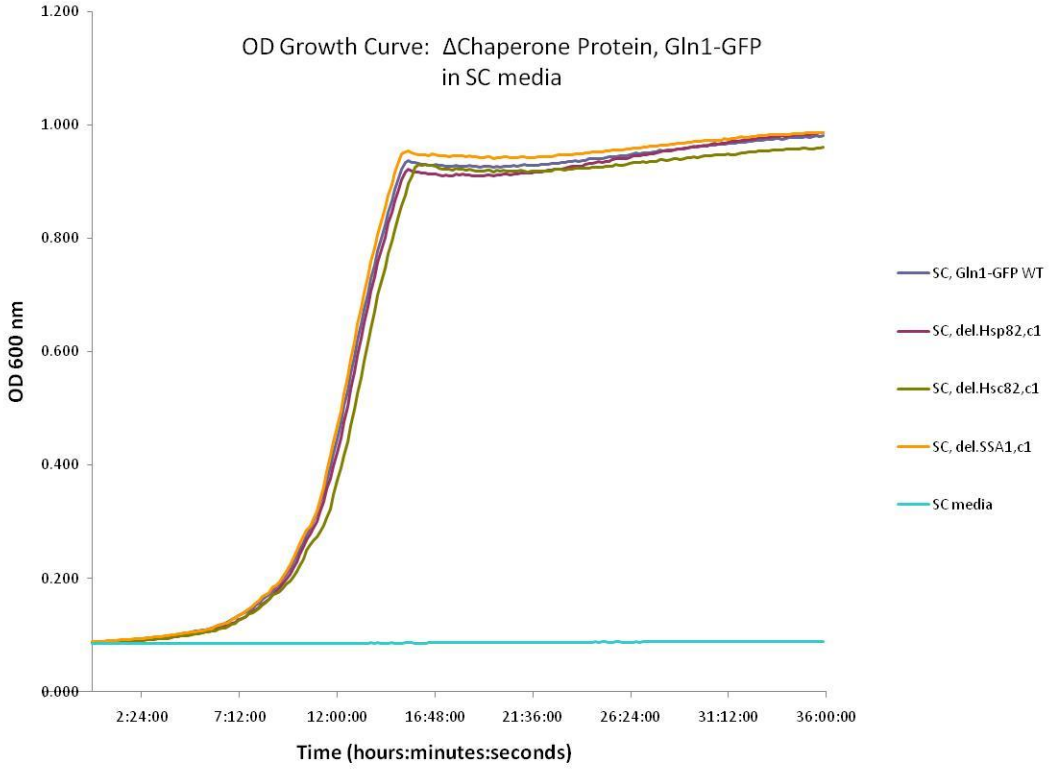

FIGURE 4-13 GROWTH CURVE CHAPERONE KNOCKOUT, GLN1-GFP, SC. Shown above are the results of the OD_{600nm} growth curves of chaperone knockout, Gln1-GFP strains in SC media (average of 3 cultures). All of the chaperone knockout strains grew similarly to the parental Gln1-GFP strain. OD_{600nm} growth curves were prepared by diluting overnight cultures to an OD_{600nm} of 0.02 and monitoring growth for 36 hours at 30˚C.

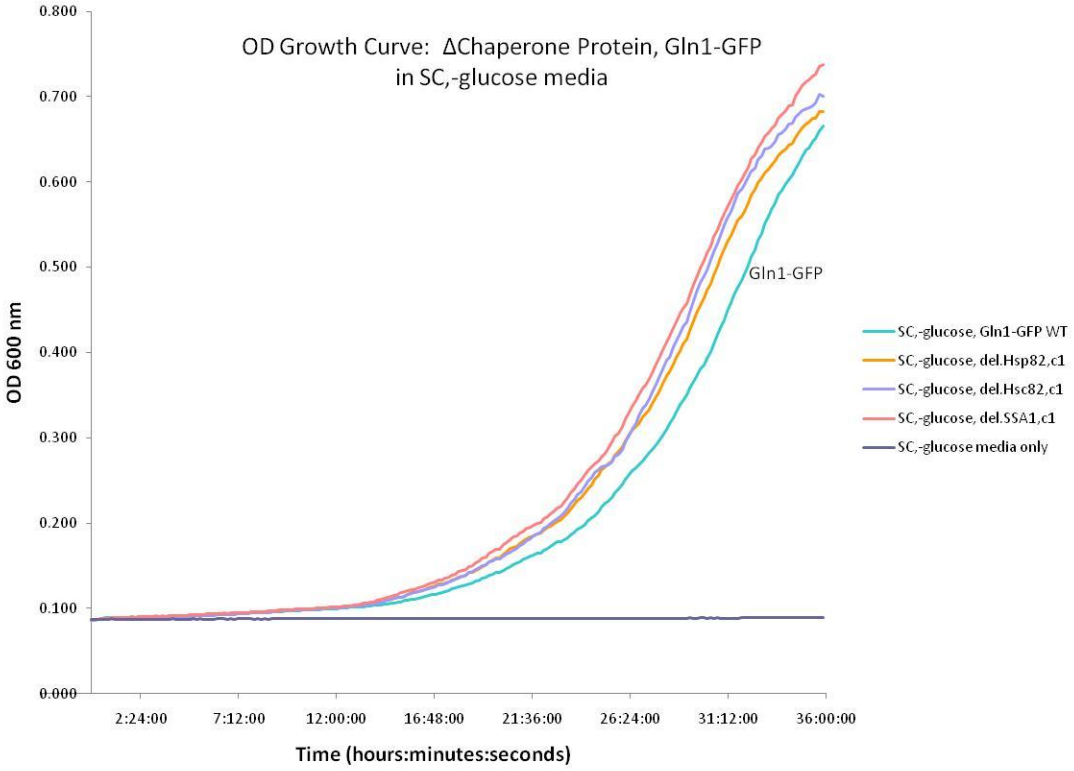

FIGURE 4-14GROWTH CURVE OF CHAPERONE KNOCKOUT, GLN1-GFP, SC,-GLUCOSE. Shown above are the OD_{600nm} growth curves of chaperone knockout, Gln1-GFP strains in SC,-glucose media (average of 3 cultures). Without usual glucose carbon source, the yeast are forced to catabolize the amino acids, thus growing slower than in richer media. OD_{600nm} growth curves were prepared by diluting overnight cultures to an OD_{600nm} of 0.02 and monitoring growth for 36 hours at 30˚C.

The *hsp82Δ::URA3*, Gln1-GFP strain punctate formation kinetics in a SC,-glucose media were examined in a time course experiment (Figure 4-15). Both of the strains achieved a 90% maximum punctate penetrance within 2 hours, which is typical for the Gln1-GFP strain (Narayanaswamy et al. 2009). A slight difference (23% difference) in the punctate formation kinetics after 1 hour of induction was observed, with the *hsp82Δ::URA3*, Gln1-GFP strain forming puncta slighter faster than the wild type Gln1-GFP strain.

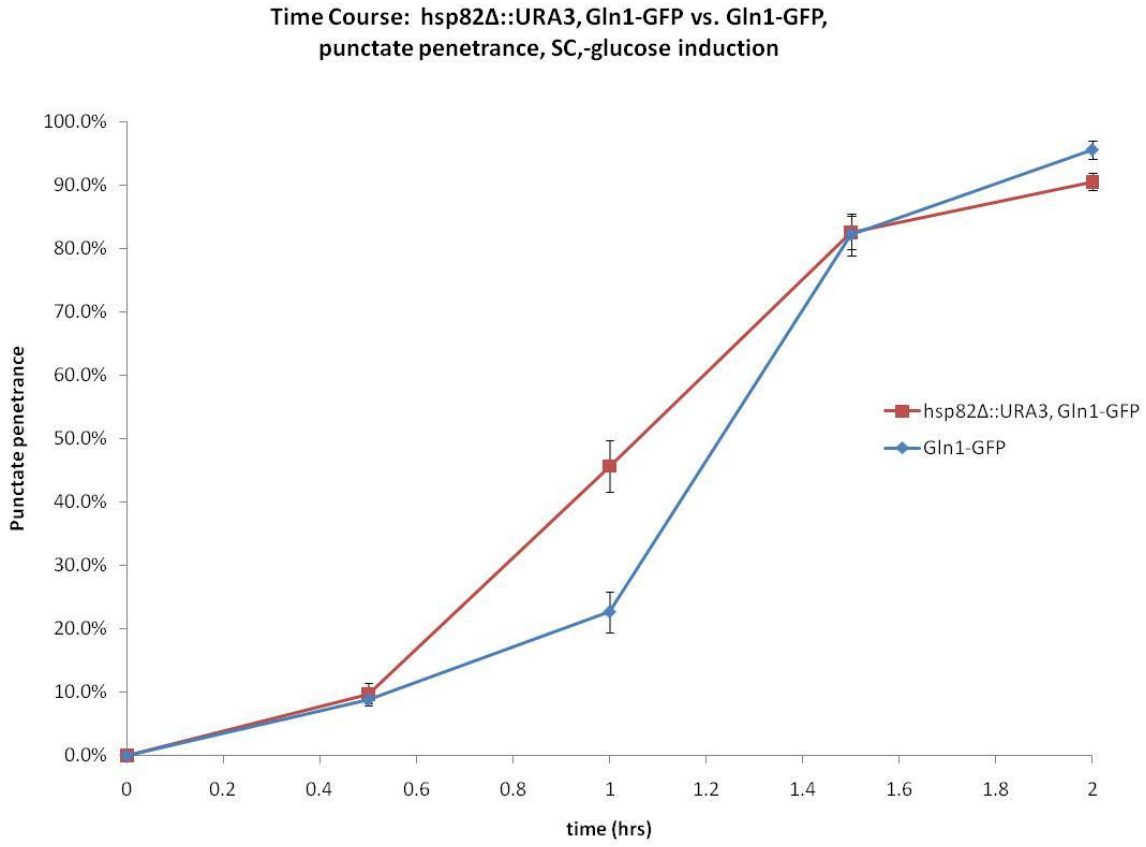

FIGURE 4-15CURSORY TIME COURSE: *HSP82Δ::URA3*, GLN1-GFP. These are the results of the time course experiment of *hsp82Δ::*URA3, Gln1-GFP with a SC,-glucose punctate induction. Both of the strains achieved a 90% maximum punctate penetrance within 2 hours, which is typical for the Gln1-GFP strain. The time course was performed in triplicate by inducing puncta in early log phase cells and quantifying the punctate penetrance manually.

Conclusions

In an effort to describe the involvement of chaperone proteins in the formation of punctate foci, we successfully generated chaperone knockouts using the Gln1-GFP parental strain and evaluated the punctate formation kinetics of one of the knockout strains. The kinetics of punctate formation were similar between the wild type Gln1-GFP

strain and the *hsp82*Δ*::URA3* strain, with the exception of a single time point (Figure 4-15). At 1 hour, the chaperone knockout strain had a greater puncta penetrance (23% greater) than the Gln1-GFP. We will attempt to reproduce these results in future experiments to further comment on the involvement of chaperone proteins in punctate formation. These results potentially support the hypothesis that the starvation induced formation of cytoplasmic proteins into punctate foci is the result of a protein misfolding or aggregation phenomenon.

As discussed previously with Ade4-GFP chaperone knockouts, the similar puncta formation kinetics between the *hsp82*Δ*::URA3*, Gln1-GFP strain and the Gln1-GFP strain might be expected. There is some evidence Hsc82p may compensate for the deletion of *hsp82* (Cox and Miller 2003), perhaps masking any aggregation and/or punctate foci effects.

FICOLL GRADIENT FRACTIONATION OF GLN1-GFP PUNCTA (NARAYANASWAMY ET AL. 2009).

Introduction

Isolation of Gln1-GFP puncta for biochemical analysis using a discontinuous Ficoll gradient was attempted. Purified puncta could provide opportunities for identification of co-purified proteins, analysis of enzymatic activity, determination of protein stoichiometry, electron microscopy imaging, detection of amyloid filaments using Thioflavin T and/or Congo Red, as well as numerous other biochemical and structural analyses.

Ficoll is a commonly used gradient medium. As a high molecular weight sucrose polymer, Ficoll is used to separate cells, organelles, and structures by density (Schneider

1987, Rieder and Emr 2001, Bode and Schirmer 1985). Ficoll solutions have a low osmotic pressure, thereby better preserving organelles. Ficoll has the additional benefit that it does not contain ionized groups, therefore minimizing reactivity (Amersham Biosciences).

Results and Discussion

Purification of puncta on a discontinuous Ficoll gradient (4%, 8%, and 16%) was attempted. Most of the Gln1-GFP pelleted. Using the Ficoll gradient fractions, GFP was quantified by Western blot analysis and punctate foci were quantified by visual inspection using fluorescent microscopy (Figure 4-16).

Punctate foci in the Ficoll gradient fractions and the clarified pellet fraction were quantitated using fluorescence microscopy. Size and fluorescence intensity criteria to quantitate the fractionated punctate foci were established based on the known cellular Gln1-GFP foci. In particular, cellular punctate foci were found to be ~1 um in size, and had fluorescence intensity greater than or equal to ~400 grayscale (MetaMorph version 6.2r6). The average density of punctate foci was determined for each fraction. Puncta were counted from 45 images (870 x 650 um^2 per image) taken from a 22 x 22 mm^2 area over which 5 uL of a Ficoll fraction was spread.

Most of the Gln1-GFP was in the pellet fraction, with only a small, floating or soluble peak (maximal at Fraction 10) detected within the gradient (Figure 4-16). The floating Gln1-GFP accounted for ~2% of total GFP. As a basis for comparison, given that vacuoles are known to float at much lower densities, these results potentially indicate that the punctates are larger or heavier than vacuoles (Rieder and Emr 2001).

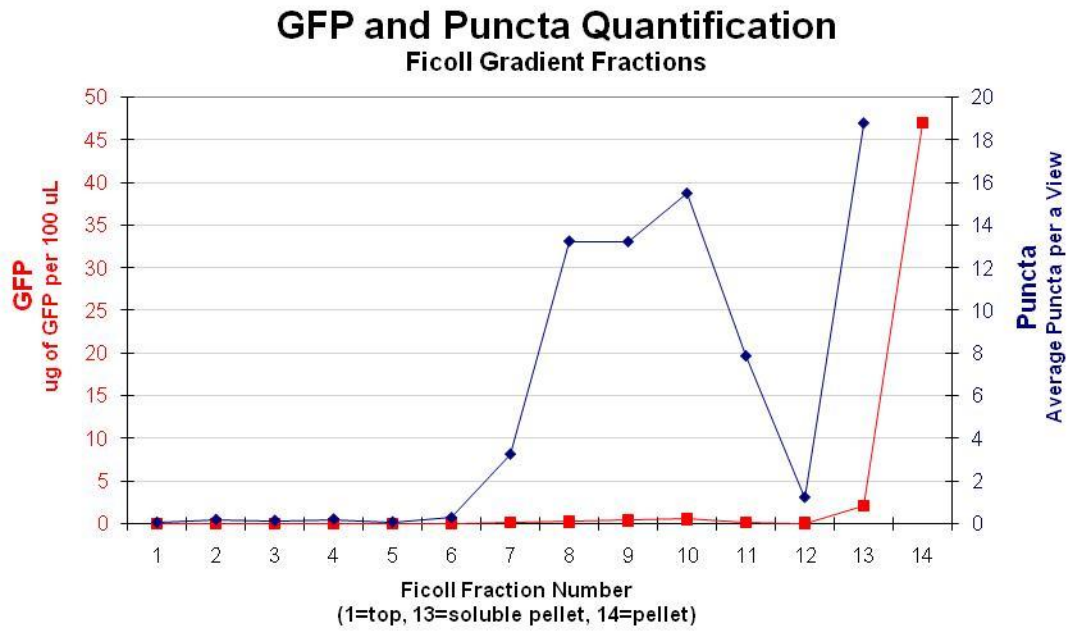

FIGURE 4-16GRADIENT FRACTIONATION AND QUANTIFICATION OF GLN1-GFP PUNCTA. These are the results of the Ficoll gradient fractionation of Gln1-GFP puncta and the quantification of GFP and puncta. The distribution of Gln1-GFP puncta separated on a Ficoll gradient, expressed as GFP (ug/100 uL of Ficoll fraction; red curve and left-hand axis) and average number of punctate foci per a view (blue curve and right-hand axis; not measurable in pellet).

Determination of the Gln1 enzymatic activity of the soluble Gln1-GFP fraction was unsuccessful. The Gln1 assay is a multienzymatic test involving the use of pyruvate kinase and lactic dehydrogenase. It couples the formation of ADP with the oxidation of NADH. Specifically, glutamate, ammonium, phosphoenolpyruvate, and β-nicotinamide adenine dinucleotide (NADH) react to form glutamine, inorganic phosphate, lactate, and NAD^+. A decrease in NADH is monitored by the decrease in UV absorption at 340 nm (Kingdon et al. 1968). The assay is subjected to interference by contaminating enzymes or glutamate and therefore does not lend itself to detection of Gln1 activity in lysate.

Conclusions

Attempts were made to isolate Gln1-GFP puncta from cell lysate using a Ficoll density gradient. The methods proved unsuccessful in isolating soluble puncta, as a majority of the Gln1-GFP puncta were collected in the insoluble pellet fraction. A small peak at fraction 10 contained <3% of the total GFP observed (Figure 4-16). While the methods were unsuccessful at isolating soluble Gln1-GFP puncta, techniques for counting puncta in cell lysate were established (Narayanaswamy et al. 2009).

ACTIN BODY STAINS (NARAYANASWAMY ET AL. 2009)

Introduction

To better describe the punctate foci phenomenon and evaluate the foci as macromolecular depots, punctate co-localization experiments were performed (Narayanaswamy et al. 2009). Specifically, the co-localization of actin bodies with Gln1-GFP puncta and Ade4-GFP puncta was examined.

Generated in quiescence, actin bodies presumably act as an actin reserve, poised to supply actin upon returning to a proliferating cycle. In contrast to the polarized, mobile, and dynamic actin network of cables and patches, actin bodies are depolarized, immobile, and actin turnover has not been observed. Similar to the punctate foci, the actin bodies are transient in nature and dissipate upon refeeding of fresh media (Sagot et al. 2006).

Results, Discussion, and Conclusions

Localization of Ade4-GFP and Gln1-GFP puncta relative to actin bodies was evaluated. Punctate foci were induced in SC medium by growing to stationary phase (56 h). Actin bodies were stained using Alexa Fluor 647 conjugated phalloidin and a modified Sagot et al. protocol (Sagot et al. 2006). The Ade4p and Gln1p puncta do not strongly colocalize with actin bodies, unlike positive control marker Cap2p. Ade4-GFP and Gln1-GFP punctate foci were fully colocalized with actin bodies in 12% and 4% of cases, respectively, in contrast to Cap2-GFP, which colocalized with actin bodies in 94% of cases (Figure 4-17, analyzing n = 51, 53, and 90 punctate foci, respectively).

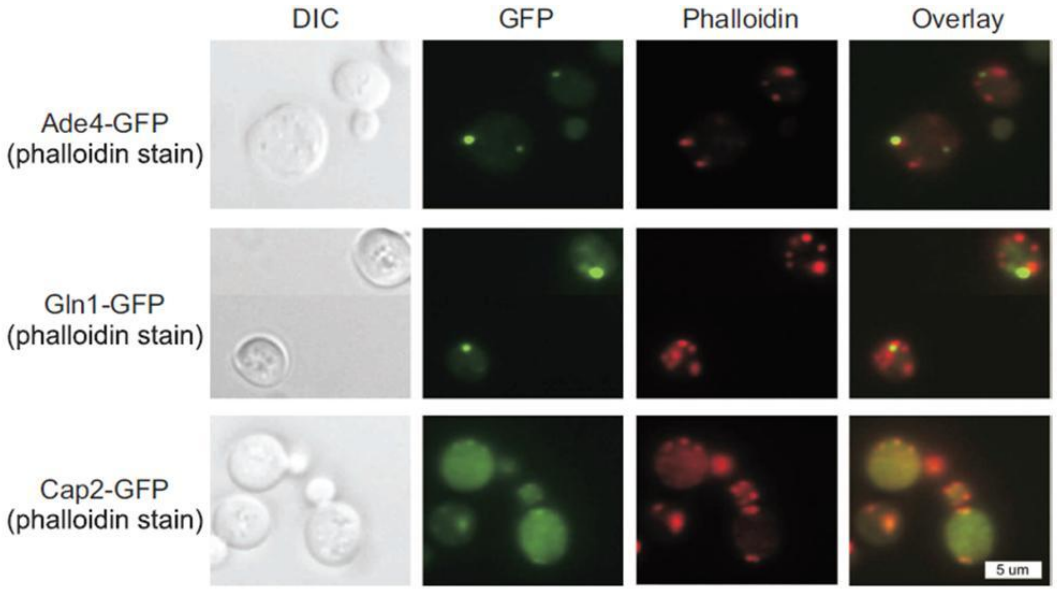

FIGURE 4-17LOCALIZATION OF ACTIN BODIES AND PUNCTAE FOCI. These are the results of the co-localization evaluation of actin bodies and Ade4-GFP and Gln1-GFP puncta. Ade4 and Gln1 puncta do not strongly colocalize with actin bodies, unlike positive control marker Cap2, as detected by counter staining of stationary phase cells expressing Ade4-GFP, Gln1-GFP or Cap2-GFP by Alexa Fluor 647 conjugated phalloidin. Ade4-GFP and Gln1-GFP punctate foci were fully colocalized with actin bodies in12% and 4%of cases, respectively, in contrast to Cap2-GFP, which colocalized with actin bodies in 94% of cases (analyzing n = 51, 53, and 90 punctate foci, respectively). Punctate foci were induced in SC medium by growing to stationary phase (56 h). (Scale bar: 5 um.)

MATERIALS AND METHODS

Time Course: Ade4 TANGO Mutants and Ade4-GFP, Chaperone Knockouts, Adenine Dropout Media Induction

Early log phase yeast Ade4-GFP cells (Invitrogen, Huh et al. 2003) and the Ade4 variants (i.e. TANGO strains and chaperone knockout strains) were prepared as follows. For the Ade4 TANGO time course experiments, 3 mL starting cultures were grown in

histidine dropout synthetic defined (SD,-histidine) media (Sunrise Science) or histidine dropout synthetic complete (SC,-histidine) media (Sunrise Science) for 8 hours at 30˚C, with one noted experiment that started in SD media (Sunrise Science). Add Ade4-GFP chaperone knockout cultures were started in SD. Cultures were diluted in SD or SC media (5 mL total volume), and grown overnight (~16 h) to an OD_{600nm} of 1.5. Cultures were again diluted in SD or SC media (5 mL or ~3.4 mL total volume) and grown for 4 hours to an OD_{600nm} of 0.5.

Ade4-GFP puncta were induced by replacing media of early log phase cells with SD or SC,-adenine media (Sunrise Science). Specifically, cells were pelleted by centrifugation (1,000 xg for 5 min). Media was aspirated and replaced with SD or SC,-adenine media. For 2 hours, 0.5 mL cell aliquots were removed and fixed every ~20 minutes using the 4% formaldehyde fixation method described below. Cells were returned to the shaking 30˚C incubator in-between time points.

Cells were fixed in 4% formaldehyde (SPI Supplies) for 20 min at room temperature. Fixed cells were washed 3 times in 0.5 mL PBS (Invitrogen) by spinning cells at 10,000 rpm (12,400 xg) for 3 minutes, aspirating media, and resuspending cell pellet in PBS.

All OD measurements were performed at 600 nm. All cultures were grown at 30˚C in a shaking incubator. All SD cultures remained in SD derived media, while the SC cultures remained in a SC derived media.

Time Course: Ade4 TANGO Mutants, Stationary Phase Punctate Induction

Early log phase yeast Ade4-GFP cells (Invitrogen, Huh et al. 2003) and Ade4 TANGO variants were prepared as follows. 3 mL starting cultures were grown in YPD

media (BD Difco) for 8 hours at 30˚C. Cultures were diluted in YPD media (5 mL total volume) and grown overnight (~11 h) to an OD_{600nm} of 1.5. Cultures were again diluted in YPD media (5 mL total volume) and grown for 4 hours to an OD_{600nm} of 0.5. Cultures were finally diluted in YPD media (5 mL total volume) at an OD_{600nm} of 0.2 to begin the time course. Cultures were grown for 48 hours in a 30˚C shaking incubator.

The cultures were regularly sampled, removing 300 uL aliquots, over 48 hours. Culture samples were fixed with 4% formaldehyde using the protocol described above in the SD or SC,-adenine induction time course method. Cells were returned to the shaking 30˚C incubator in-between time points.

Punctate penetrance was manually counted.

OD_{600nm} Growth Curves: Chaperone Knockout Evaluation

Cultures (3 mL) were generated selecting colonies from plates and growing cultures overnight in SD media in a 30˚C shaking incubator. Overnight cultures were diluted to an OD_{600nm} of 0.02 in either SD media or SD, -adenine media. Cultures, in 100 uL aliquots, were distributed to the wells of clear 96-well plates. The OD_{600nm} was read every 10 min for 36 h at 30˚C on a BioTek Synergy HT-I plate reader. The plate was shaken for 9 min and then rested for 1 min prior to each reading. Media only controls were monitored for contamination or spillover.

Time Course: Gln1-GFP, Chaperone Knockouts, Glucose Dropout Media Punctate Induction

Log phase yeast Gln1-GFP cells (Invitrogen, Huh et al. 2003) and the chaperone knockout cells were prepared as follows. Starter cultures (3 mL) grew for 24 hours in

YPD (BD Difco) at 30˚C. Diluted cultures to an OD_{600nm} of 0.125 using SC media (3 mL total volume) and grew until cells reached an OD_{600nm} of ~1.25 (~6 hours). Epifluorescence microscopy images (t=0 hours) were obtained.

Puncta were induced by replacing media of log phase cells with SC,-glucose media (Sunrise Science). Specifically, cells were pelleted by centrifugation (i.e. spun at 1,000 xg for 3 min). Media was aspirated and replaced with SC,-glucose media. For 2 hours, 0.5 mL cell aliquots were removed and imaged using fluorescence and bright field microscopy. Cells were returned to the shaking 30˚C incubator in-between time points. Puncta were manually counted.

Ficoll Gradient Fractionation of Gln1-GFP Punctate Bodies (Narayanaswamy et al. 2009)

Discontinuous Ficoll gradient fractionation of Gln1-GFP punctate was performed using a modified version of the vacuole purification protocol from Rieder and Emr (Rieder and Emr 2001). Gln1-GFP tagged *S. cerevisiae* were grown to stationary phase in YPD for 48 h and harvested by centrifugation. Punctate body formation was confirmed visual inspection using microscopy. Cells were suspended in a mixture of Roche EDTA-free protease inhibitor and gradient buffer (34 mM imidazole, pH 7.1, 60 mM MgCl2, 19 mM KCl, and 45 mM ammonium chloride), and then lysed using glass beads. Lysis was confirmed by microscopy. DEAE Dextran (Sigma, 48 ug/mL) was added to 500 uL of lysed cells (a total of 25 mL of ~8 OD_{600nm} cells). The DEAE Dextran-lysed cell mixture was loaded onto a layer of 2.9 mL of 16% (w/v) Ficoll PM 400 (Sigma) solution in gradient buffer in an ultracentrifugation tube (Beckman). 3 mL of 8% (w/v) Ficoll in gradient buffer, 4 mL of 4% Ficoll (w/v) in gradient buffer, and 2 mL of gradient buffer

were layered, respectively, onto the cell lysate. Additional gradient buffer was added as needed to balance the ultracentrifugation tubes. The density of the concentrated protein sample plus DEAE Dextran was difficult to predict in advance, and some mixing of the cell lysate with Ficoll layers was noted (although this did not likely affect the ultimate result, the pelleting of the punctate bodies). Gradients were centrifuged at 30,000 rpm in a Beckman SW41 rotor for 1.5 h at 8° Celsius. Fractions (1 mL) were taken from the top of the gradient, leaving ~1.5 mL for the final liquid fraction, 12. The pellet at the bottom of the gradient (fraction 13) was then suspended in 150 uL of PBS and clarified in a minicentrifuge for 30 seconds at ~6,000 rpm.

Western blots with purified GFP standards (minimum of 4) were used to quantitate the GFP in Ficoll gradient fractions (triplicate measurements). Briefly, 4 uL of 4x NuPAGE LDS dye (Invitrogen) was added to 10 uL of a Ficoll gradient fraction or diluted fraction. Samples and GFP standards (Millipore) were denatured for 10 min at 70° Celsius and run on 4–12% NuPAGE BisTris gels (Invitrogen). Gels were transferred to 0.45 um nitrocellulose membrane (Invitrogen), using the XCell II Blot transfer apparatus (Invitrogen). Blots were blocked with Odyssey Blocking Buffer (LI-COR) and then incubated with rabbit anti-GFP antibody (Sigma) for 2 h at room temperature or overnight at 4° Celsius. Blots were washed 3 times with PBST (PBS with 0.05% (v/v) Tween) and then incubated for 1 h with a secondary antibody (Odyssey goat anti-rabbit IR dye 680 antibody conjugate, LI-COR). Again, blots were washed 3 times with PBST, and finally scanned using the LI-COR Odyssey Imaging System. GFP was quantified using the instrument's image analytical software.

Punctate foci in the Ficoll gradient fractions and the clarified pellet fraction were quantitated using fluorescence microscopy. Size and fluorescence intensity criteria for the isolated protein aggregates were established based on the known cellular Gln1-GFP foci.

In particular, cellular bodies were found to be ~1 um in size, and had a fluorescence intensity greater than or equal to ~400 grayscale (MetaMorph version 6.2r6). The average density of punctate bodies was determined for each fraction. Puncta were counted from 45 images (870 x 650 um^2 per image) taken from a 22 x 22 mm^2 area over which 5 uL of a Ficoll fraction was spread.

Co-localization of Actin Bodies with Ade4-GFP and Gln1-GFP Puncta (Narayanaswamy et al. 2009)

For colocalization with actin bodies, punctate foci were induced in synthetic complete (SC formulation provided below) media by growing to stationary phase (56 h). Actin bodies were stained using a modified Sagot et al. protocol (Sagot et al. 2006). Cells were fixed by incubation with 4% formaldehyde at room temperature for 20 min, washed 3 times with PBS, incubated with 1/50th, 1/20th, or 1/10th the volume of Alexa Fluor 647 Phalloidin (Invitrogen) for 1 h at room temperature, washed 3 times with PBS and then imaged. Actin bodies and GFP-tagged puncta were manually counted by visual inspection.

SC media (1 L) contained: 6.7 g of yeast nitrogen base without amino acids (BD Difco), 1.92 g of yeast synthetic drop-out medium without uracil (Sigma Y1501-20G), 76 mg uracil, and 2% (w/v) glucose.

References

Bode W, Schirmer T: Determination of the protein content of crystals formed by Mastigocladus laminosus C-phycocyanin, Chroomonas spec. phycocyanin-645 and modified human fibrinogen using an improved Ficoll density gradient method. Biol Chem Hoppe Seyler 1985, 366:287-295.

Blouin C, Butt D, Roger AJ: Rapid evolution in conformational space: a study of loop regions in a ubiquitous GTP binding domain. Protein Sci 2004, 13:608-616.

Broadley SA, Hartl FU: The role of molecular chaperones in human misfolding diseases. FEBS Lett 2009, 583:2647-2653.

Chernoff YO, Lindquist SL, Ono B, Inge-Vechtomov SG, Liebman SW: Role of the chaperone protein Hsp104 in propagation of the yeast prion-like factor [psi+]. Science 1995, 268:880-884.

Cox MB, Miller CA, 3rd: Pharmacological and genetic analysis of 90-kDa heat shock isoprotein-aryl hydrocarbon receptor complexes. Mol Pharmacol 2003, 64:1549-1556.

Drummond DA, Wilke CO: The evolutionary consequences of erroneous protein synthesis. Nat Rev Genet 2009, 10:715-724.

Fernandez-Escamilla AM, Rousseau F, Schymkowitz J, Serrano L: Prediction of sequence-dependent and mutational effects on the aggregation of peptides and proteins. Nat Biotechnol 2004, 22:1302-1306.

Goldsmith M, Tawfik DS: Potential role of phenotypic mutations in the evolution of protein expression and stability. Proc Natl Acad Sci U S A 2009, 106:6197-6202.

Hartl FU, Hayer-Hartl M: Molecular chaperones in the cytosol: from nascent chain to folded protein. Science 2002, 295:1852-1858.

Hughes TR, Roberts CJ, Dai H, Jones AR, Meyer MR, Slade D, Burchard J, Dow S, Ward TR, Kidd MJ, et al.: Widespread aneuploidy revealed by DNA microarray expression profiling. Nat Genet 2000, 25:333-337.

Huh WK, Falvo JV, Gerke LC, Carroll AS, Howson RW, Weissman JS, O'Shea EK: Global analysis of protein localization in budding yeast. Nature 2003, 425:686-691.

Kaeberlein M, Kirkland KT, Fields S, Kennedy BK: Genes determining yeast replicative life span in a long-lived genetic background. Mech Ageing Dev 2005, 126:491-504.

Kingdon HS, Hubbard JS, Stadtman ER: Regulation of glutamine synthetase. XI. The nature and implications of a lag phase in the Escherichia coli glutamine synthetase reaction. Biochemistry 1968, 7:2136-2142.

Lesk AM: Introduction to protein architecture: the structural biology of proteins. Oxford; New York: Oxford University Press; 2001.

Linding R, Schymkowitz J, Rousseau F, Diella F, Serrano L: A comparative study of the relationship between protein structure and beta-aggregation in globular and intrinsically disordered proteins. J Mol Biol 2004, 342:345-353.

Matthews BW: Structural and genetic analysis of protein stability. Annu Rev Biochem 1993, 62:139-160.

Minois N, Lagona F, Frajnt M, Vaupel JW: Plasticity of death rates in stationary phase in Saccharomyces cerevisiae. Aging Cell 2009, 8:36-44.

Miyata Y, Yahara I: The 90-kDa heat shock protein, HSP90, binds and protects casein kinase II from self-aggregation and enhances its kinase activity. J Biol Chem 1992, 267:7042-7047.

Narayanaswamy R, Levy M, Tsechansky M, Stovall GM, O'Connell JD, Mirrielees J, Ellington AD, Marcotte EM: Widespread reorganization of metabolic enzymes into reversible assemblies upon nutrient starvation. Proc Natl Acad Sci U S A 2009, 106:10147-10152.

Nathan DF, Vos MH, Lindquist S: In vivo functions of the Saccharomyces cerevisiae Hsp90 chaperone. Proc Natl Acad Sci U S A 1997, 94:12949-12956.

Parsell DA, Kowal AS, Singer MA, Lindquist S: Protein disaggregation mediated by heat-shock protein Hsp104. Nature 1994, 372:475-478.

Parsell DA, Sanchez Y, Stitzel JD, Lindquist S: Hsp104 is a highly conserved protein with two essential nucleotide-binding sites. Nature 1991, 353:270-273.

Patel A: Generating Mutant Yeast and Measuring the Rate of Ade4 Punctate Foci Formation [Undergraduate Honors Thesis]. Austin: University of Texas at Austin: 2010.

Pawar AP, Dubay KF, Zurdo J, Chiti F, Vendruscolo M, Dobson CM: Prediction of "aggregation-prone" and "aggregation-susceptible" regions in proteins associated with neurodegenerative diseases. J Mol Biol 2005, 350:379-392.

Rieder SE, Emr SD: Isolation of subcellular fractions from the yeast Saccharomyces cerevisiae. Curr Protoc Cell Biol 2001, Chapter 3:Unit 3 8.

Sagot I, Pinson B, Salin B, Daignan-Fornier B: Actin bodies in yeast quiescent cells: an immediately available actin reserve? Mol Biol Cell 2006, 17:4645-4655.

Scherens B, Goffeau A: The uses of genome-wide yeast mutant collections. Genome Biol 2004, 5:229.

Schneider E, Pollard H, Lepault F, Guy-Grand D, Minkowski M, Dy M: Histamine-producing cell-stimulating activity. Interleukin 3 and granulocyte-macrophage colony-stimulating factor induce de novo synthesis of histidine decarboxylase in hemopoietic progenitor cells. J Immunol 1987, 139:3710-3717.

Tokuriki N, Stricher F, Schymkowitz J, Serrano L, Tawfik DS: The stability effects of protein mutations appear to be universally distributed. J Mol Biol 2007, 369:1318-1332.

Toombs JA, McCarty BR, Ross ED: Compositional determinants of prion formation in yeast. Mol Cell Biol 2010, 30:319-332.

Voet D, Voet JG: Biochemistry edn 3rd. New York: J. Wiley & Sons; 2004.

Winzeler EA, Shoemaker DD, Astromoff A, Liang H, Anderson K, Andre B, Bangham R, Benito R, Boeke JD, Bussey H, et al.: Functional characterization of the S. cerevisiae genome by gene deletion and parallel analysis. Science 1999, 285:901-906.

References

An S, Kumar R, Sheets ED, Benkovic SJ: Reversible compartmentalization of de novo purine biosynthetic complexes in living cells. Science 2008, 320:103-106.

Anderluh G, Gutierrez-Aguirre I, Rabzelj S, Ceru S, Kopitar-Jerala N, Macek P, Turk V, Zerovnik E: Interaction of human stefin B in the prefibrillar oligomeric form with membranes. Correlation with cellular toxicity. FEBS J 2005, 272:3042-3051.

Bajorek M, Finley D, Glickman MH: Proteasome disassembly and downregulation is correlated with viability during stationary phase. Curr Biol 2003, 13:1140-1144.

Bacher JM, de Crecy-Lagard V, Schimmel PR: Inhibited cell growth and protein functional changes from an editing-defective tRNA synthetase. Proc Natl Acad Sci U S A 2005, 102:1697-1701.

Blouin C, Butt D, Roger AJ: Rapid evolution in conformational space: a study of loop regions in a ubiquitous GTP binding domain. Protein Sci 2004, 13:608-616.

Bode W, Schirmer T: Determination of the protein content of crystals formed by Mastigocladus laminosus C-phycocyanin, Chroomonas spec. phycocyanin-645 and modified human fibrinogen using an improved Ficoll density gradient method. Biol Chem Hoppe Seyler 1985, 366:287-295.

Bousset L, Thomson NH, Radford SE, Melki R: The yeast prion Ure2p retains its native alpha-helical conformation upon assembly into protein fibrils in vitro. EMBO J 2002, 21:2903-2911.

Brengues M, Teixeira D, Parker R: Movement of eukaryotic mRNAs between polysomes and cytoplasmic processing bodies. Science 2005, 310:486-489.

Breslow DK, Cameron DM, Collins SR, Schuldiner M, Stewart-Ornstein J, Newman HW, Braun S, Madhani HD, Krogan NJ, Weissman JS: A comprehensive strategy enabling high-resolution functional analysis of the yeast genome. Nat Methods 2008, 5:711-718.

Broadley SA, Hartl FU: The role of molecular chaperones in human misfolding diseases. FEBS Lett 2009, 583:2647-2653.

Bucciantini M, Calloni G, Chiti F, Formigli L, Nosi D, Dobson CM, Stefani M: Prefibrillar amyloid protein aggregates share common features of cytotoxicity. J Biol Chem 2004, 279:31374-31382.

Bucciantini M, Giannoni E, Chiti F, Baroni F, Formigli L, Zurdo J, Taddei N, Ramponi G, Dobson CM, Stefani M: Inherent toxicity of aggregates implies a common mechanism for protein misfolding diseases. Nature 2002, 416:507-511.

Chen Y, Dokholyan NV: Natural selection against protein aggregation on self-interacting and essential proteins in yeast, fly, and worm. Mol Biol Evol 2008, 25:1530-1533.

Chernoff YO, Lindquist SL, Ono B, Inge-Vechtomov SG, Liebman SW: Role of the chaperone protein Hsp104 in propagation of the yeast prion-like factor [psi+]. Science 1995, 268:880-884.

Chiti F, Calamai M, Taddei N, Stefani M, Ramponi G, Dobson CM: Studies of the aggregation of mutant proteins in vitro provide insights into the genetics of amyloid diseases. Proc Natl Acad Sci U S A 2002, 99 Suppl 4:16419-16426.

Chiti F, Stefani M, Taddei N, Ramponi G, Dobson CM: Rationalization of the effects of mutations on peptide and protein aggregation rates. Nature 2003, 424:805-808.

Chiti F, Taddei N, Baroni F, Capanni C, Stefani M, Ramponi G, Dobson CM: Kinetic partitioning of protein folding and aggregation. Nat Struct Biol 2002, 9:137-143.

Choder M: A general topoisomerase I-dependent transcriptional repression in the stationary phase in yeast. Genes Dev 1991, 5:2315-2326.

Cox MB, Miller CA, 3rd: Pharmacological and genetic analysis of 90-kDa heat shock isoprotein-aryl hydrocarbon receptor complexes. Mol Pharmacol 2003, 64:1549-1556.

Crapeau M, Marchal C, Cullin C, Maillet L: The cellular concentration of the yeast Ure2p prion protein affects its propagation as a prion. Mol Biol Cell 2009, 20:2286-2296.

Das AK, Chen BP, Story MD, Sato M, Minna JD, Chen DJ, Nirodi CS: Somatic mutations in the tyrosine kinase domain of epidermal growth factor receptor (EGFR) abrogate EGFR-mediated radioprotection in non-small cell lung carcinoma. Cancer Res 2007, 67:5267-5274.

de Nobel H, Ruiz C, Martin H, Morris W, Brul S, Molina M, Klis FM: Cell wall perturbation in yeast results in dual phosphorylation of the Slt2/Mpk1 MAP kinase and in an Slt2-mediated increase in FKS2-lacZ expression, glucanase resistance and thermotolerance. Microbiology 2000, 146 (Pt 9):2121-2132.

Dobson CM: Protein folding and misfolding. Nature 2003, 426:884-890.

Dobson CM: Principles of protein folding, misfolding and aggregation. Semin Cell Dev Biol 2004, 15:3-16.

Dong X, Stothard P, Forsythe IJ, Wishart DS: PlasMapper: a web server for drawing and auto-annotating plasmid maps. Nucleic Acids Res 2004, 32:W660-664.

Drummond DA, Wilke CO: The evolutionary consequences of erroneous protein synthesis. Nat Rev Genet 2009, 10:715-724.

Dujon B: The yeast genome project: what did we learn? Trends Genet 1996, 12:263-270.

Fernandez-Escamilla AM, Rousseau F, Schymkowitz J, Serrano L: Prediction of sequence-dependent and mutational effects on the aggregation of peptides and proteins. Nat Biotechnol 2004, 22:1302-1306.

Fuge EK, Braun EL, Werner-Washburne M: Protein synthesis in long-term stationary-phase cultures of Saccharomyces cerevisiae. J Bacteriol 1994, 176:5802-5813.

Ganesh C, Zaidi FN, Udgaonkar JB, Varadarajan R: Reversible formation of on-pathway macroscopic aggregates during the folding of maltose binding protein. Protein Sci 2001, 10:1635-1644.

Gelperin DM, White MA, Wilkinson ML, Kon Y, Kung LA, Wise KJ, Lopez-Hoyo N, Jiang L, Piccirillo S, Yu H, et al.: Biochemical and genetic analysis of the yeast proteome with a movable ORF collection. Genes Dev 2005, 19:2816-2826.

Goldsmith M, Tawfik DS: Potential role of phenotypic mutations in the evolution of protein expression and stability. Proc Natl Acad Sci U S A 2009, 106:6197-6202.

Gray JV, Petsko GA, Johnston GC, Ringe D, Singer RA, Werner-Washburne M: "Sleeping beauty": quiescence in Saccharomyces cerevisiae. Microbiol Mol Biol Rev 2004, 68:187-206.

Greenfield NJ: Using circular dichroism spectra to estimate protein secondary structure. Nat Protoc 2006, 1:2876-2890.

Guerois R, Nielsen JE, Serrano L: Predicting changes in the stability of proteins and protein complexes: a study of more than 1000 mutations. J Mol Biol 2002, 320:369-387.

Haataja L, Gurlo T, Huang CJ, Butler PC: Islet amyloid in type 2 diabetes, and the toxic oligomer hypothesis. Endocr Rev 2008, 29:303-316.

Hartl FU, Hayer-Hartl M: Molecular chaperones in the cytosol: from nascent chain to folded protein. Science 2002, 295:1852-1858.

Hughes TR, Roberts CJ, Dai H, Jones AR, Meyer MR, Slade D, Burchard J, Dow S, Ward TR, Kidd MJ, et al.: Widespread aneuploidy revealed by DNA microarray expression profiling. Nat Genet 2000, 25:333-337.

Huh WK, Falvo JV, Gerke LC, Carroll AS, Howson RW, Weissman JS, O'Shea EK: Global analysis of protein localization in budding yeast. Nature 2003, 425:686-691.

Jarrett JT, Lansbury PT, Jr.: Seeding "one-dimensional crystallization" of amyloid: a pathogenic mechanism in Alzheimer's disease and scrapie? Cell 1993, 73:1055-1058.

Jona G, Choder M, Gileadi O: Glucose starvation induces a drastic reduction in the rates of both transcription and degradation of mRNA in yeast. Biochim Biophys Acta 2000, 1491:37-48.

Kabsch W, Sander C: Dictionary of protein secondary structure: pattern recognition of hydrogen-bonded and geometrical features. Biopolymers 1983, 22:2577-2637.

Kaeberlein M, Kirkland KT, Fields S, Kennedy BK: Genes determining yeast replicative life span in a long-lived genetic background. Mech Ageing Dev 2005, 126:491-504.

Kayed R, Head E, Thompson JL, McIntire TM, Milton SC, Cotman CW, Glabe CG: Common structure of soluble amyloid oligomers implies common mechanism of pathogenesis. Science 2003, 300:486-489.

Kingdon HS, Hubbard JS, Stadtman ER: Regulation of glutamine synthetase. XI. The nature and implications of a lag phase in the Escherichia coli glutamine synthetase reaction. Biochemistry 1968, 7:2136-2142.

Krahn JM, Kim JH, Burns MR, Parry RJ, Zalkin H, Smith JL: Coupled formation of an amidotransferase interdomain ammonia channel and a phosphoribosyltransferase active site. Biochemistry 1997, 36:11061-11068.

Krishnan L, Sad S, Patel GB, Sprott GD: Archaeosomes induce enhanced cytotoxic T lymphocyte responses to entrapped soluble protein in the absence of interleukin 12 and protect against tumor challenge. Cancer Res 2003, 63:2526-2534.

Kumar A, Agarwal S, Heyman JA, Matson S, Heidtman M, Piccirillo S, Umansky L, Drawid A, Jansen R, Liu Y, et al.: Subcellular localization of the yeast proteome. Genes Dev 2002, 16:707-719.

Kwon KS, Lee S, Yu MH: Refolding of alpha 1-antitrypsin expressed as inclusion bodies in Escherichia coli: characterization of aggregation. Biochim Biophys Acta 1995, 1247:179-184.

Lansbury PT, Jr.: Yeast prions: inheritance by seeded protein polymerization? Curr Biol 1997, 7:R617-619.

Laporte D, Salin B, Daignan-Fornier B, Sagot I: Reversible cytoplasmic localization of the proteasome in quiescent yeast cells. J Cell Biol 2008, 181:737-745.

Lee JW, Beebe K, Nangle LA, Jang J, Longo-Guess CM, Cook SA, Davisson MT, Sundberg JP, Schimmel P, Ackerman SL: Editing-defective tRNA synthetase causes protein misfolding and neurodegeneration. Nature 2006, 443:50-55.

Lesk AM: Introduction to protein architecture: the structural biology of proteins. Oxford; New York: Oxford University Press; 2001.

LeVine H, 3rd: Thioflavine T interaction with synthetic Alzheimer's disease beta-amyloid peptides: detection of amyloid aggregation in solution. Protein Sci 1993, 2:404-410.

LeVine H, 3rd, Walker LC: Molecular polymorphism of Abeta in Alzheimer's disease. Neurobiol Aging 2010, 31:542-548.

Lewis DL, and D. K. Gattie: The ecology of quiescent microbes. ASM News 1991, 57:27-32.

Li Z, Lee I, Moradi E, Hung NJ, Johnson AW, Marcotte EM: Rational extension of the ribosome biogenesis pathway using network-guided genetics. PLoS Biol 2009, 7:e1000213.

Linding R, Schymkowitz J, Rousseau F, Diella F, Serrano L: A comparative study of the relationship between protein structure and beta-aggregation in globular and intrinsically disordered proteins. J Mol Biol 2004, 342:345-353.

Liu JL: The enigmatic cytoophidium: compartmentation of CTP synthase via filament formation. Bioessays 2010, 33:159-164.

Longtine MS, McKenzie A, 3rd, Demarini DJ, Shah NG, Wach A, Brachat A, Philippsen P, Pringle JR: Additional modules for versatile and economical PCR-based gene deletion and modification in Saccharomyces cerevisiae. Yeast 1998, 14:953-961.

Ludin KM, Hilti N, Schweingruber ME: The ade4 gene of Schizosaccharomyces pombe: cloning, sequence and regulation. Curr Genet 1994, 25:465-468.

Ma J, Bharucha N, Dobry CJ, Frisch RL, Lawson S, Kumar A: Localization of autophagy-related proteins in yeast using a versatile plasmid-based resource of fluorescent protein fusions. Autophagy 2008, 4:792-800.

Malinchik SB, Inouye H, Szumowski KE, Kirschner DA: Structural analysis of Alzheimer's beta(1-40) amyloid: protofilament assembly of tubular fibrils. Biophys J 1998, 74:537-545.

Manivasakam P, Weber SC, McElver J, Schiestl RH: Micro-homology mediated PCR targeting in Saccharomyces cerevisiae. Nucleic Acids Res 1995, 23:2799-2800.

Martzen MR, McCraith SM, Spinelli SL, Torres FM, Fields S, Grayhack EJ, Phizicky EM: A biochemical genomics approach for identifying genes by the activity of their products. Science 1999, 286:1153-1155.

Matthews BW: Structural and genetic analysis of protein stability. Annu Rev Biochem 1993, 62:139-160.

Miller S, Janin J, Lesk AM, Chothia C: Interior and surface of monomeric proteins. J Mol Biol 1987, 196:641-656.

Minois N, Lagona F, Frajnt M, Vaupel JW: Plasticity of death rates in stationary phase in Saccharomyces cerevisiae. Aging Cell 2009, 8:36-44.

Mitchell AP, Magasanik B: Purification and properties of glutamine synthetase from Saccharomyces cerevisiae. J Biol Chem 1983, 258:119-124.

Miyata Y, Yahara I: The 90-kDa heat shock protein, HSP90, binds and protects casein kinase II from self-aggregation and enhances its kinase activity. J Biol Chem 1992, 267:7042-7047.

Mnaimneh S, Davierwala AP, Haynes J, Moffat J, Peng WT, Zhang W, Yang X, Pootoolal J, Chua G, Lopez A, et al.: Exploration of essential gene functions via titratable promoter alleles. Cell 2004, 118:31-44.

Muchmore CR, Krahn JM, Kim JH, Zalkin H, Smith JL: Crystal structure of glutamine phosphoribosylpyrophosphate amidotransferase from Escherichia coli. Protein Sci 1998, 7:39-51.

Nadkarni AK, McDonough VM, Yang WL, Stukey JE, Ozier-Kalogeropoulos O, Carman GM: Differential biochemical regulation of the URA7- and URA8-encoded CTP synthetases from Saccharomyces cerevisiae. J Biol Chem 1995, 270:24982-24988.

Nangle LA, Motta CM, Schimmel P: Global effects of mistranslation from an editing defect in mammalian cells. Chem Biol 2006, 13:1091-1100.

Narayanaswamy R, Levy M, Tsechansky M, Stovall GM, O'Connell JD, Mirrielees J, Ellington AD, Marcotte EM: Widespread reorganization of metabolic enzymes into reversible assemblies upon nutrient starvation. Proc Natl Acad Sci U S A 2009, 106:10147-10152.

Nathan DF, Vos MH, Lindquist S: In vivo functions of the Saccharomyces cerevisiae Hsp90 chaperone. Proc Natl Acad Sci U S A 1997, 94:12949-12956.

Noda T, Ohsumi Y: Tor, a phosphatidylinositol kinase homolog, controls autophagy in yeast. J Biol Chem 1998, 273:3963-3966.

O'Nuallain B, Wetzel R: Conformational Abs recognizing a generic amyloid fibril epitope. Proc Natl Acad Sci U S A 2002, 99:1485-1490.

Ozier-Kalogeropoulos O, Adeline MT, Yang WL, Carman GM, Lacroute F: Use of synthetic lethal mutants to clone and characterize a novel CTP synthetase gene in Saccharomyces cerevisiae. Mol Gen Genet 1994, 242:431-439.

Ozier-Kalogeropoulos O, Fasiolo F, Adeline MT, Collin J, Lacroute F: Cloning, sequencing and characterization of the Saccharomyces cerevisiae URA7 gene encoding CTP synthetase. Mol Gen Genet 1991, 231:7-16.

Parsell DA, Kowal AS, Singer MA, Lindquist S: Protein disaggregation mediated by heat-shock protein Hsp104. Nature 1994, 372:475-478.

Parsell DA, Sanchez Y, Stitzel JD, Lindquist S: Hsp104 is a highly conserved protein with two essential nucleotide-binding sites. Nature 1991, 353:270-273.

Patel A: Generating Mutant Yeast and Measuring the Rate of Ade4 Punctate Foci Formation [Undergraduate Honors Thesis]. Austin: University of Texas at Austin: 2010.

Pauling L, Corey RB: Configurations of Polypeptide Chains With Favored Orientations Around Single Bonds: Two New Pleated Sheets. Proc Natl Acad Sci U S A 1951, 37:729-740.

Pawar AP, Dubay KF, Zurdo J, Chiti F, Vendruscolo M, Dobson CM: Prediction of "aggregation-prone" and "aggregation-susceptible" regions in proteins associated with neurodegenerative diseases. J Mol Biol 2005, 350:379-392.

Pecorari F, Minard P, Desmadril M, Yon JM: Occurrence of transient multimeric species during the refolding of a monomeric protein. J Biol Chem 1996, 271:5270-5276.

Perutz MF, Windle AH: Cause of neural death in neurodegenerative diseases attributable to expansion of glutamine repeats. Nature 2001, 412:143-144.

Plesset J, Ludwig JR, Cox BS, McLaughlin CS: Effect of cell cycle position on thermotolerance in Saccharomyces cerevisiae. J Bacteriol 1987, 169:779-784.

Plost B: Protein Aggregation Optimization: An Algorithmic Approach [Undergraduate Honors Thesis]. Austin: University of Texas at Austin: 2009.

Pringle JR, Hartwell LH: The Saccharomyces cerevisiae cell cycle. In Molecular biology of the yeast Saccharomyces cerevisiae: life cycle and inheritance. Edited by J. R. Broach JS, and E. Jones Cold Spring Harbor Laboratory; 1981:97-142.

Pruyne D, Legesse-Miller A, Gao L, Dong Y, Bretscher A: Mechanisms of polarized growth and organelle segregation in yeast. Annu Rev Cell Dev Biol 2004, 20:559-591.

Radonjic M, Andrau JC, Lijnzaad P, Kemmeren P, Kockelkorn TT, van Leenen D, van Berkum NL, Holstege FC: Genome-wide analyses reveal RNA polymerase II located upstream of genes poised for rapid response upon S. cerevisiae stationary phase exit. Mol Cell 2005, 18:171-183.

Redon CE, Nakamura AJ, Gouliaeva K, Rahman A, Blakely WF, Bonner WM: The use of gamma-H2AX as a biodosimeter for total-body radiation exposure in non-human primates. PLoS One 2010, 5:e15544.

Rieder SE, Emr SD: Isolation of subcellular fractions from the yeast Saccharomyces cerevisiae. Curr Protoc Cell Biol 2001, Chapter 3:Unit 3 8.

Roberts RL, Metz M, Monks DE, Mullaney ML, Hall T, Nester EW: Purine synthesis and increased Agrobacterium tumefaciens transformation of yeast and plants. Proc Natl Acad Sci U S A 2003, 100:6634-6639.

Rochelle PA, Ferguson DM, Johnson AM, De Leon R: Quantitation of Cryptosporidium parvum infection in cell culture using a colorimetric in situ hybridization assay. J Eukaryot Microbiol 2001, 48:565-574.

Ross CA, Poirier MA: Protein aggregation and neurodegenerative disease. Nat Med 2004, 10 Suppl:S10-17.

Sagot I, Pinson B, Salin B, Daignan-Fornier B: Actin bodies in yeast quiescent cells: an immediately available actin reserve? Mol Biol Cell 2006, 17:4645-4655.

Saxena AM: Phycocyanin aggregation. A small angle neutron scattering and size exclusion chromatographic study. J Mol Biol 1988, 200:579-591.

Scherens B, Goffeau A: The uses of genome-wide yeast mutant collections. Genome Biol 2004, 5:229.

Schneider E, Pollard H, Lepault F, Guy-Grand D, Minkowski M, Dy M: Histamine-producing cell-stimulating activity. Interleukin 3 and granulocyte-macrophage colony-stimulating factor induce de novo synthesis of histidine decarboxylase in hemopoietic progenitor cells. J Immunol 1987, 139:3710-3717.

Selkoe DJ: Folding proteins in fatal ways. Nature 2003, 426:900-904.

Shirahama T, Cohen AS: High-resolution electron microscopic analysis of the amyloid fibril. J Cell Biol 1967, 33:679-708.

Silow M, Oliveberg M: Transient aggregates in protein folding are easily mistaken for folding intermediates. Proc Natl Acad Sci U S A 1997, 94:6084-6086.

Silow M, Tan YJ, Fersht AR, Oliveberg M: Formation of short-lived protein aggregates directly from the coil in two-state folding. Biochemistry 1999, 38:13006-13012.

Simpson RJ: Proteins and proteomics: a laboratory manual. Cold Spring Harbor, NY: Cold Spring Harbor Laboratory Press; 2003.

Smolina VS, Bekker ML: [Properties of 5-phosphoryl-1-pyrophosphate amidotransferase from the yeast Saccharomyces cerevisiae wild type and mutant with altered purine biosynthesis regulation]. Biokhimiia 1982, 47:162-167.

Som I, Mitsch RN, Urbanowski JL, Rolfes RJ: DNA-bound Bas1 recruits Pho2 to activate ADE genes in Saccharomyces cerevisiae. Eukaryot Cell 2005, 4:1725-1735.

Stefani M, Dobson CM: Protein aggregation and aggregate toxicity: new insights into protein folding, misfolding diseases and biological evolution. J Mol Med 2003, 81:678-699.

Sugiyama M, Yamagishi K, Kim YH, Kaneko Y, Nishizawa M, Harashima S: Advances in molecular methods to alter chromosomes and genome in the yeast Saccharomyces cerevisiae. Appl Microbiol Biotechnol 2009, 84:1045-1052.

Sunde M, Serpell LC, Bartlam M, Fraser PE, Pepys MB, Blake CC: Common core structure of amyloid fibrils by synchrotron X-ray diffraction. J Mol Biol 1997, 273:729-739.

Thevelein JM, Cauwenberg L, Colombo S, De Winde JH, Donation M, Dumortier F, Kraakman L, Lemaire K, Ma P, Nauwelaers D, et al.: Nutrient-induced signal transduction through the protein kinase A pathway and its role in the control of

metabolism, stress resistance, and growth in yeast. Enzyme Microb Technol 2000, 26:819-825.

Thompson JD, Higgins DG, Gibson TJ: CLUSTAL W: improving the sensitivity of progressive multiple sequence alignment through sequence weighting, position-specific gap penalties and weight matrix choice. Nucleic Acids Res 1994, 22:4673-4680.

Tokuriki N, Stricher F, Schymkowitz J, Serrano L, Tawfik DS: The stability effects of protein mutations appear to be universally distributed. J Mol Biol 2007, 369:1318-1332.

Toombs JA, McCarty BR, Ross ED: Compositional determinants of prion formation in yeast. Mol Cell Biol 2010, 30:319-332.

Unno H, Uchida T, Sugawara H, Kurisu G, Sugiyama T, Yamaya T, Sakakibara H, Hase T, Kusunoki M: Atomic structure of plant glutamine synthetase: a key enzyme for plant productivity. J Biol Chem 2006, 281:29287-29296.

van den Oetelaar PJ, de Man BM, Hoenders HJ: Protein folding and aggregation studied by isoelectric focusing across a urea gradient and isoelectric focusing in two dimensions. Biochim Biophys Acta 1989, 995:82-90.

Voet D, Voet JG: Biochemistry edn 3rd. New York: J. Wiley & Sons; 2004.

von Bergen M, Friedhoff P, Biernat J, Heberle J, Mandelkow EM, Mandelkow E: Assembly of tau protein into Alzheimer paired helical filaments depends on a local sequence motif ((306)VQIVYK(311)) forming beta structure. Proc Natl Acad Sci U S A 2000, 97:5129-5134.

Werner-Washburne M, Braun EL, Crawford ME, Peck VM: Stationary phase in Saccharomyces cerevisiae. Mol Microbiol 1996, 19:1159-1166.

Winzeler EA, Shoemaker DD, Astromoff A, Liang H, Anderson K, Andre B, Bangham R, Benito R, Boeke JD, Bussey H, et al.: Functional characterization of the S. cerevisiae genome by gene deletion and parallel analysis. Science 1999, 285:901-906.

Woods RA, Roberts DG, Friedman T, Jolly D, Filpula D: Hypoxanthine: guanine phosphoribosyltransferase mutants in Saccharomyces cerevisiae. Mol Gen Genet 1983, 191:407-412.

Zhu H, Bilgin M, Bangham R, Hall D, Casamayor A, Bertone P, Lan N, Jansen R, Bidlingmaier S, Houfek T, et al.: Global analysis of protein activities using proteome chips. Science 2001, 293:2101-2105.

Zhou T, Weems M, Wilke CO: Translationally optimal codons associate with structurally sensitive sites in proteins. Mol Biol Evol 2009, 26:1571-1580.

Vita

Gwendolyn Marie Motz Stovall was born in Spartanburg, South Carolina and moved to Duluth, Georgia at the age of three. After graduating Duluth High School, she entered the University of Georgia, Athens in 1995. Upon completing the American Chemical Society recommended courses, Gwen received her Bachelor of Science Chemistry degree (BS Chem) and Bachelor of Science (BS) in biochemistry and molecular biology in 1999. In 2002 she entered the laboratory of Dr. Andrew D. Ellington and began studying aptamer selections. In the fall of 2004, she entered graduate school at the University of Texas, Austin where she studied aptamers and a starvation phenomenon in yeast under the supervision of Dr. Andrew D. Ellington.

Permanent email: gwenstovall@gmail.com
This dissertation was typed by the author.